UNIVERSITÀ DEGLI STUDI DI PADOVA

Dipartimento di Fisica e Astronomia “Galileo Galilei”

Master Degree in Astrophysics and Cosmology

Final Dissertation

Cosmic Birefringence with the Cosmic Microwave Background:

A Harmonic-Based Methodology

Supervisor

Prof. Nicola BARTOLO

UNIVERSITÀ DEGLI STUDI DI PADOVA

Co-supervisor

Dr. Alessandro GRUPPUSO

INAF OAS Bologna

Master Candidate

Idil Ezgi KARAASLAN

Academic Year

2023/24

To my dad

Abstract

This thesis explores parity-violating extensions of standard electromagnetism, which can be realized through a Chern-Simons term coupling the dual of the electromagnetic tensor to a scalar field (or pseudo-scalar field, such as an axion-like field) where the latter may act as dark matter or dark energy. This interaction rotates the linear polarization of light in a manner similar to birefringent materials and is therefore commonly referred to as the Cosmic Birefringence (CB) effect. Since the Cosmic Microwave Background (CMB) is linearly polarized due to Thomson scattering at the last scattering surface, the CMB is often used to probe this phenomenon. In fact, recent analyses on Planck data, have intriguingly hinted at a detection of CB with a statistical significance ranging from 2.4 to 3.6 sigma [1, 2, 3, 4]. These measurements have attracted significant attention in recent years, as they hold the potential to uncover new physics beyond the standard model of particle physics and cosmology. In this thesis, we compute how CB affects the CMB angular power spectra. Additionally, we analytically derive two harmonic-based estimators, known in the literature as D-estimators, which constrain the CB effect by utilizing information from the TB (temperature anisotropies and B-mode polarization) and EB (E- and B-mode polarization) CMB angular power spectra. We verify that these estimators correctly recover the birefringence angle and assess their expected statistical efficiency, recovering known results from the literature. Additionally, we perform a detailed analysis of the joint estimator, obtained by combining the two D-estimators, and provide an analytical expression for the total joint uncertainty. While it is known that the joint estimator is dominated by the one derived from the EB spectrum, the final expression for the combined estimator can be considered new.

Contents

1 Introduction

The Cosmic Microwave Background (CMB) is a relic radiation from the early universe, originating approximately 380,000 years after the Big Bang. During this epoch, so-called recombination, photons were allowed to travel freely for the first time once the universe had cooled enough to combine protons and electrons into neutral hydrogen atoms. This nearly uniform radiation field is observed in microwavelength, today, with a current temperature of 2.725 K, and its nearly perfect blackbody spectrum is defined by Planck's law:

$$B(\nu, T) = \frac{2h\nu^3}{c^2} \frac{1}{\exp(\frac{h\nu}{k_B T}) - 1}, \tag{1.1}$$

where $B(\nu, T)$ is the spectral radiance at frequency ν and absolute temperature T (K), h is Planck's constant, c is the speed of light, and k_B is Boltzmann's constant. The spectral radiance describes the amount of energy emitted by a black body per unit area, per unit solid angle, per unit frequency, in units $W.m^{-2}.s^{-1}.Hz^{-1}$.

The observations and study of CMB provide an important window into the early universe since its accidental discovery by Penzias and Wilson in 1965. These observations played a significant role in developing the standard model of cosmology, the ΛCDM model, also known as the concordance model. COBE satellite was the first to map temperature anisotropies of CMB radiation [5], this was followed by later missions such as WMAP [6] and Planck [7], which provided increasingly sensitive measurements of the temperature and polarization spectra of CMB. The angular power spectrum is

used to describe the distribution of the anisotropies arising from the temperature fluctuations in the CMB radiation across different angular scales. By using spherical harmonics, these anisotropies can be decomposed into multipole moments, ℓ, where smaller multipoles correspond to larger angular scales. Using this mathematical representation, we can analyze the observed anisotropies to get information on the structure and evolution of the universe, obtain important cosmological parameters, and distinguish between different models of the universe.

Figure 1.1 represents the 2018 SMICA temperature map of CMB observed by the Planck satellite, illustrating the distribution of temperature anisotropies in the CMB, which correspond to the small density fluctuations in the photon-baryon fluid at the time of photon decoupling.

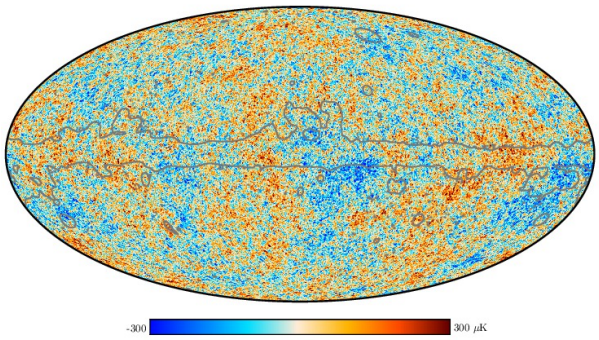

Figure 1.1: Planck CMB sky from the 2018 SMICA temperature map, smoothed to 5°. Source: Planck Collaboration [8]

The measured temperature in a direction $\hat{n}$ in the sky divided by the average CMB temperature today (T_0) is given by [9]:

$$\frac{T(\hat{n})}{T_0} = 1 + \Theta(\hat{n}) \,, \tag{1.2}$$

where the fractional temperature fluctuation $\Theta(\hat{n})$ is defined as:

$$\Theta(\hat{n}) = \frac{\delta T(\hat{n})}{T_0} \,. \tag{1.3}$$

The statistical analysis of the CMB temperature fluctuations are done by measuring the correlations between hot and cold spots as a function of their angular separation. This results as the angular power spectrum shown in Figure 1.2. We can write the two-point correlation function to make a comparison

of the temperatures at two different points $\hat{n}$ and $\hat{n}'$:

$$C(\theta) = \langle \Theta(\hat{n})\Theta(\hat{n}') \rangle \tag{1.4}$$

where $\hat{n} \cdot \hat{n}' = cos\theta$. Let us expand the temperature field in spherical harmonics since the observations of anisotropies are done on the spherical last scattering surface:

$$\Theta(\hat{n}) = \sum_{l=-2}^{\infty} \sum_{m=-l}^{l} a_{lm} Y_{lm}(\hat{n}) \,, \tag{1.5}$$

where a_{lm} are the expansion coefficients that quantify the contribution of each spherical harmonic Y_{lm} indexed by the multipole moment ℓ and the azimuthal index m. The functions Y_{lm} represent scalar spherical harmonics, which describe the angular dependence of the temperature fluctuations observed in the universe.

We can define the two point function of expansion coefficients as:

$$\langle a_{lm} a^*_{l'm'} \rangle = C_l \delta_{ll'} \delta_{mm'} \,, \tag{1.6}$$

where the superscript * denotes complex conjugation, C_l is the angular power spectrum and Kronecker deltas occur due the statistical isotropy. The angular power spectrum serves as the harmonic space counterpart to the two-point correlation function in real space. Let us substitute 1.5 into 1.4:

$$\begin{aligned} C(\theta) &= \langle \Theta(\hat{n})\Theta(\hat{n}') \rangle \\ &= \sum_{lm} \sum_{l'm'} \langle a_{lm} a^*_{l'm'} \rangle Y_{lm}(\hat{n}) Y^*_{l'm'}(\hat{n}') \\ &= \sum_{l} C_l \sum_{m} Y_{lm}(\hat{n}) Y^*_{l'm'}(\hat{n}') \\ &= \frac{2l+1}{4\pi} C_l P_l(\cos\theta) \,, \end{aligned} \tag{1.7}$$

where $P_l(\cos\theta)$ are Legendre polynomials. As a result, we can observe that the information in the C_l's is exactly the same as that of the function $C(\theta)$.

Figure 1.2 illustrates the Planck mission's observed power spectrum that contributed to determining the concordance model's parameters. In this figure, D_ℓ is equivalent to $\ell(2\ell+1)C_l$). The angular power spectrum shows distinctive peaks corresponding to sound waves in the early universe. These peaks contain crucial details on the composition and the initial conditions of the universe, as well as

its expansion history.

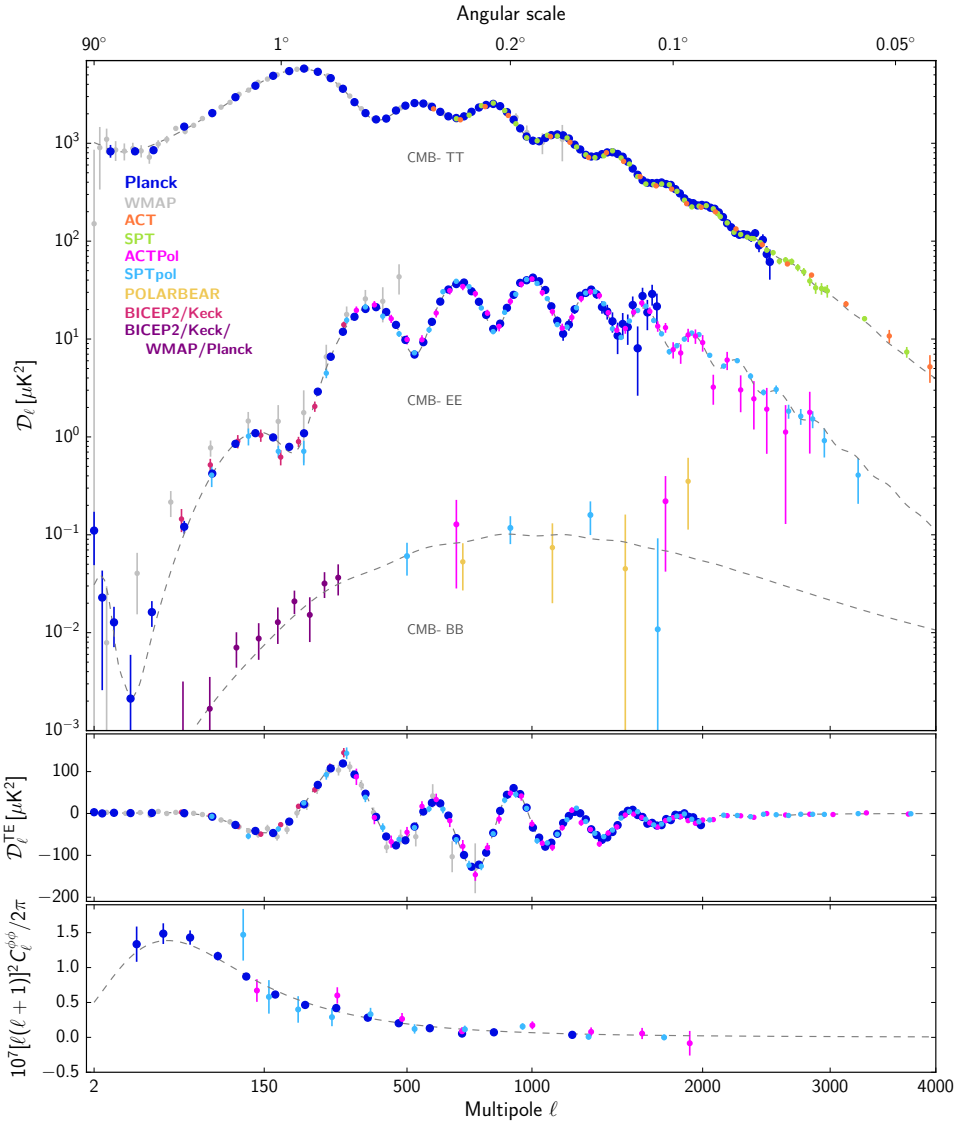

Figure 1.2: A compilation of recent measurements of the angular power spectra of the CMB, which form the foundation for most cosmological analyses. The top panel displays the power spectra of the temperature anisotropies, as well as the E-mode and B-mode polarization signals. The middle panel illustrates the T-E cross-correlation spectrum, while the bottom panel presents the lensing deflection power spectrum. Different colors represent data from various experiments, each shown with its original binning. The dashed line represents the best-fit ΛCDM model based on the Planck temperature, polarization, and lensing data. Source: Planck Collaboration [8].

1.1 ΛCDM Model

The ΛCDM model, is currently the most successful cosmological model that describes large-scale structure and evolution of the universe from the Big Bang to the present day. It is based on the Cosmological Principle, which assumes that the universe is homogeneous and isotropic on large scales. This model explains the dynamics of the universe through three main components: dark matter (CDM, or Cold Dark Matter), dark energy (Λ, represented by the cosmological constant), and ordinary matter (baryons). According to current observations [10], the universe's composition is approximately 68% dark energy, 27% dark matter, and only 5% baryonic matter. Interactions of these components are well explained within the framework of General Relativity, and the dynamics of the universe's expansion are governed by the Friedmann equations. These equations give the relation between the scale factor $a(t)$, the energy densities of each component, and the curvature of spacetime. The spacetime metric used is the Friedmann-Lemaître-Robertson-Walker metric (FLRW metric). It describes a homogeneous, isotropic, expanding universe that satisfies the cosmological principle, using an exact solution of Einstein's field equations of general relativity:

$$ds^2 = -c^2dt^2 + a(t)^2\left(\frac{dr^2}{1-kr^2} + r^2d\theta^2 + r^2\sin^2\theta\, d\varphi^2\right), \tag{1.8}$$

where t represents time, $a(t)$ is the scale factor describing the relative expansion of the universe, c is the speed of light, k denotes the spatial curvature (with values $k = 0$ for flat, $k = +1$ for closed, and $k = -1$ for open universes), and (r, θ, φ) are comoving coordinates.

Alexander Friedmann derived the Friedmann equations in 1922 from Einstein's field equations for the FLRW metric and a perfect fluid with a mass density ρ and pressure p to describe the universe's expansion. The first Friedmann equation describes the evolution of the scale factor:

$$H^2 = \left(\frac{\dot{a}}{a}\right)^2 = \frac{8\pi G}{3}\rho - \frac{kc^2}{a^2} + \frac{\Lambda c^2}{3}, \tag{1.9}$$

where H is the Hubble parameter, $\dot{a}$ is the time derivative of the scale factor, G is the gravitational constant, ρ is the total energy density of the universe.

The second Friedmann equation describes the acceleration of the universe's expansion, and it is given by:

$$\frac{\ddot{a}}{a} = -\frac{4\pi G}{3}\left(\rho + \frac{3p}{c^2}\right) + \frac{\Lambda c^2}{3}, \tag{1.10}$$

where $\ddot{a}$ is the second time derivative of the scale factor, and p is the pressure. Together, these equations describe the behavior of the expanding universe under the influence of dark matter, dark energy, and baryonic matter. The scale factor a (which is set to 1 at the present time, t_0) is related to the redshift z of the universe as follows:

$$a(t) = \frac{1}{1+z}\,. \tag{1.11}$$

Thus, as the universe expands (and redshift decreases), the scale factor a increases. This reflects the stretching of spacetime itself.

We can express the energy density ρ in terms of a dimensionless parameter called the density parameter Ω, which quantifies the total energy density of the universe relative to a critical density ρ_c. The critical density ρ_c is defined as the density required for a flat universe ($k = 0$):

$$\rho_c = \frac{3H^2}{8\pi G}\,. \tag{1.12}$$

The total energy density ρ is the sum of the densities of different components, such as matter (including both dark matter and baryonic matter), dark energy, and radiation:

$$\rho = \rho_m + \rho_\Lambda + \rho_r\,. \tag{1.13}$$

Now, we define the density parameters Ω_i for each component i as:

$$\Omega_i = \frac{\rho_i}{\rho_c}\,. \tag{1.14}$$

Thus, the total density parameter Ω becomes:

$$\Omega_{tot} = \Omega_m + \Omega_\Lambda + \Omega_r\,, \tag{1.15}$$

where Ω_m, Ω_Λ, and Ω_r are the density parameters for matter, dark energy, and radiation, respectively.

Table 1.1 represents key cosmological parameter constraints derived from CMB observations with Planck, combining temperature, polarization, and lensing data. Additional results incorporate Baryon Acoustic Oscillations (BAO) for refined constraints.

Table 1.1: Parameter confidence limits derived from Planck CMB temperature, polarization, and lensing power spectra, including BAO data. The first set of rows provides 68% confidence limits for the base-ΛCDM model. The second set presents 68% constraints on derived parameters inferred from the base-ΛCDM model. Further details can be found in [7]. Adapted from: [8].

Parameter	Planck alone	Planck + BAO
$\Omega_b h^2$	0.02237 ± 0.00015	0.02242 ± 0.00014
$\Omega_c h^2$	0.1200 ± 0.0012	0.11933 ± 0.00091
$100\theta_{MC}$	1.04092 ± 0.00031	1.04101 ± 0.00029
τ	0.0544 ± 0.0073	0.0561 ± 0.0071
$\ln(10^{10} A_s)$	3.044 ± 0.014	3.047 ± 0.014
n_s	0.9649 ± 0.0042	0.9665 ± 0.0038
H_0	67.36 ± 0.54	67.66 ± 0.42
Ω_Λ	0.6847 ± 0.0073	0.6889 ± 0.0056
Ω_m	0.3153 ± 0.0073	0.3111 ± 0.0056
$\Omega_m h^2$	0.1430 ± 0.0011	0.14240 ± 0.00087
$\Omega_m h^3$	0.09633 ± 0.00030	0.09635 ± 0.00030
σ_8	0.8111 ± 0.0060	0.8102 ± 0.0060
$\sigma_8(\Omega_m/0.3)^{0.5}$	0.832 ± 0.013	0.825 ± 0.011
z_{re}	7.67 ± 0.73	7.82 ± 0.71
Age[Gyr]	13.797 ± 0.023	13.787 ± 0.020
r_*[Mpc]	144.43 ± 0.26	144.57 ± 0.22
$100\theta_*$	1.04110 ± 0.00031	1.04119 ± 0.00029
r_{drag}[Mpc]	147.09 ± 0.26	147.57 ± 0.22
z_{eq}	3402 ± 26	3387 ± 21
k_{eq}[Mpc^{-1}]	0.010384 ± 0.000081	0.010339 ± 0.000063

1.2 Cosmic Microwave Background Radiation: Features and Observational Support for the ΛCDM Model

Different observations, such as Type Ia supernovae [11, 12], large-scale structure [13], and baryon acoustic oscillations [14] support the ΛCDM model. However, CMB provides particularly powerful data because it represents the universe at an early stage, and allows precise measurements of cosmological parameters [7], such as the Hubble constant H_0, baryon density parameter Ω_b, and dark matter

density parameter Ω_c. The Hubble constant H_0 is the present value of the Hubble parameter $H(t)$, which describes the expansion rate of the universe. It is expressed in units of kilometers per second per megaparsec (km/s/Mpc) and is a critical parameter in determining the age, size, and evolution of the universe.

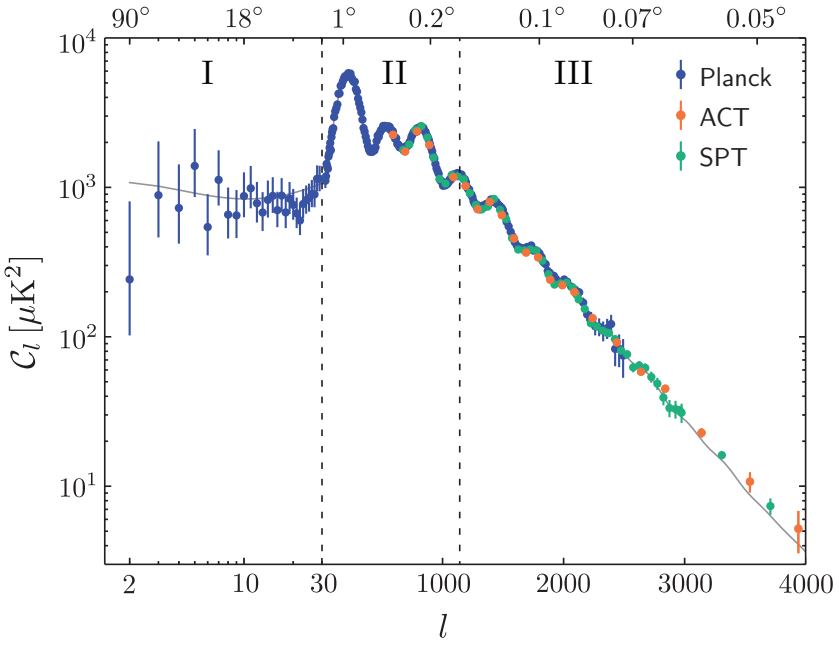

Figure 1.3: The angular variations in the CMB power spectrum reflect the dynamics of sound waves in the photon-baryon fluid. At large scales (region I), the fluctuations are frozen, revealing the spectrum of the initial conditions. At intermediate scales (region II), we observe the oscillatory behavior of the fluid at the moment of last scattering. On small scales (region III), fluctuations are suppressed as their wavelengths are shorter than the photons' mean free path, leading to damping. **Note:** The correct y-axis label should be $l(l+1)C_l/2\pi$ rather than C_l. Source: TASI Lectures on Primordial Cosmology-Daniel Baumann [15]

Figure 1.3 illustrates the CMB power spectrum measured by the Planck satellite, along with ground-based observations from the Atacama Cosmology Telescope (ACT) and the South Pole Telescope (SPT). These measurements highlight the acoustic peaks and the damping tail that characterize this spectrum. Through these features, we can gain insight into the physical mechanisms that took place in the early universe, as well as the initial conditions and the components of the universe, and the dynamics of these components during recombination. Each region of the CMB power spectrum corresponds to different physical processes with interesting aspects. These regions can be categorized as low multipoles (large angular scales), intermediate multipoles, and high multipoles (small scales), which are characterized by large angle correlations, acoustic peaks, and a damping tail, respectively [9]:

1. **Large-Angle Correlations (Region I)**: Large angular scales in the CMB spectrum correspond

to fluctuations that remained outside the horizon at recombination. These fluctuations could not evolve before photon decoupling. Therefore, they directly reflect the initial conditions of the density fluctuations of the universe.

2. **Acoustic Peaks and Intermediate-Angle Oscillations (Region II)**: On intermediate scales, perturbations with shorter wavelengths entered the horizon before recombination. Within this horizon, photon-baryon fluid was tightly coupled and perturbations in this fluid propagated as sound waves, driven by the photon pressure and baryonic mass. These sound waves were frozen in different phases when photons decoupled, resulting in an oscillatory pattern of peaks in the CMB power spectrum. The first acoustic peak represents fluctuations on the scale of horizon at the last scattering surface, the point at which the universe changed from being opaque to transparent, providing insights into the total density of the universe. Higher acoustic peaks are influenced by the composition of the photon-baryon fluid and the gravitational effects of dark matter.

   Another interesting feature of the acoustic peaks is the strong correlation between the peak heights and the matter density. If Ω_Λ at fixed $\Omega_m h^2$ (h is the dimensionless Hubble constant) increases, the Hubble rate increases mutually. Therefore, this causes the distance to the last scattering surface to decrease, and the peaks to move to larger angular scales (smaller multipoles).

3. **Small-Scale Damping and the Damping Tail (Region III)**: At small angular scales that are smaller than the mean free path of photons, photon diffusion begins to erase density variations (anisotropies) in the fluid, which leads to a damping effect. As interactions and scattering rates in the photon-baryon fluid affect the amount of damping, this damping tail limits the baryon-to-photon ratio and sheds light on the early thermal history of the universe.

To understand the physical mechanisms that produced the observed temperature anisotropies and the polarization patterns in CMB, we need to discuss the processes at the last scattering surface, approximately 380,000 years after the Big Bang.

1.3 Temperature Anisotropies and the Last Scattering Surface

The temperature anisotropies observed in CMB arise from density fluctuations in the photon-baryon fluid at the time of photon decoupling. Before recombination, the universe was a hot, dense plasma

in which all atoms were ionized, and photons and baryons were tightly coupled through Thomson scattering. Hence, it was opaque to photons due to the scattering of photons by free electrons. As the universe expanded, the temperature of this plasma started to decrease, and this caused combining protons, helium nuclei, and electrons into neutral atoms, which did not scatter photons as before. This moment is referred to as the 'last scattering', after which photons could propagate their journey freely for more than 13 billion years until they reach our instruments today.

The small density fluctuations that existed in this hot plasma correspond to small variations in temperature at photon decoupling. While higher density regions are associated with slightly hotter regions of the universe, lower density regions are associated with cooler regions, at the last scattering surface. These density variations originated from gravitational potentials, which had been induced by quantum fluctuations in the early universe, from inflationary processes. Acoustic oscillations traveling through the photon-baryon fluid are the direct consequences of these fluctuations, and they are imprinted in the CMB power spectrum as a series of acoustic peaks, indicating the competition between photon pressure and gravitational collapse. Therefore, the temperature anisotropies in CMB reflect the initial conditions of the universe at recombination.

1.4 E-mode Polarization

Thomson scattering is the main mechanism for establishing the polarization of the CMB radiation during the epoch of recombination. When photons scatter off free electrons in the plasma, they become polarized in regions where the radiation is not isotropic. This polarization is strongest at angles corresponding to the acoustic peaks, where the photon-baryon fluid was oscillating.

CMB polarization was first detected in 2002 by the Degree Angular Scale Interferometer (DASI) [16]. The polarization produced in the early universe is predominantly E-mode polarization (even-parity fluctuations), which corresponds to the gradient of density perturbations in the universe. The observed E-mode polarization is directly associated with temperature anisotropies in the primordial plasma. Let us consider a plane wave photon density perturbation propagating in a direction transverse to the line of sight [9], where the plane wave corresponds to hot and cold alterations of the photon temperature. The polarization direction of the outgoing radiation will be aligned with the hot regions, and the polarization directions will be either parallel or perpendicular to the wavevector k. This type of polarization pattern is called an E-mode.

We can obtain information about the geometry of the universe as the distribution of polarization will be sensitive to the curvature of the universe [17]. E-mode pattern will change when the geometry deviates from flatness. From this, we can get insights into the overall shape of the observed universe.

Additionally, E-mode polarization is influenced by the contributions of baryonic matter, dark matter, and dark energy as their densities affect the evolution of the sound waves in the universe [9]. These aspects of E-mode polarization provide crucial information in understanding the main properties of our universe.

Figure 1.4 represents polarization map of CMB observed by the Planck satellite. We can see the polarization field, represented as rods of varying length, superimposed on the temperature map given in Figure 1.1. This polarization field highlights the E-mode and B-mode patterns.

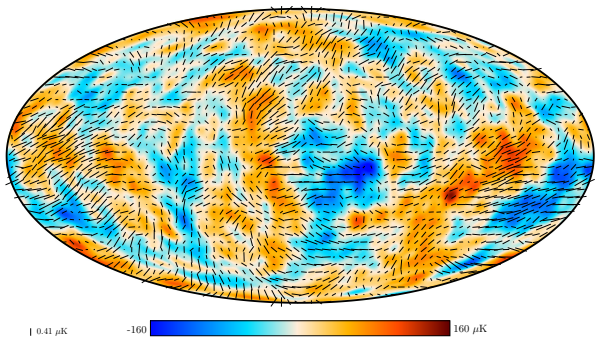

Figure 1.4: The map shows the polarization field as rods of varying length superimposed on the 2018 SMICA temperature map, smoothed to 5°. Source: Planck Collaboration [8]

1.5 B-mode Polarization

The B-modes are odd-parity fluctuations and can be used as a powerful probe of both early and late universe physics. Scalar density fluctuations in the universe cannot produce this type of polarization pattern due to the property of symmetry, where azimuthal symmetry of these fluctuations prohibits this polarization pattern [9]. Therefore, the B-mode pattern can be a key probe of non-scalar, tensor fluctuations that took place in the early universe, where they can arise from primordial gravitational waves during inflation, a period of rapid expansion that occurred during the first fraction of a second after the Big Bang. Inflation generates gravitational waves, which imprint a characteristic B-mode signature on CMB. These primordial B-modes are expected to be detectable at larger angular scales and would provide direct evidence for inflationary models if discovered [18, 19, 20]. Theoretical models predict that the amplitude of these primordial B-modes is related to the energy scale of inflation, and their detection could provide crucial information about the very early universe.

A possible detection of primordial B-modes was reported in 2014 from the BICEP2 experiment [21]. However, this result was later revised due to the contamination from galactic dust. Despite this, the detection of primordial B-modes remains a key goal for future experiments such as LiteBIRD

[22, 23], CMB-S4 [24] and the Simons Observatory [25].

In addition to primordial B-modes, gravitational lensing by large-scale structure can also generate B-mode polarization at smaller angular scales [26]. As CMB photons pass through the universe, they are deflected by the gravitational fields of large-scale structures, such as galaxies and galaxy clusters, producing a lensing B-mode signal. From this signal, we can obtain information about the distribution of mass in the universe, particularly the dark matter distribution. Measurements by experiments like Planck, ACT, SPT, and BICEP/Keck arrays support that the lensing B-modes are smaller in amplitude compared to the primordial ones but are present at much higher multipoles.

Figure 1.5 shows the B-mode polarization power spectra with contributions from primordial gravitational waves generated during inflation represented by two models; the blue solid line and the orange dashed line, lensing B-modes produced by the deflection of CMB photons by large-scale structures represented by the grey solid line, and effects from cosmic birefringence with the red dashed line.

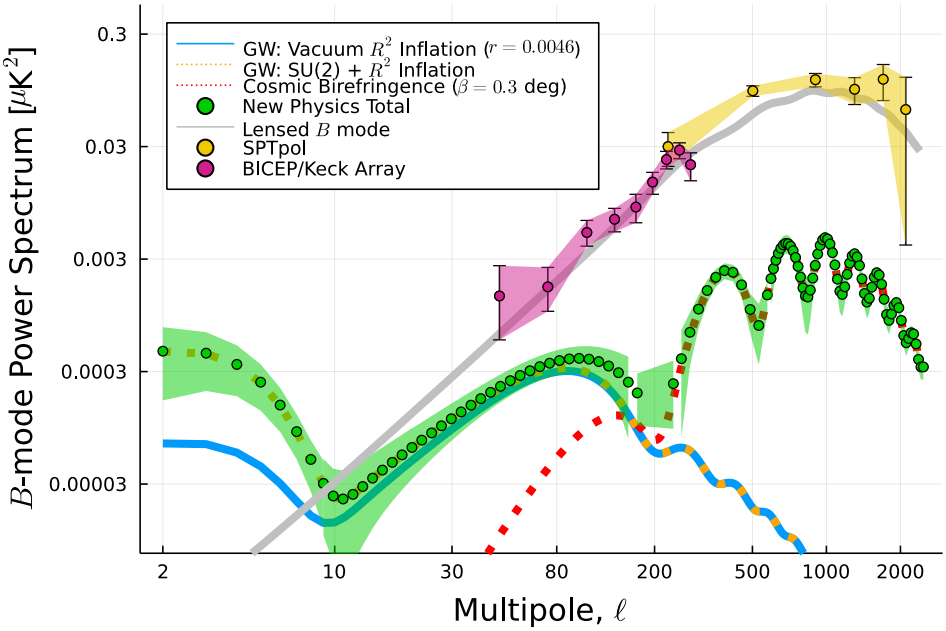

Figure 1.5: The B-mode polarization power spectra display $\ell(\ell+1)C_\ell^{BB}/2\pi$ in units of μK^2. Contributions include cosmic birefringence with $\beta = 0.3°$ (red dashed) and a sourced GW signal from SU(2) gauge fields combined with the vacuum contribution of R^2 inflation (orange dashed). The green filled circles represent the summed contributions, averaged over multipoles in bins centered at ℓ. The grey solid line corresponds to the lensed B-mode power spectrum, which is subtracted. The bands indicate 68% confidence intervals for full-sky, noiseless experiments (including the lensed B-mode contribution). The blue solid line shows the vacuum contribution alone. Source: [27].

An interesting aspect of polarization in CMB is the potential for parity violation. In a universe with perfect symmetry, the polarization pattern of the CMB should be symmetric under a mirror

transformation, i.e., no preferred direction for polarization. However, certain physical effects can break this symmetry, leading to the violation of parity. One such effect is cosmic birefringence (CB), which could arise if there is an interaction between photons and hypothetical particles (such as axions) in the early or late universe [28]. This interaction causes a rotation in the polarization of photons, distorting the observed E-mode and B-mode patterns. As a result, cosmic birefringence would produce cross-correlations between the temperature anisotropies, E-modes, and B-modes, i.e., non-zero TB, and EB correlations, making it detectable in the CMB data. This contribution is most prominent at $\ell \gtrsim 200$ [27].

Although there is no direct evidence for cosmic birefringence currently, recent measurements have placed tight constraints on its magnitude. Studies have reported values for the birefringence angle α with statistical significances ranging from $2.4\,\sigma$ to $3.6\,\sigma$, with results such as $\alpha = 0.35^\circ \pm 0.14^\circ$ [1], $\alpha = 0.30^\circ \pm 0.11^\circ$ [2], and $\alpha = 0.33^\circ\,^{+0.094^\circ}_{-0.091^\circ}$ [3, 4]. Although these results are exciting, a convincing detection has not yet been made. If a confirmed signal of cosmic birefringence, with a higher statistical significance achieved in future observations, this would open a fascinating window for physics beyond the standard model, as it would imply that the parity symmetry is violated, as well as contributing to the physics of dark matter and dark energy.

Ground-based experiments like the Simons Observatory and the CMB-S4 array, along with space missions like LiteBIRD, are designed to achieve the sensitivity required to detect these B-mode signals. The detection of B-modes would provide a groundbreaking test of inflation and offer insights into new physics beyond the ΛCDM model, potentially including cosmic birefringence.

Figure 1.6 shows the current measurements of the angular power spectrum for the temperature and polarization anisotropies in CMB. The projections shown in grey illustrate the anticipated improvements from CMB-S4, an upcoming ground-based experiment designed to enhance the precision of CMB measurements, especially in polarization modes.

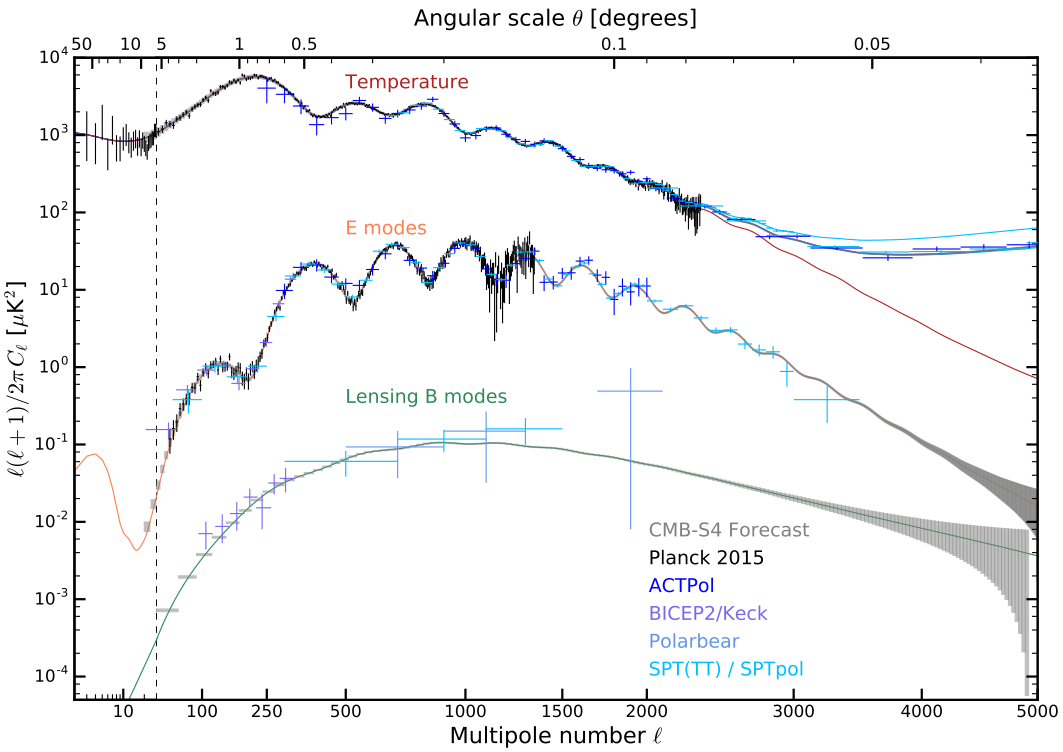

Figure 1.6: Current measurements of the angular power spectrum of the CMB temperature and polarization anisotropy are shown. The horizontal axis is scaled logarithmically in multipole ℓ for $\ell < 30$ (left of the vertical dashed line) and as $\ell^{0.6}$ at higher multipoles. Best-fit models of residual foregrounds combined with primary CMB anisotropy power for TT datasets are also plotted. To illustrate expected advancements with CMB-S4, projections for a strawman instrumental configuration are shown in grey (binned with $\Delta\ell = 5$ for TT and EE spectra and $\Delta\ell = 30$ for BB) for a ΛCDM cosmological model with $r = 0$. [24]

2

Cosmic Birefringence

Cosmic birefringence refers to the rotation of the polarization plane of the CMB radiation as it propagates across the universe, potentially caused by a pseudoscalar field that could be linked to dark matter or dark energy. This effect, if present, leaves a distinct signature in the polarization field of CMB. We will first present the Stokes parameters, which provide a framework for describing the polarization of radiation. It will be followed by a discussion on how this pseudoscalar field could modify the Lagrangian of the electromagnetic sector with an extra term, the so-called Chern-Simons term, through the interaction between photons and axion-like particles. This additional term leads to a mixing between the Q and U Stokes parameters, causing a rotation of the polarization plane by an angle α. We will then derive the equations for how this rotation affects the observed temperature and polarization cross-power spectra, and discuss its potential observable consequences, which could provide a valuable understanding of the physics beyond the standard model.

Figure 2.1 illustrates a sketch of the cosmic birefringence effect as the a clockwise rotation of the plane of polarization of the CMB radiation on the sky, as observed on Earth.

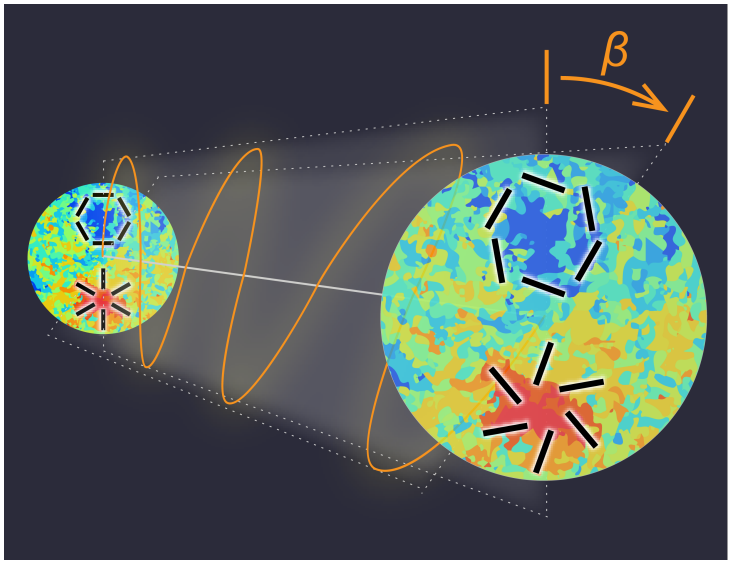

Figure 2.1: Rotation of linear polarization by cosmic birefringence. Polarization pattern at the surface of last scattering (black lines inside the left circle) changes when the plane of linear polarization (orange line) rotates by an angle β as CMB photons travel to reach us today (right circle). Source: [27]. Credit: Y. Minami.

2.1 Stokes Parameters

The polarization of radiation is often described using the Stokes parameters Q, U, and V. Let us consider a (quasi)monochromatic electromagnetic wave with a frequency ω_0 traveling along the z-direction where the amplitudes and phases vary slowly over time relative to the wave's inverse frequency. The electric field at a given location in space can be represented by its components [20]:

$$E_x = a_x(t)\cos[\omega_0 t - \theta_x(t)]\,, \tag{2.1}$$

$$E_y = a_y(t)\cos[\omega_0 t - \theta_y(t)]\,. \tag{2.2}$$

The Stokes parameters quantify this polarization and are calculated as time-averaged values based on the electric field components.

$$I = \langle a_x^2 \rangle + \left\langle a_y^2 \right\rangle\,, \tag{2.3}$$

$$Q = \langle a_x^2 \rangle - \left\langle a_y^2 \right\rangle\,, \tag{2.4}$$

$$U = \left\langle 2a_x a_y \cos(\theta_x - \theta_y) \right\rangle\,, \tag{2.5}$$

$$V = \left\langle 2a_x a_y \sin(\theta_x - \theta_y) \right\rangle\,. \tag{2.6}$$

where I represents the total intensity of the wave, combining the contributions from both the x- and y-polarized components. Q and U describe linear polarization, with Q indicating the intensity difference between horizontal and vertical polarization, and U corresponding to the intensity difference between polarized components oriented at 45° angles. When the x and y-components of the field oscillate in phase (or anti-phase), the polarization ellipse degenerates into a line. We say that the wave is linearly polarized. V characterizes circular polarization, measuring the difference in intensity between left- and right-handed circularly polarized light. For unpolarized radiation, $Q = U = V = 0$. The Stokes parameter V is expected to be zero for the CMB radiation because the processes generating CMB, such as Thomson scattering, do not produce circular polarization (see, however, e.g [29] and other references therein). As a result, V is generally considered negligible in CMB studies under standard assumptions, and is not considered further.

From Eqs. 2.4 and 2.5, we can show that a rotation of the coordinate system by an angle α transforms the Stokes parameters describing the same radiation field as:

$$Q' = Q\cos(2\alpha) + U\sin(2\alpha)\,, \tag{2.7}$$

$$U' = -Q\sin(2\alpha) + U\cos(2\alpha)\,. \tag{2.8}$$

This rotational behavior of the Stokes parameters forms the basis for describing linear polarization in terms of its amplitude, P, and position angle, ψ. The relationship $Q \pm iU = Pe^{\pm 2i\psi}$ shows that polarization transforms like a spin-2 field. According to the International Astronomical Union (IAU) definition, $\psi > 0$ corresponds to a counter-clockwise rotation of the polarization plane on the sky. In contrast, the CMB community often adopts a right-handed coordinate system, where the z-axis aligns with the observer's line of sight, resulting in an opposite sign convention for U and the position angle. Therefore, we define the position angle (PA) $\alpha = -\psi$, where $\alpha > 0$ indicates a clockwise rotation on the sky and $Q \pm iU = Pe^{\pm 2i\alpha} = Pe^{\mp 2i\psi}$.

2.2 A Pseudoscalar Field

In this section, we will discuss the possible existence of a psuedoscalar field, χ, which changes sign when the spatial coordinates are inverted, using some of the results from [27, 28, 30]. This pseudoscalar field could be linked to a hypothetical, axionlike particle that affects the polarization of the CMB radiation in a parity-violating way if coupled to the electromangetic field, through its journey from the last scattering surface to the present day. Furthermore, we can relate this field to dark matter (see [31, 32, 33]) or dark energy (see [27], and [34, 35, 36, 37]), depending on its dynamics.

The FLRW spacetime metric in Eq. 1.8 for a spatially flat universe ($k = 0$) in Cartesian coordinates, simplifies to:

$$ds^2 = -c^2dt^2 + a(t)^2(dx^2 + dy^2 + dz^2)\,. \tag{2.9}$$

Introducing the conformal time η, defined by:

$$\eta = \int \frac{dt}{a(t)}, \quad dt = a(t)d\eta\,, \tag{2.10}$$

the metric becomes:

$$ds^2 = a^2(\eta)\left(-c^2d\eta^2 + dx^2 + dy^2 + dz^2\right)\,. \tag{2.11}$$

This can be expressed in terms of the metric tensor:

$$ds^2 = \sum_{\mu\nu} g_{\mu\nu}dx^\mu dx^\nu\,, \tag{2.12}$$

with the metric tensor given by:

$$g_{\mu\nu} = a^2(\eta)\mathrm{diag}(-1, 1, 1, 1)\,, \tag{2.13}$$

where μ, ν run over $(0, 1, 2, 3)$, corresponding to η, x, y, z ($c \equiv 1$ in natural units).

We can write the action and the Lagrangian density for a free electromagnetic field as [27]:

$$I_{EM} = \int d^4x\sqrt{-g}\mathcal{L}_{EM}\,, \tag{2.14}$$

$$\mathcal{L}_{EM} = -\frac{1}{4}\sum_{\mu\nu} F_{\mu\nu}F^{\mu\nu}\,, \tag{2.15}$$

where $F_{\mu\nu} \equiv \partial A_\nu/\partial x^\mu - \partial A_\mu/\partial x^\nu$ is the antisymmetric electromagnetic tensor defined in terms of the electromagnetic four-potential A_μ and g is the determinant of $g_{\mu\nu}$.

The equation of motion for $\mathbf{A}$ with gauge conditions $A_0 = 0$ and $\nabla \cdot \mathbf{A} = 0$ is given by:

$$\mathbf{A}'' - \nabla^2\mathbf{A} = 0\,, \tag{2.16}$$

where $\nabla \equiv \partial/\partial x$ and the prime denotes $\partial/\partial\eta$. We can write the equation of motion for $\pm$ helicity states:

$$A''_{\pm} + k^2 A_{\pm} = 0\,, \tag{2.17}$$

where k is comoving wavenumber.

A pseudoscalar field, χ, can couple to the electromagnetic field through a Chern-Simons term. In this scenario, the standard Maxwell Lagrangian density is modified with an extra term [30, 27]:

$$\mathcal{L} = \mathcal{L}_{EM} + \mathcal{L}_{CS}\,, \tag{2.18}$$

where

$$\mathcal{L}_{CS} = -\frac{\alpha_{em}}{4f}\chi F\tilde{F}, \tag{2.19}$$

and

$$F\tilde{F} \equiv \sum_{\mu\nu} F_{\mu\nu} \sum_{\mu'\nu'} \frac{\varepsilon^{\mu\nu\mu'\nu'}}{2\sqrt{-g}} F_{\mu'\nu'}\,. \tag{2.20}$$

Here, α_{em} is a dimensionless coupling constant, f is a characteristic energy scale, often called the "decay constant", with the dimension of energy, and $\varepsilon^{\mu\nu\mu'\nu'}$ is the Levi-Civita symbol, fully antisymmetric with $\varepsilon^{0123} = 1$. α_{em}/f can be considered as a free parameter, linked to the properties of dark matter or dark energy. Its value can be constrained using observational data, such as the CMB polarization.

The parity violation arises because $F\tilde{F} = -4\mathbf{B}\cdot\mathbf{E}$, where $\mathbf{E}$ (electric field vector) has odd parity and $\mathbf{B}$ (magnetic field vector) has even parity ($\mathbf{E}$ and $\mathbf{B}$ should not be confused with E and B polarization modes). Consequently, $F\tilde{F}$ changes sign under spatial inversion. For the interaction term $\chi F\tilde{F}$ to remain invariant, the field χ must be pseudoscalar.

From Eq. 2.19, it is evident that when χ is constant, the term $\chi F\tilde{F}$ does not contribute to the equation of motion since $F\tilde{F}$ is a total derivative. The Chern-Simons term can only affect the dynamics, if the field χ varies in spacetime, meaning that the derivative of the pseudoscalar field, χ', is non-zero, resulting in violation of parity. If χ is constant, then $\chi' = 0$, and the contribution of the $\chi F\tilde{F}$ term vanishes. This results in no parity-violating effect.

The equation of motion for modified **A** is now given by:

$$\mathbf{A}'' - \nabla^2 \mathbf{A} - (\frac{\alpha_{em}\chi'}{f})\nabla \times \mathbf{A} = 0\,. \tag{2.21}$$

The coupling modifies the wave's dispersion relation, which defines the connection between its frequency ω and wavenumber k. This modification causes the relation to depend on the wave's helicity, distinguishing between the two polarization states:

$$A''_{\pm} + \left(k^2 \mp \frac{k\alpha_{em}\chi'}{f}\right) A_{\pm} = 0\,. \tag{2.22}$$

When the effective angular frequency, $\omega_{\pm}^2 \equiv k^2 \mp k\alpha_{em}\chi'/f$, changes slowly over time during a single oscillation period, such that $|\omega'_{\pm}|/\omega_{\pm}^2 \ll 1$, the WKB approximation gives the solution, as shown in [27]:

$$A_{\pm} \simeq (2\omega_{\pm})^{-1/2} e^{-i\int d\eta\, \omega_{\pm} + i\delta_{\pm}}\,, \tag{2.23}$$

where $\delta_{\pm}$ is the initial phase for the $\pm$ states. The phase velocity, describing how the wave propagates, is approximately:

$$\frac{\omega_{\pm}}{k} \simeq 1 \mp \frac{\alpha_{em}\chi'}{2kf}\,. \tag{2.24}$$

where the correction term is extremely small. The ratio of the photon wavelength to the size of the observable universe gives a measure of how small the correction is. Despite the smallness of this correction term, the effect becomes important over the long period of time, more than 13 billion years, for the CMB radiation, meaning that the difference $\int d\eta(\omega_+ - \omega_-)$ becomes large enough to be detected in the CMB data. This integral represents the total accumulated difference in frequencies $(\omega_+ - \omega_-)$ (which are time dependent) over this long time. As a result, the difference in the phase velocity causes the plane of linear polarization to rotate (see [27] and other ref.s therein). We can now define the birefringence angle, α as:

$$\alpha = \frac{1}{2}\left(\delta_+ - \delta_-\right) - \frac{1}{2}\int d\eta\,(\omega_+ - \omega_-)\,. \tag{2.25}$$

For simplicity, we assume the initial rotation angle at the last scattering surface $\delta_+ - \delta_- = 0$. From

Eq. 2.24, the isotropic birefringence angle, α becomes:

$$\alpha = \frac{\alpha_{em}}{2f} \int_{\eta_{LS}}^{\eta_0} d\eta \chi' \,, \tag{2.26}$$

where η_{LS} and η_0 correspond to the conformal times at the last scattering surface and the present epoch, respectively. The varying nature of χ introduces a rotation of the polarization plane of the CMB photons as they propagate across the universe, which results in a mixing between Q and U Stokes parameters.

Although the standard treatment of CB is based on the isotropic birefringence, it is also important to consider the possibility of anisotropic birefringence, where the rotation angle can be expressed as the sum of isotropic and anisotropic components. Ref.s [38, 39, 34, 40] provide a detailed treatment of these models. The anisotropic birefringence angle in these models depends on the direction of the photon. This effect may arise when considering fluctuations in the scalar field. During this thesis, we will always consider a homogeneous field $\chi = \chi(\eta)$ sourcing isotropic birefringence.

2.3 The Impact of Cosmic Birefringence on CMB Spectra

In this section, we assume that the rotation angle α characterizes the rotation of the CMB polarization spectra due to a birefringence effect. This angle represents the amount of rotation of the E-mode and B-mode polarization components compared to their primordial (unrotated) form. This rotation mixes the E-mode and B-mode spectra, modifying the observed CMB power spectra.

Observed Stokes Parameters with the modification of the Chern-Simons term is given by [28]:

$$(Q \pm iU)^o = \exp\left(\pm i2\alpha\right)(Q \pm iU) \,. \tag{2.27}$$

Here, the superscript "o" indicates the observed Stokes parameters, while Q and U without the superscript represent the intrinsic (unrotated) Stokes parameters.

In a spatially flat universe, we perform multiple expansions for temperature and polarization anisotropies in terms of spin-weighted spherical harmonic functions for describing the CMB fluctuations across the sky [28, 38, 20, 18]:

$$T(\hat{n}) = \sum_{lm} a_{T,lm} Y_{lm}(\hat{n}) \tag{2.28}$$

$$(Q \pm iU)(\hat{n}) = \sum_{lm} a_{\pm 2,lm\pm 2} Y_{lm}(\hat{n}) \tag{2.29}$$

Here, the term ${}_{\pm 2}Y_{lm}$ refers to the spin-weighted spherical harmonics with spin-weight ± 2 for the two polarization states. The expressions for the expansion coefficients are given as:

$$a_{T,lm} = \int d\Omega \; Y^*_{lm}(\hat{n}) T(\hat{n}) \,, \tag{2.30}$$

$$a_{\pm 2,lm} = \int d\Omega \; {}_{\pm 2}Y^*_{lm}(\hat{n}) (Q \pm iU)(\hat{n}) \,. \tag{2.31}$$

We can introduce the linear combinations of $a_{2,lm}$ and $a_{-2,lm}$ to define the polarization E- and B-mode harmonic coefficients:

$$a_{E,lm} = -(a_{2,lm} + a_{-2,lm})/2 \,, \tag{2.32}$$

$$a_{B,lm} = i(a_{2,lm} - a_{-2,lm})/2 \,. \tag{2.33}$$

For a real field X, we can write [20]:

$$Y^*_{lm} = Y_{l-m}(-1)^{-m} \,, \tag{2.34}$$

so that;

$$a^{X*}_{lm} = a^X_{l-m}(-1)^{-m} \,, \tag{2.35}$$

Utilizing Eq. 1.6, we can rewrite the two-point function of the expansion coefficients by the following relation:

$$\langle a^X_{lm} (a^Y_{l'm'})^* \rangle = \delta_{ll'} \delta_{mm'} C^{XY}_l \,, \tag{2.36}$$

where X and Y stand for T (temperature), E-mode polarization, and B-mode polarization and the power spectra are defined as:

$$C^{XY}_l = \frac{1}{2l+1} \sum_{l=-m}^{m} a^X_{lm} (a^Y_{lm})^* \,. \tag{2.37}$$

The expansion coefficients after the rotation in Eq. 2.27 can be written as:

$$a^o_{\pm 2,lm} = \int d\Omega_{\pm 2} Y^*_{lm}(\hat{n}) (Q \pm iU)^o(\hat{n}) \tag{2.38}$$

$$= \int d\Omega \; {}_{\pm 2}Y^*_{lm}(\hat{n}) \exp\left(\pm i2\alpha\right)(Q \pm iU)(\hat{n}) \,, \tag{2.39}$$

and $a_{T,lm}$ remains unchanged.

The following equations show how the primordial power spectra are transformed by this rotation, leading to the observed spectra:

$$a^{T,o}_{lm} = a^{T}_{lm} + a^{nT}_{lm} \,, \tag{2.40}$$
$$a^{E,o}_{lm} = a^{E}_{lm} \cos 2\alpha - a^{B}_{lm} \sin 2\alpha + a^{nE}_{lm} \,, \tag{2.41}$$
$$a^{B,o}_{lm} = a^{B}_{lm} \cos 2\alpha + a^{E}_{lm} \sin 2\alpha + a^{nB}_{lm} \,. \tag{2.42}$$

Here, $a^{T}_{lm}, a^{E}_{lm}, a^{B}_{lm}$ without the superscript "o" represent the primordial signal components, and $a^{nT}_{lm}, a^{nE}_{lm}, a^{nB}_{lm}$ denote the corresponding instrumental noise.

In the ideal case where noise is absent from the calculation, the observed spectra takes the form of:

$$\begin{aligned}
C^{EB,o}_{l} &= \frac{1}{2l+1} \sum_{l=-m}^{m} a^{E,o}_{lm} (a^{B,o}_{lm})^* \\
&= \frac{1}{2l+1} \sum_{l=-m}^{m} \left[(a^{E}_{lm} \cos 2\alpha - a^{B}_{lm} \sin 2\alpha)(a^{B^*}_{lm} \cos 2\alpha + a^{E^*}_{lm} \sin 2\alpha) \right] \\
&= \frac{1}{2l+1} \sum_{l=-m}^{m} \left[a^{E}_{lm} a^{B^*}_{lm} \cos^2 2\alpha + a^{E}_{lm} a^{E^*}_{lm} \cos 2\alpha \sin 2\alpha - a^{B}_{lm} a^{B^*}_{lm} \cos 2\alpha \sin 2\alpha - a^{B}_{lm} a^{E^*}_{lm} \sin^2 2\alpha \right] \\
&= C^{EB}_{l} \cos^2 2\alpha + C^{EE}_{l} \cos 2\alpha \sin 2\alpha - C^{BB}_{l} \cos 2\alpha \sin 2\alpha + C^{EB}_{l} \sin^2 2\alpha \\
&= C^{EB}_{l} (\cos^2 2\alpha - \sin^2 2\alpha) + (C^{EE}_{l} - C^{BB}_{l}) \cos 2\alpha \sin 2\alpha \\
&= C^{EB}_{l} \cos 4\alpha + \frac{1}{2} (C^{EE}_{l} - C^{BB}_{l}) \sin 4\alpha \,,
\end{aligned} \tag{2.43}$$

$$\begin{aligned}
C^{EE,o}_{l} &= \frac{1}{2l+1} \sum_{l=-m}^{m} a^{E,o}_{lm} (a^{E,o}_{lm})^* \\
&= \frac{1}{2l+1} \sum_{l=-m}^{m} \left[(a^{E}_{lm} \cos 2\alpha - a^{B}_{lm} \sin 2\alpha)(a^{E^*}_{lm} \cos 2\alpha - a^{B^*}_{lm} \sin 2\alpha) \right] \\
&= \frac{1}{2l+1} \sum_{l=-m}^{m} \left[a^{E}_{lm} a^{E^*}_{lm} \cos^2 2\alpha - a^{E}_{lm} a^{B^*}_{lm} \cos 2\alpha \sin 2\alpha - a^{B}_{lm} a^{E^*}_{lm} \cos 2\alpha \sin 2\alpha + a^{B}_{lm} a^{B^*}_{lm} \sin^2 2\alpha \right] \\
&= C^{EE}_{l} \cos^2 2\alpha - C^{EB}_{l} \cos 2\alpha \sin 2\alpha - C^{EB}_{l} \cos 2\alpha \sin 2\beta + C^{BB}_{l} \sin^2 2\alpha
\end{aligned}$$

$$= C_l^{EE}\cos^2 2\alpha + C_l^{BB}\sin^2 2\alpha - 2C_l^{EB}\cos 2\alpha \sin 2\alpha\,, \tag{2.44}$$

$$\begin{aligned}
C_l^{BB,o} &= \frac{1}{2l+1}\sum_{l=-m}^{m} a_{lm}^{B,o}(a_{lm}^{B,o})^* \\
&= \frac{1}{2l+1}\sum_{l=-m}^{m} \left[(a_{lm}^{B}\cos 2\alpha + a_{lm}^{E}\sin 2\alpha)(a_{lm}^{B^*}\cos 2\alpha + a_{lm}^{E^*}\sin 2\alpha)\right] \\
&= \frac{1}{2l+1}\sum_{l=-m}^{m} \left[a_{lm}^{B}a_{lm}^{B^*}\cos^2 2\alpha + a_{lm}^{E}a_{lm}^{B^*}\cos 2\alpha\sin 2\alpha + a_{lm}^{B}a_{lm}^{E^*}\cos 2\alpha\sin 2\alpha + a_{lm}^{E}a_{lm}^{E^*}\sin^2 2\alpha\right] \\
&= C_l^{BB}\cos^2 2\alpha + C_l^{EB}\cos 2\alpha\sin 2\alpha + C_l^{EB}\cos 2\alpha\sin 2\beta + C_l^{EE}\sin^2 2\alpha \\
&= C_l^{BB}\cos^2 2\alpha + C_l^{EE}\sin^2 2\alpha + 2C_l^{EB}\cos 2\alpha\sin 2\alpha\,,
\end{aligned} \tag{2.45}$$

$$\begin{aligned}
C_l^{EE,o} - C_l^{BB,o} &= C_l^{EE}\cos^2 2\alpha + C_l^{BB}\sin^2 2\alpha - 2C_l^{EB}\cos 2\alpha\sin 2\alpha - C_l^{BB}\cos^2 2\alpha - C_l^{EE}\sin^2 2\alpha \\
&\quad - 2C_l^{EB}\cos 2\alpha\sin 2\alpha \\
&= (C_l^{EE} - C_l^{BB})\cos^2 2\alpha - (C_l^{EE} - C_l^{BB})\sin^2 2\alpha - 4C_l^{EB}\sin 2\alpha\cos 2\alpha \\
&= (C_l^{EE} - C_l^{BB})(\cos^2 2\alpha - \sin^2 2\alpha) - 4C_l^{EB}\sin 2\alpha\cos 2\alpha \\
&= (C_l^{EE} - C_l^{BB})\cos 4\alpha - 2C_l^{EB}\sin 4\alpha
\end{aligned}$$

$$\frac{1}{2}(C_l^{EE,o} - C_l^{BB,o}) = \frac{1}{2}(C_l^{EE} - C_l^{BB})\cos 4\alpha - C_l^{EB}\sin 4\alpha\,, \tag{2.46}$$

$$\begin{aligned}
C_l^{TB,o} &= \frac{1}{2l+1}\sum_{l=-m}^{m} a_{lm}^{T,o}(a_{lm}^{B,o})^* \\
&= \frac{1}{2l+1}\sum_{l=-m}^{m} \left[(a_{lm}^{T}(a_{lm}^{B^*}\cos 2\alpha + a_{lm}^{E^*}\sin 2\alpha)\right] \\
&= \frac{1}{2l+1}\sum_{l=-m}^{m} \left[a_{lm}^{T}a_{lm}^{B^*}\cos 2\alpha + a_{lm}^{T}a_{lm}^{E^*}\sin 2\alpha\right] \\
&= C_l^{TB}\cos 2\alpha + C_l^{TE}\sin 2\alpha\,,
\end{aligned} \tag{2.47}$$

$$
\begin{aligned}
C_l^{TE,o} &= \frac{1}{2l+1}\sum_{l=-m}^{m} a_{lm}^{T,o}(a_{lm}^{E,o})^* \\
&= \frac{1}{2l+1}\sum_{l=-m}^{m} \left[(a_{lm}^{T}(a_{lm}^{E^*}\cos 2\alpha - a_{lm}^{B^*}\sin 2\alpha)\right] \\
&= \frac{1}{2l+1}\sum_{l=-m}^{m} \left[a_{lm}^{T}a_{lm}^{E^*}\cos 2\alpha - a_{lm}^{T}a_{lm}^{B^*}\sin 2\alpha\right] \\
&= C_l^{TE}\cos 2\alpha - C_l^{TB}\sin 2\alpha\,. \qquad (2.48)
\end{aligned}
$$

The equations above provide the foundation for constructing the statistical estimators aimed at measuring the cosmic birefringence angle α, as discussed in the next chapter.

3
D-estimators

3.1 Definition and Main Properties

In this chapter, we introduce the D-estimators, which are harmonic-based estimators derived from the observed CMB spectra. These estimators will be used to estimate the true birefringence angle α, which is used to characterize the rotation of the CMB polarization spectra caused by a potential birefringence effect. Here, the parameter β, referred to as the estimator angle, is the quantity we aim to determine from our analysis. It serves as an estimation of the true birefringence angle α. The *D*-estimators are defined in terms of the observed power spectra as follows [41, 42]:

$$D_l^{EB,o}(\beta) = C_l^{EB,o}\cos 4\beta - \frac{1}{2}(C_l^{EE,o} - C_l^{BB,o})\sin 4\beta\,, \tag{3.1}$$

$$D_l^{TB,o}(\beta) = C_l^{TB,o}\cos 2\beta - C_l^{TE,o}\sin 2\beta\,, \tag{3.2}$$

where $C_l^{EB,o}$ and $C_l^{TB,o}$ are defined in Eq.s 2.43 and 2.47. Taking the ensemble average of Eq.s 3.1 and 3.2:

$$\langle D_l^{EB,o}(\beta)\rangle = \langle C_l^{EB,o}\rangle\cos 4\beta - \frac{1}{2}(\langle C_l^{EE,o}\rangle - \langle C_l^{BB,o}\rangle\sin 4\beta, \tag{3.3}$$

$$\langle D_l^{TB,o}(\beta)\rangle = \langle C_l^{TB,o}\rangle\cos 2\beta - \langle C_l^{TE,o}\rangle\sin 2\beta\,. \tag{3.4}$$

From now on, $D_l^{EB}(\beta)$ and $D_l^{TB}(\beta)$ will be denoted simply as D_l^{EB} and D_l^{TB}, along with their ensemble averages. Equations 3.3 and 3.4 are related to the primordial (unrotated) spectra in given way:

$$\begin{aligned}
\langle D_l^{EB,o}\rangle &= \langle C_l^{EB,o}\rangle \cos 4\beta - \frac{1}{2}\left(\langle C_l^{EE,o}\rangle - \langle C_l^{BB,o}\rangle\right)\sin 4\beta \\
&= \langle C_l^{EB}\rangle \cos 4\alpha \cos 4\beta + \frac{1}{2}\left(\langle C_l^{EE}\rangle - \langle C_l^{BB}\rangle\right)\sin 4\alpha \cos 4\beta \\
&- \frac{1}{2}\left(\langle C_l^{EE}\rangle - \langle C_l^{BB}\rangle\right)\cos 4\alpha \sin 4\beta + \langle C_l^{EB}\rangle \sin 4\alpha \sin 4\beta \\
&= \langle C_l^{EB}\rangle(\cos 4\alpha \cos 4\beta + \sin 4\alpha \sin 4\beta) + \frac{1}{2}\left(\langle C_l^{EE}\rangle - \langle C_l^{BB}\rangle\right)(\sin 4\alpha \cos 4\beta - \cos 4\alpha \sin 4\beta) \\
&= \langle C_l^{EB}\rangle \cos 4(\alpha-\beta) + \frac{1}{2}\left(\langle C_l^{EE}\rangle - \langle C_l^{BB}\rangle\right)\sin 4(\alpha-\beta)
\end{aligned}$$

where we used the following trigonometric identities (with $A = 4\alpha$ and $B = 4\beta$):

$$\begin{aligned}
&\cos A \cos B + \sin A \sin B = \cos(A-B)\,, \\
&\sin A \cos B - \cos A \sin B = \sin(A-B)\,.
\end{aligned}$$

Let us consider the scenario at the last scattering surface where the primordial $C_l^{EB} = 0$. This choice implies the absence of parity-violating physics at the last scattering surface, consistent with the standard cosmological model, which assumes no mechanisms breaking mirror symmetry in the early universe.

$$\Rightarrow \langle D_l^{EB,o}\rangle = \frac{1}{2}\left(\langle C_l^{EE}\rangle - \langle C_l^{BB}\rangle\right)\sin 4(\alpha-\beta)\,, \tag{3.5}$$

$$\begin{aligned}
\langle D_l^{TB,o}\rangle &= \langle C_l^{TB,o}\rangle \cos 2\beta - \langle C_l^{TE,o}\rangle \sin 2\beta \\
&= \langle C_l^{TB}\rangle \cos 2\beta \cos 2\alpha + \langle C_l^{TE}\rangle \cos 2\beta \sin 2\alpha - \langle C_l^{TE}\rangle \sin 2\beta \cos 2\alpha + \langle C_l^{TB}\rangle \sin 2\beta \sin 2\alpha \\
&= \langle C_l^{TB}\rangle(\cos 2\beta \cos 2\alpha + \sin 2\beta \sin 2\alpha) + \langle C_l^{TE}\rangle(\cos 2\beta \sin 2\alpha - \sin 2\beta \cos 2\alpha) \\
&= \langle C_l^{TB}\rangle \cos 2(\alpha-\beta) + \langle C_l^{TE}\rangle \sin 2(\alpha-\beta)\,.
\end{aligned}$$

At the last scattering surface, we similarly assume that $C_l^{TB} = 0$, again reflecting the assumption of no parity-violating interactions influencing the CMB. Under this condition:

$$\Rightarrow \langle D_l^{TB,o}\rangle = \langle C_l^{TE}\rangle \sin 2(\alpha-\beta)\,. \tag{3.6}$$

Equations 3.5 and 3.6 imply that the estimators D_l^{EB} and D_l^{TB} provide information about the birefringence angle through the rotation of the primordial CMB spectra. These estimators work because, in nature, $C_l^{EE} \neq C_l^{BB}$ and $C_l^{TE} \neq 0$, allowing for the detection of any non-zero rotation angle β.

However, if $C_l^{EE} = C_l^{BB}$, the estimator D_l^{EB} would not be useful for estimating the birefringence angle, as its expected value would be zero even if $\beta \neq 0$. Similarly, for D_l^{TB}, if $C_l^{TE} = 0$, this estimator would also lose its effectiveness in providing information about β. Thus, the natural asymmetries in the CMB spectra make these estimators effective tools for detecting rotation effects.

To estimate the birefringence angle α, we need to analyze the behavior of certain polarization spectra correlations, particularly the D_l^{EB} and D_l^{TB} estimators, and the covariances associated with these correlations. This involves computing expectation values and covariances for these estimators to assess how well they can detect a non-zero rotation angle.

The role of the covariances is particularly important because they determine the statistical uncertainty of the estimators, which affects the precision of the estimation of α. In this analysis, we focus on the case where $\beta = \alpha$, aligning the estimator angle β with the true birefringence angle α. Computing the covariances under this assumption allows us to evaluate the effectiveness of the estimators in inferring the actual physical rotation, assuming such a rotation is present in the universe. This approach lays the groundwork for estimating α in later sections, once the necessary covariances have been derived.

3.2 Characterization of the D_l^{EB}-Estimator

In this section, we focus on the characterization of the D_l^{EB}-estimator, which is used to estimate the angle β based on the cross-correlation between the E-mode and B-mode polarization spectra. We begin by examining the expectation value of this estimator and its covariance structure in order to evaluate the estimator's performance and uncertainty. This analysis provides a detailed understanding of the behavior of the D_l^{EB}-estimator, which will be important later for combining EB and TB correlations in the joint estimator.

3.2.1 Covariance of C_l^{EB}

In order to compute the covariance, first we need to show:

$$\left\langle (D_l^{EB,o} - \langle D_l^{EB,o} \rangle)(D_{l'}^{EB,o} - \langle D_{l'}^{EB,o} \rangle) \right\rangle = \left\langle D_l^{EB,o} D_{l'}^{EB,o} - D_l^{EB,o} \langle D_{l'}^{EB,o} \rangle - D_{l'}^{EB,o} \langle D_l^{EB,o} \rangle + \langle D_l^{EB,o} \rangle \langle D_{l'}^{EB,o} \rangle \right\rangle .$$

Using the linearity of the expectation:

$$\begin{aligned}\left\langle (D_l^{EB,o} - \langle D_l^{EB,o}\rangle)(D_{l'}^{EB,o} - \langle D_{l'}^{EB,o}\rangle)\right\rangle &= \langle D_l^{EB,o} D_{l'}^{EB,o}\rangle - \langle D_l^{EB,o}\rangle\langle D_{l'}^{EB,o}\rangle - \langle D_{l'}^{EB,o}\rangle\langle D_l^{EB,o}\rangle + \langle D_{l'}^{EB,o}\rangle\langle D_l^{EB,o}\rangle \\ &= \langle D_l^{EB,o} D_{l'}^{EB,o}\rangle - \langle D_l^{EB,o}\rangle\langle D_{l'}^{EB,o}\rangle\,.\end{aligned}$$

Using Eq. 3.1, we can write:

$$\begin{aligned}\langle D_l^{EB,o} D_{l'}^{EB,o}\rangle &= \left\langle \left[C_l^{EB,o}\cos 4\beta - \frac{1}{2}(C_l^{EE,o} - C_l^{BB,o})\sin 4\beta\right]\right. \\ &\quad \left.\cdot \left[C_{l'}^{EB,o}\cos 4\beta - \frac{1}{2}(C_{l'}^{EE,o} - C_{l'}^{BB,o})\sin 4\beta\right]\right\rangle \\ &= \langle C_l^{EB,o} C_{l'}^{EB,o}\rangle\cos^2 4\beta - \langle C_l^{EB,o}\frac{1}{2}(C_{l'}^{EE,o} - C_{l'}^{BB,o})\rangle\cos 4\beta\sin 4\beta \\ &\quad - \langle\frac{1}{2}(C_l^{EE,o} - C_l^{BB,o})C_{l'}^{EB,o}\rangle\sin 4\beta\cos 4\beta + \langle\frac{1}{2}(C_l^{EE,o} - C_l^{BB,o})\frac{1}{2}(C_{l'}^{EE,o} - C_{l'}^{BB,o})\rangle\sin^2 4\beta\,.\end{aligned}$$

To compute $\langle D_l^{EB,o} D_{l'}^{EB,o}\rangle$, we must first evaluate the expectation values of each term, utilizing Equations 2.43, and 2.46:

$$\begin{aligned}1.\ \langle C_l^{EB,o} C_{l'}^{EB,o}\rangle\cos^2 4\beta &= \left\langle \left[C_l^{EB}\cos 4\alpha + \frac{1}{2}(C_l^{EE} - C_l^{BB})\sin 4\alpha\right]\right. \\ &\quad \left.\cdot \left[C_{l'}^{EB}\cos 4\alpha + \frac{1}{2}(C_{l'}^{EE} - C_{l'}^{BB})\sin 4\alpha\right]\right\rangle\cos^2 4\beta \\ &= \langle C_l^{EB} C_{l'}^{EB}\rangle\cos^2 4\alpha\cos^2 4\beta \\ &\quad + \langle C_l^{EB}\frac{1}{2}(C_{l'}^{EE} - C_{l'}^{BB})\rangle\cos 4\alpha\sin 4\alpha\cos^2 4\beta \\ &\quad + \langle\frac{1}{2}(C_l^{EE} - C_l^{BB})C_{l'}^{EB}\rangle\cos 4\alpha\sin 4\alpha\cos^2 4\beta \\ &\quad + \langle\frac{1}{2}(C_l^{EE} - C_l^{BB})\frac{1}{2}(C_{l'}^{EE} - C_{l'}^{BB})\rangle\sin^2 4\alpha\cos^2 4\beta\end{aligned}$$

$$\begin{aligned}2.\ \langle C_l^{EB,o}\frac{1}{2}(C_{l'}^{EE,o} - C_{l'}^{BB,o})\rangle\cos 4\beta\sin 4\beta &= \left\langle \left[C_l^{EB}\cos 4\alpha + \frac{1}{2}(C_l^{EE} - C_l^{BB})\sin 4\alpha\right]\right. \\ &\quad \left.\cdot \left[\frac{1}{2}(C_{l'}^{EE} - C_{l'}^{BB})\cos 4\alpha - C_{l'}^{EB}\sin 4\alpha\right]\right\rangle\cos 4\beta\sin 4\beta \\ &= \langle C_l^{EB}\frac{1}{2}(C_{l'}^{EE} - C_{l'}^{BB})\rangle\cos^2 4\alpha\cos 4\beta\sin 4\beta\end{aligned}$$

$$
\begin{aligned}
&- \langle C_l^{EB} C_{l'}^{EB} \rangle \cos 4\alpha \sin 4\alpha \cos 4\beta \sin 4\beta \\
&+ \langle \frac{1}{2}(C_l^{EE} - C_l^{BB}) \frac{1}{2}(C_{l'}^{EE} - C_{l'}^{BB}) \rangle \cos 4\alpha \sin 4\alpha \cos 4\beta \sin 4\beta \\
&- \langle \frac{1}{2}(C_l^{EE} - C_l^{BB}) C_{l'}^{EB} \rangle \sin^2 4\alpha \cos 4\beta \sin 4\beta
\end{aligned}
$$

$$
\begin{aligned}
3.\ \langle \frac{1}{2}(C_l^{EE,o} - C_l^{BB,o}) C_{l'}^{EB,o} \rangle \cos 4\beta \sin 4\beta &= \Big\langle \Big[\frac{1}{2}(C_l^{EE} - C_l^{BB}) \cos 4\alpha - C_l^{EB} \sin 4\alpha \Big] \\
&\cdot \Big[C_{l'}^{EB} \cos 4\alpha + \frac{1}{2}(C_{l'}^{EE} - C_{l'}^{BB}) \sin 4\alpha \Big] \Big\rangle \cos 4\beta \sin 4\beta \\
&= \langle \frac{1}{2}(C_l^{EE} - C_l^{BB}) C_{l'}^{EB} \rangle \cos^2 4\alpha \cos 4\beta \sin 4\beta \\
&+ \langle \frac{1}{2}(C_l^{EE} - C_l^{BB}) \frac{1}{2}(C_{l'}^{EE} - C_{l'}^{BB}) \rangle \cos 4\alpha \sin 4\alpha \cos 4\beta \sin 4\beta \\
&- \langle C_l^{EB} C_{l'}^{EB} \rangle \cos 4\alpha \sin 4\alpha \cos 4\beta \sin 4\beta \\
&- \langle C_l^{EB} \frac{1}{2}(C_{l'}^{EE} - C_{l'}^{BB}) \rangle \sin^2 4\alpha \cos 4\beta \sin 4\beta
\end{aligned}
$$

$$
\begin{aligned}
4.\ \langle \frac{1}{2}(C_l^{EE,o} - C_l^{BB,o}) \frac{1}{2}(C_{l'}^{EE,o} - C_{l'}^{BB,o}) \rangle \sin^2 4\beta &= \Big\langle \Big[\frac{1}{2}(C_l^{EE} - C_l^{BB}) \cos 4\alpha - C_l^{EB} \sin 4\alpha \Big] \\
&\cdot \Big[\frac{1}{2}(C_{l'}^{EE} - C_{l'}^{BB}) \cos 4\alpha - C_{l'}^{EB} \sin 4\alpha \Big] \Big\rangle \sin^2 4\beta \\
&= \langle \frac{1}{2}(C_l^{EE} - C_l^{BB}) \frac{1}{2}(C_{l'}^{EE} - C_{l'}^{BB}) \rangle \cos^2 4\alpha \sin^2 4\beta \\
&- \langle C_l^{EB} \frac{1}{2}(C_{l'}^{EE} - C_{l'}^{BB}) \rangle \cos 4\alpha \sin 4\alpha \sin^2 4\beta \\
&- \langle \frac{1}{2}(C_l^{EE} - C_l^{BB}) C_{l'}^{EB} \rangle \cos 4\alpha \sin 4\alpha \sin^2 4\beta \\
&+ \langle C_l^{EB} C_{l'}^{EB} \rangle \sin^2 4\alpha \sin^2 4\beta \,.
\end{aligned}
$$

Now, let us combine all the terms we have computed individually:

$$
\begin{aligned}
\langle D_l^{EB} D_{l'}^{EB} \rangle &= \langle C_l^{EB} C_{l'}^{EB} \rangle \cos^2 4\alpha \cos^2 4\beta \\
&+ \langle C_l^{EB} \frac{1}{2}(C_{l'}^{EE} - C_{l'}^{BB}) \rangle \cos 4\alpha \sin 4\alpha \cos^2 4\beta \\
&+ \langle \frac{1}{2}(C_l^{EE} - C_l^{BB}) C_{l'}^{EB} \rangle \cos 4\alpha \sin 4\alpha \cos^2 4\beta
\end{aligned}
$$

$$
\begin{aligned}
&+ \langle \frac{1}{2}(C_l^{EE} - C_l^{BB}) \frac{1}{2}(C_{l'}^{EE} - C_{l'}^{BB}) \rangle \sin^2 4\alpha \cos^2 4\beta \\
&- \langle C_l^{EB} \frac{1}{2}(C_{l'}^{EE} - C_{l'}^{BB}) \rangle \cos^2 4\alpha \sin 4\beta \cos 4\beta \\
&+ \langle C_l^{EB} C_{l'}^{EB} \rangle \cos 4\alpha \sin 4\alpha \cos 4\beta \sin 4\beta \\
&- \langle \frac{1}{2}(C_l^{EE} - C_l^{BB}) \frac{1}{2}(C_{l'}^{EE} - C_{l'}^{BB}) \rangle \cos 4\alpha \sin 4\alpha \cos 4\beta \sin 4\beta \\
&+ \langle \frac{1}{2}(C_l^{EE} - C_l^{BB}) C_{l'}^{EB} \rangle \sin^2 4\alpha \cos 4\beta \sin 4\beta \\
&- \langle \frac{1}{2}(C_l^{EE} - C_l^{BB}) C_{l'}^{EB} \rangle \cos^2 4\alpha \cos 4\beta \sin 4\beta \\
&- \langle \frac{1}{2}(C_l^{EE} - C_l^{BB}) \frac{1}{2}(C_{l'}^{EE} - C_{l'}^{BB}) \rangle \cos 4\alpha \sin 4\alpha \cos 4\beta \sin 4\beta \\
&+ \langle C_l^{EB} C_{l'}^{EB} \rangle \cos 4\alpha \sin 4\alpha \cos 4\beta \sin 4\beta \\
&+ \langle C_l^{EB} \frac{1}{2}(C_{l'}^{EE} - C_{l'}^{BB}) \rangle \sin^2 4\alpha \cos 4\beta \sin 4\beta \\
&+ \langle \frac{1}{2}(C_l^{EE} - C_l^{BB}) \frac{1}{2}(C_{l'}^{EE} - C_{l'}^{BB}) \rangle \cos^2 4\alpha \sin^2 4\beta \\
&- \langle C_l^{EB} \frac{1}{2}(C_{l'}^{EE} - C_{l'}^{BB}) \rangle \cos 4\alpha \sin 4\alpha \sin^2 4\beta \\
&- \langle \frac{1}{2}(C_l^{EE} - C_l^{BB}) C_{l'}^{EB} \rangle \cos 4\alpha \sin 4\alpha \sin^2 4\beta \\
&+ \langle C_l^{EB} C_{l'}^{EB} \rangle \sin^2 4\alpha \sin^2 4\beta \,.
\end{aligned}
$$

After modifying the trigonometric terms in the above expression using the previously introduced trigonometric identities for angle summation and subtraction, the expectation value of the D-estimators for the EB-EB case becomes:

$$
\begin{aligned}
\langle D_l^{EB} D_{l'}^{EB} \rangle = &\langle C_l^{EB} C_{l'}^{EB} \rangle \cos^2 4(\alpha - \beta) \\
&+ \langle C_l^{EB} \frac{1}{2}(C_{l'}^{EE} - C_{l'}^{BB}) \rangle \frac{1}{2} \sin 8(\alpha - \beta) \\
&+ \langle \frac{1}{2}(C_l^{EE} - C_l^{BB}) C_{l'}^{EB} \rangle \frac{1}{2} \sin 8(\alpha - \beta) \\
&+ \langle \frac{1}{2}(C_l^{EE} - C_l^{BB}) \frac{1}{2}(C_{l'}^{EE} - C_{l'}^{BB}) \rangle \sin^2 4(\alpha - \beta) \,. \qquad (3.7)
\end{aligned}
$$

Recalling Eq.s 3.7 and 3.5, we can rewrite the expression for the covariance:

$$\begin{aligned}\langle D_l^{EB,o} D_{l'}^{EB,o}\rangle - \langle D_l^{EB,o}\rangle\langle D_{l'}^{EB,o}\rangle = \langle C_l^{EB} C_{l'}^{EB}\rangle \cos^2 4(\alpha-\beta) \\ + \langle C_l^{EB}\frac{1}{2}(C_{l'}^{EE} - C_{l'}^{BB})\rangle \frac{1}{2}\sin 8(\alpha-\beta) \\ + \langle \frac{1}{2}(C_l^{EE} - C_l^{BB}) C_{l'}^{EB}\rangle \frac{1}{2}\sin 8(\alpha-\beta) \\ + \langle \frac{1}{2}(C_l^{EE} - C_l^{BB})\frac{1}{2}(C_{l'}^{EE} - C_{l'}^{BB})\rangle (\sin^2 4(\alpha-\beta)) \\ - \frac{1}{2}\left(\langle C_l^{EE}\rangle - \langle C_l^{BB}\rangle\right)\frac{1}{2}\left(\langle C_{l'}^{EE}\rangle - \langle C_{l'}^{BB}\rangle\right)\sin^2 4(\alpha-\beta)\,.\end{aligned}$$

Let us analyze the expectation of the each angular power spectra separately, for clarity, using Eq. 2.37:

1. $C_l^{EB} = \dfrac{1}{2l+1}\sum_{m=-l}^{l} a_{lm}^E (a_{lm}^B)^*\,,$

and

$$\begin{aligned}\langle C_l^{EB} C_{l'}^{EB}\rangle &= \frac{1}{2l+1}\frac{1}{2l'+1}\Big\langle \sum_{m=-l}^{l}\sum_{m'=-l'}^{l'} a_{lm}^E (a_{lm}^B)^* a_{l'm'}^E (a_{l'm'}^B)^*\Big\rangle \\ &= \frac{1}{2l+1}\frac{1}{2l'+1}\sum_{mm'}\langle a_{lm}^E (a_{lm}^B)^* a_{l'm'}^E (a_{l'm'}^B)^*\rangle\,.\end{aligned}$$

Applying the Wick's theorem;

$$\begin{aligned}\langle C_l^{EB} C_{l'}^{EB}\rangle = \frac{1}{2l+1}\frac{1}{2l'+1}\sum_{mm'}\Big\{ &\langle a_{lm}^E (a_{lm}^B)^*\rangle\langle a_{l'm'}^E (a_{l'm'}^B)^*\rangle + \langle a_{lm}^E a_{l'm'}^E\rangle\langle (a_{lm}^B)^* (a_{l'm'}^B)^*\rangle \\ &+ \langle a_{lm}^E (a_{l'm'}^B)^*\rangle\langle (a_{lm}^B)^* a_{l'm'}^E\rangle\Big\}\,.\end{aligned}$$

Using Eq.s 2.36 and 2.35, the above expression becomes:

$$= \frac{1}{2l+1}\frac{1}{2l'+1}\Big\{\sum_m\sum_{m'} C_l^{EB} C_{l'}^{EB} + \sum_m\sum_{m'} C_l^{EE}\delta_{ll'}\delta_{m-m'} C_l^{BB}\delta_{ll'}\delta_{-mm'} + \sum_m\sum_{m'}(C_l^{EB})^2\delta_{ll'}\delta_{mm'}\Big\}\,,$$

where we used the property of Kronecker delta;

$$\delta_{lm,l'm'} = \begin{cases} 1, & \text{if } l = l' \text{ and } m = m' \\ 0, & \text{otherwise} \end{cases} . \tag{3.8}$$

Given the sums:

$$\sum_{m=-l}^{l} = 2l+1, \sum_{m'=-l'}^{l'} = 2l'+1\,,$$

and the condition that:

$$\delta_{ll'} \neq 0 \Leftrightarrow l = l'$$
$$\Rightarrow 2l+1 = 2l'+1\,,$$

we can now express the following:

$$\begin{aligned} \langle C_l^{EB} C_{l'}^{EB} \rangle &= \frac{1}{(2l+1)^2}\Big\{(2l+1)^2 C_l^{EB} C_{l'}^{EB} + \delta_{ll'} C_l^{EE} C_l^{BB} \sum_{mm'} \delta_{m-m'} + \delta_{ll'} (C_l^{EB})^2 \sum_{mm'} \delta_{mm'}\Big\} \\ &= C_l^{EB} C_{l'}^{EB} + \frac{\delta_{ll'}}{(2l+1)^2}(2l+1) C_l^{EE} C_l^{BB} + \frac{\delta_{ll'}}{(2l+1)^2}(2l+1)(C_l^{EB})^2 \\ &= C_l^{EB} C_{l'}^{EB} + \frac{\delta_{ll'}}{2l+1}\left(C_l^{EE} C_l^{BB} + (C_l^{EB})^2\right) . \end{aligned}$$

Considering $C_l^{EB} = 0$,

$$\langle C_l^{EB} C_{l'}^{EB} \rangle = \frac{\delta_{ll'}}{2l+1} C_l^{EE} C_l^{BB}\,.$$

2. Using the following definitions:

$$C_l^{EB} = \frac{1}{2l+1} \sum_{l=-m}^{m} a_{lm}^{E} (a_{lm}^{B})^*\,,$$

$$C_{l'}^{EE} = \frac{1}{2l'+1} \sum_{l'=-m'}^{m'} a_{l'm'}^{E} (a_{l'm'}^{E})^*\,,$$

$$C_{l'}^{BB} = \frac{1}{2l'+1}\sum_{l'=-m'}^{m'} a^B_{l'm'}(a^B_{l'm'})^*\,,$$

and applying the property of linearity of expectation, Wick's theorem and following the previous rules, we have:

$$\begin{aligned}
\langle C_l^{EB}\frac{1}{2}(C_{l'}^{EE}-C_{l'}^{BB})\rangle &= \langle C_l^{EB}\frac{1}{2}C_{l'}^{EE} - \frac{1}{2}C_l^{EB}C_{l'}^{BB}\rangle \\
&= \frac{1}{2}\langle C_l^{EB}C_{l'}^{EE}\rangle - \frac{1}{2}\langle C_l^{EB}C_{l'}^{BB}\rangle \\
&= \frac{1}{2}\left\langle \frac{1}{2l+1}\frac{1}{2l'+1}\sum_m\sum_{m'} a^E_{lm}(a^B_{lm})^* a^E_{l'm'}(a^E_{l'm'})^*\right\rangle \\
&\quad - \frac{1}{2}\left\langle \frac{1}{2l+1}\frac{1}{2l'+1}\sum_m\sum_{m'} a^E_{lm}(a^B_{lm})^* a^B_{l'm'}(a^B_{l'm'})^*\right. \\
&\quad \textit{rangle} \\
&= \frac{1}{2}\frac{1}{2l+1}\frac{1}{2l'+1}\sum_{mm'}\Big\{\langle a^E_{lm}(a^B_{lm})^*\rangle\langle a^E_{l'm'}(a^E_{l'm'})^*\rangle + \\
&\quad \langle a^E_{lm}a^E_{l'm'}\rangle\langle (a^B_{lm})^*(a^E_{l'm'})^*\rangle + \langle a^E_{lm}(a^E_{l'm'})^*\rangle\langle (a^B_{lm})^* a^E_{l'm'}\rangle\Big\} \\
&\quad - \frac{1}{2}\frac{1}{2l+1}\frac{1}{2l'+1}\sum_{mm'}\Big\{\langle a^E_{lm}(a^B_{lm})^*\rangle\langle a^B_{l'm'}(a^B_{l'm'})^*\rangle \\
&\quad + \langle a^E_{lm}a^B_{l'm'}\rangle\langle (a^B_{lm})^*(a^B_{l'm'})^*\rangle + \langle a^E_{lm}(a^B_{l'm'})^*\rangle\langle (a^B_{lm})^* a^B_{l'm'}\rangle\Big\}\,.
\end{aligned}$$

After some algebra we find:

$$\langle C_l^{EB}\frac{1}{2}(C_{l'}^{EE}-C_{l'}^{BB})\rangle = \frac{1}{2}\left(C_l^{EB}C_{l'}^{EE} + 2\frac{\delta_{ll'}}{2l+1}C_l^{EE}C_l^{EB}\right) - \frac{1}{2}\left(C_l^{EB}C_{l'}^{BB} + 2\frac{\delta_{ll'}}{2l+1}C_l^{BB}C_l^{EB}\right).$$

Considering $C_l^{EB} = 0$,

$$\langle C_l^{EB}\frac{1}{2}(C_{l'}^{EE}-C_{l'}^{BB})\rangle = 0\,.$$

$$
\begin{aligned}
3.\ \langle\frac{1}{2}(C_l^{EE}-C_l^{BB})C_{l'}^{EB}\rangle &= \langle\frac{1}{2}C_l^{EE}C_{l'}^{EB}-\frac{1}{2}C_l^{BB}C_{l'}^{EB}\rangle \\
&= \frac{1}{2}\langle C_l^{EE}C_{l'}^{EB}\rangle-\frac{1}{2}\langle C_l^{BB}C_{l'}^{EB}\rangle \\
&= \frac{1}{2}\frac{1}{2l+1}\frac{1}{2l'+1}\sum_{mm'}\langle a_{lm}^E(a_{lm}^E)^* a_{l'm'}^E(a_{l'm'}^B)^*\rangle \\
&- \frac{1}{2}\frac{1}{2l+1}\frac{1}{2l'+1}\sum_{mm'}\langle a_{lm}^B(a_{lm}^B)^* a_{l'm'}^E(a_{l'm'}^B)^*\rangle \\
&= \frac{1}{2}\frac{1}{2l+1}\frac{1}{2l'+1}\sum_{mm'}\Bigg\{\langle a_{lm}^E(a_{lm}^E)^*\rangle\langle a_{l'm'}^E(a_{l'm'}^B)^*\rangle \\
&+ \langle a_{lm}^E a_{l'm'}^E\rangle\langle(a_{lm}^E)^*(a_{l'm'}^B)^*\rangle+\langle a_{lm}^E(a_{l'm'}^B)^*\rangle\langle(a_{lm}^E)^* a_{l'm'}^E\rangle\Bigg\} \\
&- \frac{1}{2}\frac{1}{2l+1}\frac{1}{2l'+1}\sum_{mm'}\Bigg\{\langle a_{lm}^B(a_{lm}^B)^*\rangle\langle a_{l'm'}^E(a_{l'm'}^B)^*\rangle \\
&+ \langle a_{lm}^B a_{l'm'}^E\rangle\langle(a_{lm}^B)^*(a_{l'm'}^B)^*\rangle+\langle a_{lm}^B(a_{l'm'}^B)^*\rangle\langle(a_{lm}^B)^* a_{l'm'}^E\rangle\Bigg\} \\
&= \frac{1}{2}\left(C_l^{EE}C_{l'}^{EB}+2\frac{\delta_{ll'}}{2l+1}C_l^{EE}C_l^{EB}\right)-\frac{1}{2}\left(C_l^{BB}C_{l'}^{EB}+2\frac{\delta_{ll'}}{2l+1}C_l^{BB}C_l^{EB}\right)
\end{aligned}
$$

Considering $C_l^{EB}=0$,

$$\langle\frac{1}{2}(C_l^{EE}-C_l^{BB})C_{l'}^{EB}\rangle = 0\,.$$

$$
\begin{aligned}
4.\ \langle\frac{1}{2}(C_l^{EE}-C_l^{BB})\frac{1}{2}(C_{l'}^{EE}-C_{l'}^{BB})\rangle &= \left\langle\frac{1}{2}C_l^{EE}\frac{1}{2}C_{l'}^{EE}-\frac{1}{2}C_l^{EE}\frac{1}{2}C_{l'}^{BB}-\frac{1}{2}C_l^{BB}\frac{1}{2}C_{l'}^{EE}+\frac{1}{2}C_l^{BB}\frac{1}{2}C_{l'}^{BB}\right\rangle \\
&= \frac{1}{4}\left(\langle C_l^{EE}C_{l'}^{EE}\rangle-\langle C_l^{EE}C_{l'}^{BB}\rangle\right)+\frac{1}{4}\left(\langle C_l^{BB}C_{l'}^{BB}\rangle-\langle C_l^{BB}C_{l'}^{EE}\rangle\right)
\end{aligned}
$$

For clarity, let us break this expression into two parts. We will analyze the following:

$$
\begin{aligned}
\text{a)}\ \frac{1}{4}(\langle C_l^{EE} C_{l'}^{EE}\rangle - \langle C_l^{EE} C_{l'}^{BB}\rangle) &= \frac{1}{4}\frac{1}{2l+1}\frac{1}{2l'+1}\sum_{mm'}\langle a^E_{lm}(a^E_{lm})^* a^E_{l'm'}(a^E_{l'm'})^*\rangle \\
&- \frac{1}{4}\frac{1}{2l+1}\frac{1}{2l'+1}\sum_{mm'}\langle a^E_{lm}(a^E_{lm})^* a^B_{l'm'}(a^B_{l'm'})^*\rangle \\
&= \frac{1}{4}\frac{1}{2l+1}\frac{1}{2l'+1}\sum_{mm'}\Bigg\{\langle a^E_{lm}(a^E_{lm})^*\rangle\langle a^E_{l'm'}(a^E_{l'm'})^*\rangle \\
&+ \langle a^E_{lm}a^E_{l'm'}\rangle\langle (a^E_{lm})^*(a^E_{l'm'})^*\rangle + \langle a^E_{lm}(a^E_{l'm'})^*\rangle\langle (a^E_{lm})^* a^E_{l'm'}\rangle\Bigg\} \\
&- \frac{1}{4}\frac{1}{2l+1}\frac{1}{2l'+1}\sum_{mm'}\Bigg\{\langle a^E_{lm}(a^E_{lm})^*\rangle\langle a^B_{l'm'}(a^B_{l'm'})^*\rangle \\
&+ \langle a^E_{lm}a^B_{l'm'}\rangle\langle (a^E_{lm})^*(a^B_{l'm'})^*\rangle + \langle a^E_{lm}(a^E_{l'm'})^*\rangle\langle (a^E_{lm})^* a^B_{l'm'}\rangle\Bigg\} \\
&= \frac{1}{4}\left(C_l^{EE}C_{l'}^{EE} + 2\frac{\delta_{ll'}}{2l+1}C_l^{EE}C_l^{EE}\right) - \frac{1}{4}\left(C_l^{EE}C_{l'}^{BB} + 2\frac{\delta_{ll'}}{2l+1}C_l^{EB}C_l^{EB}\right).
\end{aligned}
$$

$$
\begin{aligned}
\text{b)}\ \frac{1}{4}(\langle C_l^{BB} C_{l'}^{BB}\rangle - \langle C_l^{BB} C_{l'}^{EE}\rangle) &= \frac{1}{4}\frac{1}{2l+1}\frac{1}{2l'+1}\sum_{mm'}\langle a^B_{lm}(a^B_{lm})^* a^B_{l'm'}(a^B_{l'm'})^*\rangle \\
&- \frac{1}{4}\frac{1}{2l+1}\frac{1}{2l'+1}\sum_{mm'}\langle a^B_{lm}(a^B_{lm})^* a^E_{l'm'}(a^E_{l'm'})^*\rangle \\
&= \frac{1}{4}\frac{1}{2l+1}\frac{1}{2l'+1}\sum_{mm'}\Bigg\{\langle a^B_{lm}(a^B_{lm})^*\rangle\langle a^B_{l'm'}(a^B_{l'm'})^*\rangle \\
&+ \langle a^B_{lm}a^B_{l'm'}\rangle\langle (a^B_{lm})^*(a^B_{l'm'})^*\rangle + \langle a^B_{lm}(a^B_{l'm'})^*\rangle\langle (a^B_{lm})^* a^B_{l'm'}\rangle\Bigg\} \\
&- \frac{1}{4}\frac{1}{2l+1}\frac{1}{2l'+1}\sum_{mm'}\Bigg\{\langle a^B_{lm}(a^B_{lm})^*\rangle\langle a^E_{l'm'}(a^E_{l'm'})^*\rangle \\
&+ \langle a^B_{lm}a^E_{l'm'}\rangle\langle (a^B_{lm})^*(a^E_{l'm'})^*\rangle + \langle a^B_{lm}(a^E_{l'm'})^*\rangle\langle (a^B_{lm})^* a^E_{l'm'}\rangle\Bigg\} \\
&= \frac{1}{4}\left(C_l^{BB}C_{l'}^{BB} + 2\frac{\delta_{ll'}}{2l+1}C_l^{BB}C_l^{BB}\right) - \frac{1}{4}\left(C_l^{BB}C_{l'}^{EE} + 2\frac{\delta_{ll'}}{2l+1}C_l^{EB}C_l^{EB}\right).
\end{aligned}
$$

Now, let's combine the final results from parts (a) and (b):

$$\langle\frac{1}{2}(C_l^{EE}-C_l^{BB})\frac{1}{2}(C_{l'}^{EE}-C_{l'}^{BB})\rangle = \frac{1}{4}\left(C_l^{EE}C_{l'}^{EE}+C_l^{BB}C_{l'}^{BB}-C_l^{EE}C_{l'}^{BB}-C_l^{BB}C_{l'}^{EE}\right) + \frac{1}{2}\frac{\delta_{ll'}}{2l+1}\left((C_l^{EE})^2+(C_l^{BB})^2-2(C_l^{EB})^2\right) .$$

Where $C_l^{EB}=0$,

$$\langle\frac{1}{2}(C_l^{EE}-C_l^{BB})\frac{1}{2}(C_{l'}^{EE}-C_{l'}^{BB})\rangle = \frac{1}{4}\left(C_l^{EE}C_{l'}^{EE}+C_l^{BB}C_{l'}^{BB}-C_l^{EE}C_{l'}^{BB}-C_l^{BB}C_{l'}^{EE}\right) + \frac{1}{2}\frac{\delta_{ll'}}{2l+1}\left((C_l^{EE})^2+(C_l^{BB})^2\right) .$$

5. $\langle C_l^{EE}\rangle = \frac{1}{2l+1}\sum_m \langle a_{lm}^E (a_{lm}^E)^*\rangle$

$$\frac{1}{2l+1}\sum_m \delta_{ll}\delta_{mm}C_l^{EE}$$
$$= \frac{1}{2l+1}C_l^{EE}\sum_m$$
$$= \frac{1}{2l+1}(2l+1)C_l^{EE}$$
$$= C_l^{EE}$$

In the same way,

$$\langle C_l^{BB}\rangle = C_l^{BB},$$
$$\langle C_{l'}^{EE}\rangle = C_{l'}^{EE},$$
$$\langle C_{l'}^{BB}\rangle = C_{l'}^{BB}.$$

Then;

$$\frac{1}{2}(\langle C_l^{EE}\rangle-\langle C_l^{BB}\rangle)\frac{1}{2}(\langle C_{l'}^{EE}\rangle-\langle C_{l'}^{BB}\rangle) = \frac{1}{2}(C_l^{EE}-C_l^{BB})\frac{1}{2}(C_{l'}^{EE}-C_{l'}^{BB}) = \frac{1}{4}\left(C_l^{EE}C_{l'}^{EE}+C_l^{BB}C_{l'}^{BB}-C_l^{EE}C_{l'}^{BB}-C_l^{BB}C_{l'}^{EE}\right) .$$

Now, combining all the terms computed separately earlier:

$$\begin{aligned}
\langle D_l^{EB,o} D_{l'}^{EB,o} \rangle &= \frac{\delta_{ll'}}{2l+1} C_l^{EE} C_l^{BB} \cos^2 4(\alpha-\beta) \\
&+ \frac{1}{4}\left(C_l^{EE} C_{l'}^{EE} + C_l^{BB} C_{l'}^{BB} - C_l^{EE} C_{l'}^{BB} - C_l^{BB} C_{l'}^{EE}\right) \sin^2 4(\alpha-\beta) \\
&+ \frac{1}{2}\frac{\delta_{ll'}}{2l+1}\left((C_l^{EE})^2 + (C_l^{BB})^2\right) \sin^2 4(\alpha-\beta) \\
&= \frac{\delta_{ll'}}{2l+1} C_l^{EE} C_l^{BB} (1 - \sin^2 4(\alpha-\beta)) \\
&+ \frac{1}{4}\left(C_l^{EE} C_{l'}^{EE} + C_l^{BB} C_{l'}^{BB} - C_l^{EE} C_{l'}^{BB} - C_l^{BB} C_{l'}^{EE}\right) \sin^2 4(\alpha-\beta) \\
&+ \frac{1}{2}\frac{\delta_{ll'}}{2l+1}\left((C_l^{EE})^2 + (C_l^{BB})^2\right) \sin^2 4(\alpha-\beta) \\
&= \frac{1}{2}\frac{\delta_{ll'}}{2l+1}\left((C_l^{EE})^2 + (C_l^{BB})^2 - 2C_l^{EE} C_l^{BB}\right) \sin^2 4(\alpha-\beta) + \frac{\delta_{ll'}}{2l+1} C_l^{EE} C_l^{BB} \\
&+ \frac{1}{4}\left(C_l^{EE} C_{l'}^{EE} + C_l^{BB} C_{l'}^{BB} - C_l^{EE} C_{l'}^{BB} - C_l^{BB} C_{l'}^{EE}\right) \sin^2 4(\alpha-\beta)\,.
\end{aligned}$$

Then;

$$\begin{aligned}
\langle D_l^{EB,o} D_{l'}^{EB,o} \rangle &= \frac{\delta_{ll'}}{2l+1}\left[\frac{1}{2}(C_l^{EE} - C_l^{BB})^2 \sin^2 4(\alpha-\beta) + C_l^{EE} C_l^{BB}\right] \\
&+ \frac{1}{4}\left(C_l^{EE} C_{l'}^{EE} + C_l^{BB} C_{l'}^{BB} - C_l^{EE} C_{l'}^{BB} - C_l^{BB} C_{l'}^{EE}\right) \sin^2 4(\alpha-\beta)\,, \qquad (3.9)
\end{aligned}$$

and

$$\begin{aligned}
\langle D_l^{EB,o} D_{l'}^{EB,o} \rangle - \langle D_l^{EB,o} \rangle \langle D_{l'}^{EB,o} \rangle &= \frac{\delta_{ll'}}{2l+1}\left[\frac{1}{2}(C_l^{EE} - C_l^{BB})^2 \sin^2 4(\alpha-\beta) + C_l^{EE} C_l^{BB}\right] \\
&+ \frac{1}{4}\left(C_l^{EE} C_{l'}^{EE} + C_l^{BB} C_{l'}^{BB} - C_l^{EE} C_{l'}^{BB} - C_l^{BB} C_{l'}^{EE}\right) \sin^2 4(\alpha-\beta) \\
&- \frac{1}{4}\left(C_l^{EE} C_{l'}^{EE} + C_l^{BB} C_{l'}^{BB} - C_l^{EE} C_{l'}^{BB} - C_l^{BB} C_{l'}^{EE}\right) \sin^2 4(\alpha-\beta)\,.
\end{aligned}$$

Finally, the covariance of EB correlation is:

$$\langle D_l^{EB,o} D_{l'}^{EB,o} \rangle - \langle D_l^{EB,o} \rangle \langle D_{l'}^{EB,o} \rangle = \frac{\delta_{ll'}}{2l+1}\left[\frac{1}{2}(C_l^{EE} - C_l^{BB})^2 \sin^2 4(\alpha-\beta) + C_l^{EE} C_l^{BB}\right]\,. \qquad (3.10)$$

In the case $\alpha = \beta$, our result becomes:

$$\langle D_l^{EB,o} D_{l'}^{EB,o} \rangle - \langle D_l^{EB,o} \rangle \langle D_{l'}^{EB,o} \rangle = \frac{\delta_{ll'}}{2l+1} C_l^{EE} C_l^{BB} \,. \tag{3.11}$$

Setting the physical birefringence angle α equal to the estimator angle β is necessary to ensure consistency between the actual polarization rotation in the observed signal and the angle assumed in our model when estimating correlations. If α and β differ, the model would not accurately account for the true rotation effect, introducing discrepancies in the correlation terms. By setting $\alpha = \beta$, we align the physical reality with our estimation framework, allowing the covariance result to simplify to the form shown in Eq.3.11, where the covariance reduces to $\frac{\delta_{ll'}}{2l+1} C_l^{EE} C_l^{BB}$. This result reflects an idealized, unbiased case with no misalignment in the assumed and actual rotation angles, enabling a straightforward interpretation of the *EB-EB* correlation as a product of *EE* and *BB* power spectra.

3.2.2 Uncertainty of β

We now evaluate the uncertainty in the D-estimators for the EB-EB correlation using a chi-squared expression based on the Gaussian approximation. We assume that the difference $(\alpha - \beta)$ follows a Gaussian distribution centered around zero, indicating that β is an unbiased estimator of α. The chi-squared expression is given by [43]:

$$\mathcal{L}(\alpha, \beta, \sigma^2) = \frac{1}{\sqrt{2\pi\sigma^2}} \exp\left(-\frac{\chi^2}{2}\right) \tag{3.12}$$

$$= \frac{1}{\sqrt{2\pi\sigma^2}} \exp\left(-\frac{(\alpha-\beta)^2}{2\sigma^2}\right), \tag{3.13}$$

where:

- $(\alpha - \beta)$ represents the deviation between the true angle and the estimator,
- σ^2 is the variance in the measurement, indicating the spread or uncertainty in the estimator's accuracy. Smaller values of σ^2 imply a more precise estimator with less deviation between α and β, while larger values suggest greater variability in β as an approximation of α.

Modeling $(\alpha - \beta)$ as a Gaussian variable with variance σ^2 allows us to assess the uncertainty in the estimator β and strengthen the robustness of our analysis of the cosmic birefringence effect. These analysis helps identify the most likely value for β while ensuring its consistency with the true birefringence angle α.

In the χ^2 analysis, we assume $\alpha = \beta$ within the covariance matrix to model statistical uncertainty. In this way, we assume that the D-estimators D^{TB} and D^{EB} are unbiased estimators of the theoretical spectra C^{TB} and C^{EB} when $\beta = \alpha$. Meanwhile, by allowing $\alpha \neq \beta$ in $\langle D_l^{EB} D_{l'}^{EB} \rangle$, we maintain sensitivity to potential discrepancies between the true birefringence angle α and the estimator angle β. This allows us to assess whether the β that minimizes χ^2 aligns with α, providing a reliable method for detecting the true birefringence angle.

Let us analyze the χ^2 statistic for the EB component:

$$\begin{aligned}\langle \chi^2_{EB} \rangle &= \sum_{ll'} \langle D_l^{EB,o}\, Cov^{-1}_{ll'}\, D_{l'}^{EB,o} \rangle \\ &= \sum_{ll'} Cov^{-1}_{ll'} \langle D_l^{EB,o}\, D_{l'}^{EB,o} \rangle,\end{aligned}$$

where the covariance matrix $Cov_{ll'}$ is defined by Eq. 3.11. In above expression, the inverse covariance matrix $Cov^{-1}_{ll'}$ can be factored out of the expectation as it acts as a fixed, known matrix with respect to the D-estimators. Then, using Eq.s 3.11 and 3.9 the χ^2 becomes:

$$\begin{aligned}\langle \chi^2_{EB} \rangle = \sum_{ll'} \Bigg\{ \left(\frac{\delta_{ll'}}{2l+1} C_l^{EE} C_l^{BB} \right)^{-1} \Bigg[\frac{\delta_{ll'}}{2l+1} \left(\frac{1}{2} (C_l^{EE} - C_l^{BB})^2 \sin^2 4(\alpha - \beta) + C_l^{EE} C_l^{BB} \right) \\ + \frac{1}{4} \left(C_l^{EE} C_{l'}^{EE} + C_l^{BB} C_{l'}^{BB} - C_l^{EE} C_{l'}^{BB} - C_l^{BB} C_{l'}^{EE} \right) \sin^2 4(\alpha - \beta) \Bigg] \Bigg\}.\end{aligned}$$

Using the property of $\delta_{ll'}$ we simplify the sum by setting l = l', leading to:

$$\begin{aligned}\langle \chi^2_{EB} \rangle &= \sum_{l} \Bigg\{ \left(\frac{1}{2l+1} C_l^{EE} C_l^{BB} \right)^{-1} \Bigg[\frac{1}{2l+1} \left(\frac{1}{2} (C_l^{EE} - C_l^{BB})^2 \sin^2 4(\alpha - \beta) + C_l^{EE} C_l^{BB} \right) \\ &\quad + \frac{1}{4} \left(C_l^{EE} C_l^{EE} + C_l^{BB} C_l^{BB} - C_l^{EE} C_l^{BB} - C_l^{BB} C_l^{EE} \right) \sin^2 4(\alpha - \beta) \Bigg] \Bigg\} \\ &= \sum_l \frac{1}{2} \frac{(C_l^{EE} - C_l^{BB})^2}{C_l^{EE} C_l^{BB}} sin^2 4(\alpha - \beta) + \sum_l 1 + \sum_l \frac{1}{4} \frac{(C_l^{EE} - C_l^{BB})^2}{C_l^{EE} C_l^{BB}} sin^2 4(\alpha - \beta)(2l+1).\end{aligned}$$

Considering the Gaussian approximation, we focus on terms up to the second-order in the Taylor

expansion for small γ defined as $\gamma = \alpha - \beta$, where $\gamma \ll 1$:

$$\langle \chi^2_{EB} \rangle \simeq (2l+1) + \gamma^2 \sum_l 4 \frac{(C_l^{EE} - C_l^{BB})^2}{C_l^{EE} C_l^{BB}} [(2l+1) + 2] \,. \tag{3.14}$$

Given the expression in Eq. 3.13, now we can write:

$$\mathcal{L}(\alpha, \beta, \sigma^2) \propto \exp\left(-\frac{1}{2} \gamma^2 \sum_l 4 \frac{(C_l^{EE} - C_l^{BB})^2}{C_l^{EE} C_l^{BB}} [(2l+1) + 2] \right) .$$

We focus on the dependence of $\mathcal{L}$ on σ and simplify this as:

$$\mathcal{L}(\alpha, \beta, \sigma^2) \propto \exp\left(-\frac{\gamma^2}{2\sigma^2} \right) . \tag{3.15}$$

Here, we disregard the normalization factor since our aim is to concentrate on the effect of $(\alpha - \beta)$ and σ. We can now express the uncertainty as follows:

$$\sigma_{EB} = \left(4 \sum_l \frac{(C_l^{EE} - C_l^{BB})^2}{C_l^{EE} C_l^{BB}} [(2l+1) + 2] \right)^{-\frac{1}{2}} . \tag{3.16}$$

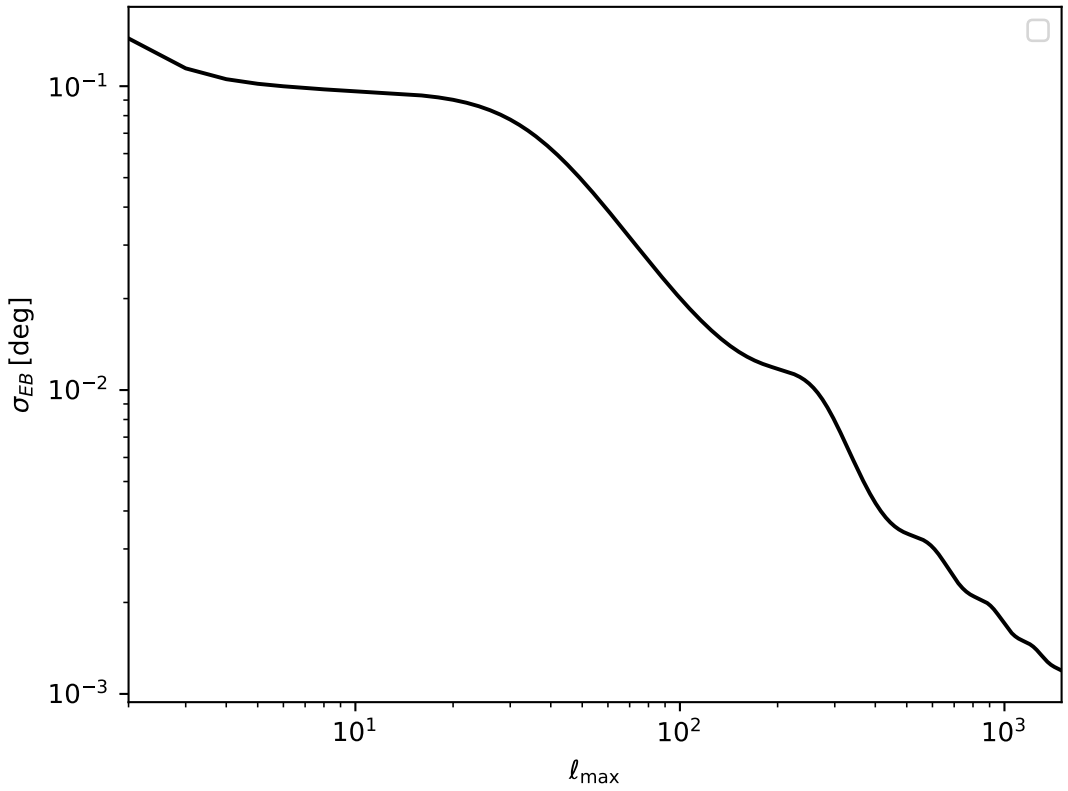

Figure 3.1: Uncertainty of the EB-EB correlation

These results demonstrate that our method is effective because $EE \gg BB$, which is a natural feature of the CMB polarization. The ratio of BB/EE is not constant and varies with ℓ, since EE exhibits an oscillatory behavior. This ratio, and consequently the uncertainty, becomes smallest when ℓ's are near the peaks of EE, due to the acoustic oscillations that occurred in the early universe. In Figure 3.1, the σ_{EB} curve exhibits a characteristic decrease as the multipole moment ℓ increases. This trend indicates that the uncertainty is higher at lower multipoles (large angular scales) and decreases at higher multipoles, which are more sensitive to smaller-scale features of the CMB. This behavior arises because, at low multipoles, the EE and BB spectra typically have higher power. As a result, the uncertainty in the correlation between these spectra is larger at these scales, where the system is dominated by large-scale cosmological features.

3.3 Characterization of the D_l^{TB}-Estimator

In this section, we focus on the characterization of the D_l^{TB}-estimator, based on the cross-correlation between the T-mode and B-mode polarization spectra. The expectation value and covariance structure of this estimator are derived in Appendix A. Here, we summarize how these analyses are used to assess the estimator's uncertainty.

3.3.1 Uncertainty of β

Let us analyze the χ^2 statistic for the *TB* component:

$$\langle \chi^2_{TB}(\beta) \rangle = \left\langle \sum_{ll'} D_l^{TB,o}(\beta) Cov_{ll'}(\beta) D_{l'}^{TB,o}(\beta) \right\rangle ,$$

where the covariance matrix $Cov_{ll'}$ is defined by Eq. A.7. Then, using Eq.s A.7 and A.5, the χ^2 becomes:

$$\langle \chi^2_{TB} \rangle = \sum_{ll'} \left\{ \left(\frac{\delta_{ll'}}{2l+1} C_l^{TT} C_l^{BB} \right)^{-1} \left[\frac{\delta_{ll'}}{2l+1} \left[\left(C_l^{TT} C_l^{EE} + (C_l^{TE})^2 - C_l^{TT} C_l^{BB} \right) \sin^2 2(\alpha - \beta) + C_l^{TT} C_l^{BB} \right] + C_l^{TE} C_{l'}^{TE} \sin^2 2(\alpha - \beta) \right] \right\} .$$

Using the property of $\delta_{ll'}$, we simplify the sum by setting l = l', leading to:

$$\langle \chi^2_{TB} \rangle = \sum_{l} \left\{ \left(\frac{1}{2l+1} C_l^{TT} C_l^{BB} \right)^{-1} \left[\frac{1}{2l+1} \left[\left(C_l^{TT} C_l^{EE} + (C_l^{TE})^2 - C_l^{TT} C_l^{BB} \right) \sin^2 2(\alpha - \beta) + C_l^{TT} C_l^{BB} \right] + (C_l^{TE})^2 \sin^2 2(\alpha - \beta) \right] \right\}$$

Considering the Gaussian approximation, we focus on terms up the second-order in the Taylor expansion for small γ defined as $\gamma = \alpha - \beta$, where $\gamma \ll 1$:

$$\langle \chi^2_{TB} \rangle \simeq (2l+1) + \gamma^2 \sum_l 4 \left[\frac{\left(C_l^{TT} C_l^{EE} + (C_l^{TE})^2 - C_l^{TT} C_l^{BB} \right)}{C_l^{TT} C_l^{BB}} + (2l+1) \frac{(C_l^{TE})^2}{C_l^{TT} C_l^{BB}} \right] .$$

After modifying the above equation, the final expression for the $\langle \chi^2_{TB} \rangle$ becomes:

$$\langle \chi^2_{TB} \rangle \simeq (2l+1) + \gamma^2 \sum_l 4 \left[\frac{C_l^{EE} - C_l^{BB}}{\substack{BB \\ l}} + \frac{(C_l^{TE})^2}{C_l^{TT} C_l^{BB}} + (2l+1) \frac{(C_l^{TE})^2}{C_l^{TT} C_l^{BB}} \right] . \tag{3.17}$$

Focusing on the dependence of $\mathcal{L}$ on σ, as defined in the previous section, we can express the uncertainty as follows:

$$\sigma_{TB} = \left[4 \sum_l \frac{C_l^{EE} - C_l^{BB}}{C_l^{BB}} + \frac{(C_l^{TE})^2}{C_l^{TT} C_l^{BB}} + (2l+1) \frac{(C_l^{TE})^2}{C_l^{TT} C_l^{BB}} \right]^{-\frac{1}{2}} . \tag{3.18}$$

Equation 3.18 defines the analytical expression of σ_{TB}, where the uncertainty is dominated by the term $(2l+1)(C_l^{TE})^2 / C_l^{TT} C_l^{BB}$. We can see that the uncertainty is inversely related to the expression

$$\left(\frac{C_l^{EE} - C_l^{BB}}{C_l^{BB}} + \frac{(C_l^{TE})^2}{C_l^{TT} C_l^{BB}} + (2l+1) \frac{(C_l^{TE})^2}{C_l^{TT} C_l^{BB}} \right) .$$

This means that when the C_l^{EE} and C_l^{TE} terms dominate over C_l^{BB}, the uncertainty is minimized.

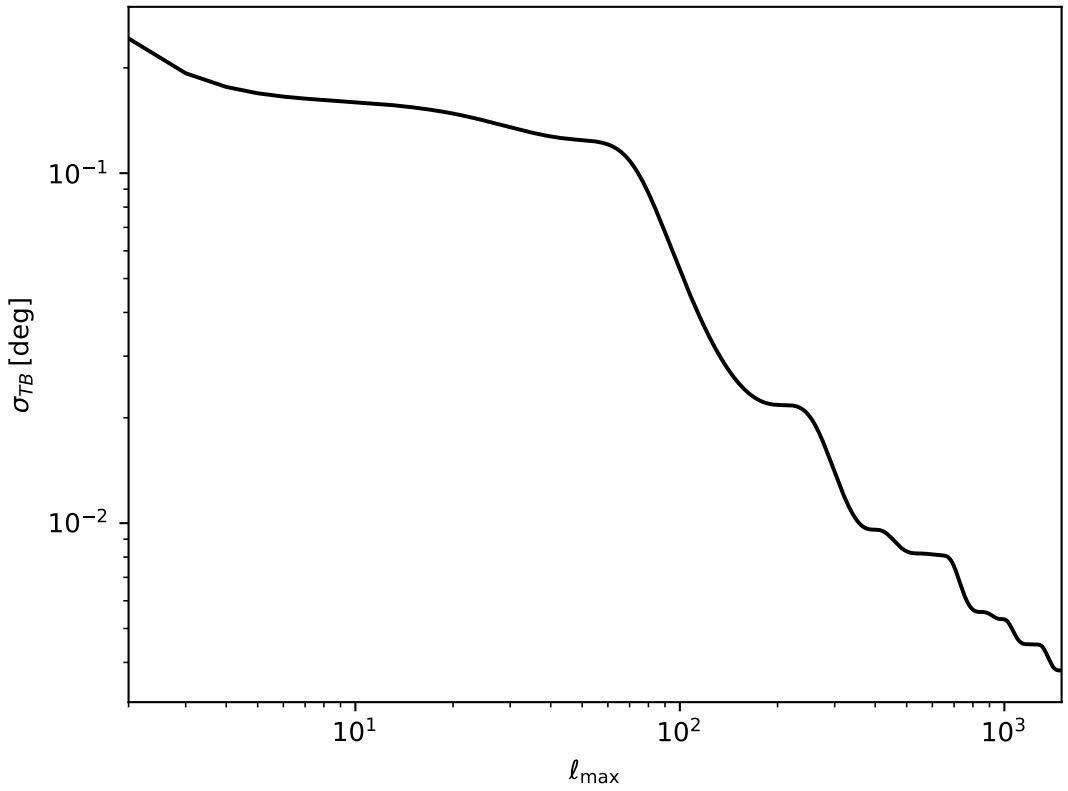

Figure 3.2: Uncertainty of the TB-TB correlation

Figure 3.2 shows how the uncertainty from the TB-TB correlation varies among multipoles. In the figure, σ_{TB} decreases as ℓ grows, indicating increased precision for estimating the birefringence angle for higher multipoles. The observed trend is consistent with theoretical assumptions, since the impact of large-scale characteristics (which contribute to larger uncertainty) decreases with higher multipoles.

3.4 Joint Estimator

In this section, we introduce a methodology to estimate the joint covariance between the TB and EB estimators. Our goal is to determine the combined covariance and associated uncertainty in estimating the angle β. This approach involves calculating the joint χ^2 statistic, which is given by the

following expression:

$$\left\langle \chi^2_{joint} \right\rangle = \sum_{ll'} \left\langle \begin{pmatrix} D_l^{TB,o}(\beta) & D_l^{EB,o}(\beta) \end{pmatrix} Cov_{ll'}^{-1} \begin{pmatrix} D_{l'}^{TB,o}(\beta) \\ D_{l'}^{EB,o}(\beta) \end{pmatrix} \right\rangle ,$$

and

$$Cov_{ll'}^{-1} = \begin{pmatrix} \left\langle \left(D_l^{TB,o} - \langle D_l^{TB,o} \rangle\right) \left(D_{l'}^{TB,o} - \langle D_{l'}^{TB,o} \rangle\right) \right\rangle & \left\langle \left(D_l^{TB,o} - \langle D_l^{TB,o} \rangle\right) \left(D_{l'}^{EB,o} - \langle D_{l'}^{EB,o} \rangle\right) \right\rangle \\ \left\langle \left(D_l^{EB,o} - \langle D_l^{EB,o} \rangle\right) \left(D_{l'}^{TB,o} - \langle D_{l'}^{TB,o} \rangle\right) \right\rangle & \left\langle \left(D_l^{EB,o} - \langle D_l^{EB,o} \rangle\right) \left(D_{l'}^{EB,o} - \langle D_{l'}^{EB,o} \rangle\right) \right\rangle \end{pmatrix}^{-1} ,$$

where $Cov_{ll'}^{-1}$ represents the inverse of the covariance matrix for the joint estimator of β, which we will compute for the correlation between TB and EB. To simplify the analysis, we express the covariance matrix as a block matrix containing four components:

$$Cov_{ll'} = \begin{pmatrix} A_{ll'} & B_{ll'} \\ C_{ll'} & D_{ll'} \end{pmatrix} ,$$

and its inverse as:

$$Cov_{ll'}^{-1} = \begin{pmatrix} X_{ll'} & Y_{ll'} \\ Z_{ll'} & W_{ll'} \end{pmatrix} .$$

Each of these components, $A_{ll'}$, $B_{ll'}$, $C_{ll'}$, and $D_{ll'}$ corresponds to the covariance between different combinations of the TB and EB, capturing the relationships both within and between the two. These sub-matrices are the components of the inverse covariance matrix, which we will use to compute the joint uncertainty. The components of the inverse covariance matrix are derived using standard matrix inversion techniques. They are given by the following expressions, using the Schur complement formula [44]:

$$\begin{aligned} X_{ll'} &= A_{ll'}^{-1} + A_{ll'}^{-1} B_{ll'} (D_{ll'} - C_{ll'} A_{ll'}^{-1} B_{ll'})^{-1} C_{ll'} A_{ll'}^{-1} , \\ Y_{ll'} &= -A_{ll'}^{-1} B_{ll'} (D_{ll'} - C_{ll'} A_{ll'}^{-1} B_{ll'})^{-1} , \\ Z_{ll'} &= -(D_{ll'} - C_{ll'} A_{ll'}^{-1} B_{ll'})^{-1} C_{ll'} A_{ll'}^{-1} , \\ W_{ll'} &= (D_{ll'} - C_{ll'} A_{ll'}^{-1} B_{ll'})^{-1} . \end{aligned}$$

Using the derived components of the inverse covariance matrix, we can rewrite the expression for the χ^2 of the joint estimator as:

$$\left\langle \chi^2_{joint} \right\rangle = \left\langle \sum_{ll'} D_l^{TB,o} X_{ll'} D_{l'}^{TB,o} + \sum_{ll'} D_l^{TB,o} Y_{ll'} D_{l'}^{EB,o} + \sum_{ll'} D_l^{EB,o} Z_{ll'} D_{l'}^{TB,o} + \sum_{ll'} D_l^{EB,o} W_{ll'} D_{l'}^{EB,o} \right\rangle .$$

By applying the linearity property of expectation, we can separate these terms and compute them individually. Each of these terms corresponds to a different contribution to the joint uncertainty:

$$\begin{aligned} \left\langle \chi^2_{joint} \right\rangle = &\left\langle \sum_{ll'} D_l^{TB,o} X_{ll'} D_{l'}^{TB,o} \right\rangle + \left\langle \sum_{ll'} D_l^{TB,o} Y_{ll'} D_{l'}^{EB,o} \right\rangle + \left\langle \sum_{ll'} D_l^{EB,o} Z_{ll'} D_{l'}^{TB,o} \right\rangle \\ &+ \left\langle \sum_{ll'} D_l^{EB,o} W_{ll'} D_{l'}^{EB,o} \right\rangle . \end{aligned} \tag{3.19}$$

3.4.1 Covariances of the Joint Estimator

Let us start with the expression for $W_{ll'}$, which represents the covariance between the EB at different angular scales:

1. $W_{ll'} = (D_{ll'} - C_{ll'} A_{ll'}^{-1} B_{ll'})^{-1}$

$$\begin{aligned} &= \Bigg(\left\langle \left(D_l^{EB,o} - \langle D_l^{EB,o} \rangle\right) \left(D_{l'}^{EB,o} - \langle D_{l'}^{EB,o} \rangle\right) \right\rangle - \left\langle \left(D_l^{EB,o} - \langle D_l^{EB,o} \rangle\right) \left(D_{l'}^{TB,o} - \langle D_{l'}^{TB,o} \rangle\right) \right\rangle \\ &\cdot \left\langle \left(D_l^{TB,o} - \langle D_l^{TB,o} \rangle\right) \left(D_{l'}^{TB,o} - \langle D_{l'}^{TB,o} \rangle\right) \right\rangle^{-1} \cdot \left\langle \left(D_l^{TB,o} - \langle D_l^{TB,o} \rangle\right) \left(D_{l'}^{EB,o} - \langle D_{l'}^{EB,o} \rangle\right) \right\rangle \Bigg)^{-1} . \end{aligned}$$

Utilizing the Equations 3.11, A.7, and A.14, and using the property

$$\left\langle \left(D_l^{TB,o} - \langle D_l^{TB,o} \rangle\right) \left(D_{l'}^{EB,o} - \langle D_{l'}^{EB,o} \rangle\right) \right\rangle = \left\langle \left(D_l^{EB,o} - \langle D_l^{EB,o} \rangle\right) \left(D_{l'}^{TB,o} - \langle D_{l'}^{TB,o} \rangle\right) \right\rangle ,$$

$$W_{ll'} = \left[\frac{\delta_{ll'}}{2l+1} C_l^{EE} C_l^{BB} - \frac{\delta_{ll'}}{2l+1} C_l^{TE} C_l^{BB} \left(\frac{\delta_{ll'}}{2l+1} C_l^{TT} C_l^{BB} \right)^{-1} \frac{\delta_{ll'}}{2l+1} C_l^{TE} C_l^{BB} \right]^{-1}$$

$$= \delta_{ll'}(2l+1)\left[C_l^{EE}C_l^{BB} - \frac{(C_l^{TE})^2}{C_l^{TT}}C_l^{BB}\right]^{-1}$$
$$= \delta_{ll'}(2l+1)\frac{1}{C_l^{BB}}\left[C_l^{EE} - \frac{(C_l^{TE})^2}{C_l^{TT}}\right]^{-1}. \tag{3.20}$$

The expressions for $Z_{ll'}$ and $Y_{ll'}$ involve similar computations, but they also include the cross-covariances between TB and EB.

$$2.\ Z_{ll'} = -(D_{ll'} - C_{ll'}A_{ll'}^{-1}B_{ll'})^{-1}C_{ll'}A_{ll'}^{-1}$$
$$= -\Bigg(\left\langle\left(D_l^{EB,o} - \langle D_l^{EB,o}\rangle\right)\left(D_{l'}^{EB,o} - \langle D_{l'}^{EB,o}\rangle\right)\right\rangle - \left\langle\left(D_l^{EB,o} - \langle D_l^{EB,o}\rangle\right)\left(D_{l'}^{TB,o} - \langle D_{l'}^{TB,o}\rangle\right)\right\rangle$$
$$\cdot\left\langle\left(D_l^{TB,o} - \langle D_l^{TB,o}\rangle\right)\left(D_{l'}^{TB,o} - \langle D_{l'}^{TB,o}\rangle\right)\right\rangle^{-1}\cdot\left\langle\left(D_l^{TB,o} - \langle D_l^{TB,o}\rangle\right)\left(D_{l'}^{EB,o} - \langle D_{l'}^{EB,o}\rangle\right)\right\rangle\Bigg)^{-1}$$
$$\cdot\left\langle\left(D_l^{EB,o} - \langle D_l^{EB,o}\rangle\right)\left(D_{l'}^{TB,o} - \langle D_{l'}^{TB,o}\rangle\right)\right\rangle\left(\left\langle\left(D_l^{TB,o} - \langle D_l^{TB,o}\rangle\right)\left(D_{l'}^{TB,o} - \langle D_{l'}^{TB,o}\rangle\right)\right\rangle\right)^{-1}$$

Inserting the final expression of $W_{ll'}$ into $Z_{ll'}$:

$$Z_{ll'} = -\delta_{ll'}(2l+1)\frac{1}{C_l^{BB}}\left[C_l^{EE} - \frac{(C_l^{TE})^2}{C_l^{TT}}\right]^{-1}\frac{\delta_{ll'}}{2l+1}C_l^{TE}C_l^{BB}\left(\frac{\delta_{ll'}}{2l+1}C_l^{TT}C_l^{BB}\right)^{-1}$$
$$= -\delta_{ll'}(2l+1)\frac{C_l^{TE}}{C_l^{TT}C_l^{BB}}\left[C_l^{EE} - \frac{(C_l^{TE})^2}{C_l^{TT}}\right]^{-1}. \tag{3.21}$$

$$3.\ Y_{ll'} = -A_{ll'}^{-1}B_{ll'}(D_{ll'} - C_{ll'}A_{ll'}^{-1}B_{ll'})^{-1}$$
$$= -\left(\left\langle\left(D_l^{TB,o} - \langle D_l^{TB,o}\rangle\right)\left(D_{l'}^{TB,o} - \langle D_{l'}^{TB,o}\rangle\right)\right\rangle\right)^{-1}\left\langle\left(D_l^{TB,o} - \langle D_l^{TB,o}\rangle\right)\left(D_{l'}^{EB,o} - \langle D_{l'}^{EB,o}\rangle\right)\right\rangle$$
$$\cdot\Bigg(\left\langle\left(D_l^{EB,o} - \langle D_l^{EB,o}\rangle\right)\left(D_{l'}^{EB,o} - \langle D_{l'}^{EB,o}\rangle\right)\right\rangle - \left\langle\left(D_l^{EB,o} - \langle D_l^{EB,o}\rangle\right)\left(D_{l'}^{TB,o} - \langle D_{l'}^{TB,o}\rangle\right)\right\rangle$$
$$\cdot\left\langle\left(D_l^{TB,o} - \langle D_l^{TB,o}\rangle\right)\left(D_{l'}^{TB,o} - \langle D_{l'}^{TB,o}\rangle\right)\right\rangle^{-1}\cdot\left\langle\left(D_l^{TB,o} - \langle D_l^{TB,o}\rangle\right)\left(D_{l'}^{EB,o} - \langle D_{l'}^{EB,o}\rangle\right)\right\rangle\Bigg)^{-1}$$

$$Y_{ll'} = -\left(\frac{\delta_{ll'}}{2l+1}C_l^{TT}C_l^{BB}\right)^{-1}\frac{\delta_{ll'}}{2l+1}C_l^{TE}C_l^{BB}\delta_{ll'}(2l+1)\frac{1}{C_l^{BB}}\left[C_l^{EE} - \frac{(C_l^{TE})^2}{C_l^{TT}}\right]^{-1}$$

$$= -\delta_{ll'}(2l+1)\frac{C_l^{TE}}{C_l^{TT}C_l^{BB}}\left[C_l^{EE}-\frac{(C_l^{TE})^2}{C_l^{TT}}\right]^{-1}. \tag{3.22}$$

We see that $Y_{ll'} = Z_{ll'}$ as expected.

$$\begin{aligned}
4.\, X_{ll'} &= A_{ll'}^{-1} + A_{ll'}^{-1}B_{ll'}(D_{ll'} - C_{ll'}A_{ll'}^{-1}B_{ll'})^{-1}C_{ll'}A_{ll'}^{-1} \\
&= \left(\left\langle\left(D_l^{TB,o} - \langle D_l^{TB,o}\rangle\right)\left(D_{l'}^{TB,o} - \langle D_{l'}^{TB,o}\rangle\right)\right\rangle\right)^{-1} \\
&+ \left(\left\langle\left(D_l^{TB,o} - \langle D_l^{TB,o}\rangle\right)\left(D_{l'}^{TB,o} - \langle D_{l'}^{TB,o}\rangle\right)\right\rangle\right)^{-1}\left\langle\left(D_l^{TB,o} - \langle D_l^{TB,o}\rangle\right)\left(D_{l'}^{EB,o} - \langle D_{l'}^{EB,o}\rangle\right)\right\rangle \\
&\cdot\left(\left\langle\left(D_l^{EB,o} - \langle D_l^{EB,o}\rangle\right)\left(D_{l'}^{EB,o} - \langle D_{l'}^{EB,o}\rangle\right)\right\rangle - \left\langle\left(D_l^{EB,o} - \langle D_l^{EB,o}\rangle\right)\left(D_{l'}^{TB,o} - \langle D_{l'}^{TB,o}\rangle\right)\right\rangle\right. \\
&\left.\cdot\left\langle\left(D_l^{TB,o} - \langle D_l^{TB,o}\rangle\right)\left(D_{l'}^{TB,o} - \langle D_{l'}^{TB,o}\rangle\right)\right\rangle^{-1}\cdot\left\langle\left(D_l^{TB,o} - \langle D_l^{TB,o}\rangle\right)\left(D_{l'}^{EB,o} - \langle D_{l'}^{EB,o}\rangle\right)\right\rangle\right)^{-1} \\
&\cdot\left\langle\left(D_l^{EB,o} - \langle D_l^{EB,o}\rangle\right)\left(D_{l'}^{TB,o} - \langle D_{l'}^{TB,o}\rangle\right)\right\rangle\left(\left\langle\left(D_l^{TB,o} - \langle D_l^{TB,o}\rangle\right)\left(D_{l'}^{TB,o} - \langle D_{l'}^{TB,o}\rangle\right)\right\rangle\right)^{-1}
\end{aligned}$$

Inserting the final expression of $Y_{ll'}$ into $X_{ll'}$:

$$\begin{aligned}
X_{ll'} &= \left(\frac{\delta_{ll'}}{2l+1}C_l^{TT}C_l^{BB}\right)^{-1} + \delta_{ll'}(2l+1)\frac{C_l^{TE}}{C_l^{TT}C_l^{BB}}\left[C_l^{EE}-\frac{(C_l^{TE})^2}{C_l^{TT}}\right]^{-1} \\
&\cdot\frac{\delta_{ll'}}{2l+1}C_l^{TE}C_l^{BB}\left(\frac{\delta_{ll'}}{2l+1}C_l^{TT}C_l^{BB}\right)^{-1} \\
&= \delta_{ll'}(2l+1)\frac{1}{C_l^{TT}C_l^{BB}}\left\{1+\frac{(C_l^{TE})^2}{C_l^{TT}}\left[C_l^{EE}-\frac{(C_l^{TE})^2}{C_l^{TT}}\right]^{-1}\right\}.
\end{aligned}$$

After some modification $X_{ll'}$ becomes:

$$X_{ll'} = \delta_{ll'}(2l+1)\frac{1}{C_l^{TT}C_l^{BB}}C_l^{EE}\left[C_l^{EE}-\frac{(C_l^{TE})^2}{C_l^{TT}}\right]^{-1}. \tag{3.23}$$

3.4.2 Joint Uncertainty

We are now ready to compute the terms of the joint $\langle \chi^2_{TB-EB} \rangle$ separately:

$$1. \left\langle \sum_{ll'} D_l^{TB,o} X_{ll'} D_{l'}^{TB,o} \right\rangle = \sum_{ll'} X_{ll'} \left\langle D_l^{TB,o} D_{l'}^{TB,o} \right\rangle$$

In the above expression, $X_{ll'}$ can be factored out because it is deterministic with respect to the D-estimators and therefore treated as a constant in the expectation. Utilizing Eq.s 3.23 and A.5 we can now write:

$$\begin{aligned}
\sum_{ll'} X_{ll'} \left\langle D_l^{TB,o} D_{l'}^{TB,o} \right\rangle = \sum_{ll'} \delta_{ll'} (2l+1) \frac{1}{C_l^{TT} C_l^{BB}} C_l^{EE} \left[C_l^{EE} - \frac{(C_l^{TE})^2}{C_l^{TT}} \right]^{-1} \\
\cdot \left\{ \frac{\delta_{ll'}}{2l+1} \left[\left(C_l^{TT} C_l^{EE} + (C_l^{TE})^2 - C_l^{TT} C_l^{BB} \right) \sin^2 2(\alpha - \beta) + C_l^{TT} C_l^{BB} \right] \right. \\
\left. + C_l^{TE} C_{l'}^{TE} \sin^2 2(\alpha - \beta) \right\} \\
= \sum_{ll'} \delta_{ll'} C_l^{EE} \left[C_l^{EE} - \frac{(C_l^{TE})^2}{C_l^{TT}} \right]^{-1} \left\{ 1 + \sin^2 2(\alpha - \beta) \right. \\
\left. \cdot \left[\frac{C_l^{EE}}{C_l^{BB}} + \frac{(C_l^{TE})^2}{C_l^{TT} C_l^{BB}} - 1 + (2l+1) \frac{C_l^{TE} C_{l'}^{TE}}{C_l^{TT} C_l^{BB}} \right] \right\}.
\end{aligned}$$

Using the the property of the Kronecker delta as given in 3.8, applying Taylor expansion for small γ up to the second order, and modifying the above expression, we obtain:

$$\begin{aligned}
\sum_{ll'} X_{ll'} \left\langle D_l^{TB,o} D_{l'}^{TB,o} \right\rangle \simeq \sum_{l} C_l^{EE} \left[C_l^{EE} - \frac{(C_l^{TE})^2}{C_l^{TT}} \right]^{-1} \\
+ \gamma^2 \sum_{l} 4 C_l^{EE} \left[C_l^{EE} - \frac{(C_l^{TE})^2}{C_l^{TT}} \right]^{-1} \left[\frac{C_l^{EE} - C_l^{BB}}{C_l^{BB}} + \frac{(C_l^{TE})^2}{C_l^{TT} C_l^{BB}} + (2l+1) \frac{(C_l^{TE})^2}{C_l^{TT} C_l^{BB}} \right].
\end{aligned} \tag{3.24}$$

$$2. \left\langle \sum_{ll'} D_l^{TB,o} Y_{ll'} D_{l'}^{EB,o} \right\rangle = \sum_{ll'} Y_{ll'} \left\langle D_l^{TB,o} D_{l'}^{EB,o} \right\rangle$$

Utilizing Equations 3.22 and A.12:

$$\begin{aligned}
\sum_{ll'} Y_{ll'} \left\langle D_l^{TB,o} D_{l'}^{EB,o} \right\rangle &= -\sum_{ll'} \delta_{ll'} (2l+1) \frac{C_l^{TE}}{C_l^{TT} C_l^{BB}} \left[C_l^{EE} - \frac{(C_l^{TE})^2}{C_l^{TT}} \right]^{-1} \\
&\cdot \left[\frac{\delta_{ll'}}{2l+1} C_l^{TE} C_l^{BB} \cos 2(\alpha-\beta) \cos 4(\alpha-\beta) \right. \\
&+ \frac{1}{2} C_l^{TE} (C_{l'}^{EE} - C_{l'}^{BB}) \sin 2(\alpha-\beta) \sin 4(\alpha-\beta) \\
&\left. + \frac{\delta_{ll'}}{2l+1} C_l^{TE} C_l^{EE} \sin 2(\alpha-\beta) \sin 4(\alpha-\beta) \right] \\
&= -\sum_{ll'} \delta_{ll'} \frac{(C_l^{TE})^2}{C_l^{TT}} \left[C_l^{EE} - \frac{(C_l^{TE})^2}{C_l^{TT}} \right]^{-1} \cos 2(\alpha-\beta) \cos 4(\alpha-\beta) \\
&- \sum_{ll'} \delta_{ll'} (2l+1) \frac{(C_l^{TE})^2}{C_l^{TT}} \frac{(C_{l'}^{EE} - C_{l'}^{BB})}{C_l^{BB}} \left[C_l^{EE} - \frac{(C_l^{TE})^2}{C_l^{TT}} \right]^{-1} \frac{1}{2} \sin 2(\alpha-\beta) \sin 4(\alpha-\beta) \\
&- \sum_{ll'} \delta_{ll'} \frac{(C_l^{TE})^2}{C_l^{TT}} \frac{C_l^{EE}}{C_l^{BB}} \left[C_l^{EE} - \frac{(C_l^{TE})^2}{C_l^{TT}} \right]^{-1} \sin 2(\alpha-\beta) \sin 4(\alpha-\beta) \,.
\end{aligned}$$

Let us use the the property of the Kronecker delta, and Taylor expand the expression for small γ up to the second order:

$$\begin{aligned}
\sum_{ll'} Y_{ll'} \left\langle D_l^{TB,o} D_{l'}^{EB,o} \right\rangle &\simeq -\sum_{l} \frac{(C_l^{TE})^2}{C_l^{TT}} \left[C_l^{EE} - \frac{(C_l^{TE})^2}{C_l^{TT}} \right]^{-1} (1-2\gamma^2)(1-8\gamma^2) \\
&- \sum_{l} (2l+1) \frac{(C_l^{TE})^2}{C_l^{TT}} \frac{(C_l^{EE} - C_l^{BB})}{C_l^{BB}} \left[C_l^{EE} - \frac{(C_l^{TE})^2}{C_l^{TT}} \right]^{-1} \frac{1}{2} 2\gamma \cdot 4\gamma \\
&- \sum_{l} \frac{(C_l^{TE})^2}{C_l^{TT}} \frac{C_l^{EE}}{C_l^{BB}} \left[C_l^{EE} - \frac{(C_l^{TE})^2}{C_l^{TT}} \right]^{-1} 2\gamma \cdot 4\gamma \\
&\simeq -\sum_{l} \frac{(C_l^{TE})^2}{C_l^{TT}} \left[C_l^{EE} - \frac{(C_l^{TE})^2}{C_l^{TT}} \right]^{-1} (1-10\gamma^2) \\
&- \sum_{l} (2l+1) \frac{(C_l^{TE})^2}{C_l^{TT}} \frac{(C_l^{EE} - C_l^{BB})}{C_l^{BB}} \left[C_l^{EE} - \frac{(C_l^{TE})^2}{C_l^{TT}} \right]^{-1} 4\gamma^2 \\
&- \sum_{l} \frac{(C_l^{TE})^2}{C_l^{TT}} \frac{C_l^{EE}}{C_l^{BB}} \left[C_l^{EE} - \frac{(C_l^{TE})^2}{C_l^{TT}} \right]^{-1} 8\gamma^2 \,.
\end{aligned}$$

After some modifications, the above expression becomes:

$$\sum_{ll'} Y_{ll'} \left\langle D_l^{TB,o} D_{l'}^{EB,o} \right\rangle \simeq -\sum_l \frac{(C_l^{TE})^2}{C_l^{TT}} \left[C_l^{EE} - \frac{(C_l^{TE})^2}{C_l^{TT}} \right]^{-1} - \gamma^2 \sum_l \frac{(C_l^{TE})^2}{C_l^{TT}} C_l^{EE} \left[C_l^{EE} - \frac{(C_l^{TE})^2}{C_l^{TT}} \right]^{-1} \left[\left(\frac{8}{C_l^{BB}} - \frac{10}{C_l^{EE}} \right) + 4(2l+1) \left(\frac{C_l^{EE} - C_l^{BB}}{C_l^{BB} C_l^{EE}} \right) \right] . \tag{3.25}$$

3. $$\left\langle \sum_{ll'} D_l^{EB,o} Z_{ll'} D_{l'}^{TB,o} \right\rangle = \left\langle \sum_{ll'} D_l^{TB,o} Y_{ll'} D_{l'}^{EB,o} \right\rangle$$

as a result of $Z_{ll'} = Y_{ll'}$ and $\langle D_l^{TB,o} D_{l'}^{EB,o} \rangle = \langle D_l^{EB,o} D_{l'}^{TB,o} \rangle$. Therefore, Equation 3.25 holds also here.

4. $$\left\langle \sum_{ll'} D_l^{EB,o} W_{ll'} D_{l'}^{EB,o} \right\rangle = \sum_{ll'} W_{ll'} \left\langle D_l^{EB,o} D_{l'}^{EB,o} \right\rangle$$

Using Eq.s 3.20 and 3.9:

$$\begin{aligned}
\sum_{ll'} W_{ll'} \left\langle D_l^{EB,o} D_{l'}^{EB,o} \right\rangle &= \sum_{ll'} \delta_{ll'} (2l+1) \frac{1}{C_l^{BB}} \left[C_l^{EE} - \frac{(C_l^{TE})^2}{C_l^{TT}} \right]^{-1} \\
&\cdot \left\{ \frac{\delta_{ll'}}{2l+1} \left[\frac{1}{2} (C_l^{EE} - C_l^{BB})^2 \sin^2 4(\alpha - \beta) + C_l^{EE} C_l^{BB} \right] \right. \\
&\left. + \frac{1}{4} \left(C_l^{EE} C_{l'}^{EE} + C_l^{BB} C_{l'}^{BB} - C_l^{EE} C_{l'}^{BB} - C_l^{BB} C_{l'}^{EE} \right) \sin^2 4(\alpha - \beta) \right\} \\
&= \sum_{ll'} \delta_{ll'} C_l^{EE} \left[C_l^{EE} - \frac{(C_l^{TE})^2}{C_l^{TT}} \right]^{-1} \\
&+ \sum_{ll'} \delta_{ll'} \frac{(C_l^{EE} - C_l^{BB})^2}{C_l^{BB}} \left[C_l^{EE} - \frac{(C_l^{TE})^2}{C_l^{TT}} \right]^{-1} \frac{1}{2} \sin^2 4(\alpha - \beta) \\
&+ \sum_{ll'} \delta_{ll'} (2l+1) \frac{(C_l^{EE} C_{l'}^{EE} + C_l^{BB} C_{l'}^{BB} - C_l^{EE} C_{l'}^{BB} - C_l^{BB} C_{l'}^{EE})}{C_l^{BB}} \\
&\cdot \left[C_l^{EE} - \frac{(C_l^{TE})^2}{C_l^{TT}} \right]^{-1} \frac{1}{4} \sin^2 4(\alpha - \beta) .
\end{aligned}$$

Using the the property of the Kronecker delta 3.8, applying Taylor expansion for small γ up to the second order, and modifying the above expression, we obtain:

$$\sum_{ll'} W_{ll'} \left\langle D_l^{EB,o} D_{l'}^{EB,o} \right\rangle \simeq \sum_l C_l^{EE} \left[C_l^{EE} - \frac{(C_l^{TE})^2}{C_l^{TT}} \right]^{-1} + \gamma^2 \sum_l \frac{(C_l^{EE} - C_l^{BB})^2}{C_l^{BB}} \left[C_l^{EE} - \frac{(C_l^{TE})^2}{C_l^{TT}} \right]^{-1} (8 + 4(2l+1)) \ . \tag{3.26}$$

We now compute the total joint uncertainty by summing over all the terms derived the individually, in $\langle \chi^2_{joint} \rangle$. This provides an estimate of the total uncertainty in the joint estimator for β, taking into account both the auto- and cross-correlations between TB and EB:

$$\begin{aligned}
\left\langle \chi^2_{joint} \right\rangle &= \sum_{ll'} \left\langle \begin{pmatrix} D_l^{TB,o}(\beta) & D_l^{EB,o}(\beta) \end{pmatrix} Cov_{ll'}^{-1} \begin{pmatrix} D_{l'}^{TB,o}(\beta) \\ D_{l'}^{EB,o}(\beta) \end{pmatrix} \right\rangle \\
&= \sum_l C_l^{EE} \left[C_l^{EE} - \frac{(C_l^{TE})^2}{C_l^{TT}} \right]^{-1} \\
&+ \gamma^2 \sum_l 4 C_l^{EE} \left[C_l^{EE} - \frac{(C_l^{TE})^2}{C_l^{TT}} \right]^{-1} \left[\frac{C_l^{EE} - C_l^{BB}}{C_l^{BB}} + \frac{(C_l^{TE})^2}{C_l^{TT} C_l^{BB}} + (2l+1) \frac{(C_l^{TE})^2}{C_l^{TT} C_l^{BB}} \right] \\
&- 2 \sum_l \frac{(C_l^{TE})^2}{C_l^{TT}} \left[C_l^{EE} - \frac{(C_l^{TE})^2}{C_l^{TT}} \right]^{-1} \\
&- 2\gamma^2 \sum_l \frac{(C_l^{TE})^2}{C_l^{TT}} \frac{C_l^{EE}}{\left[C_l^{EE} - \frac{(C_l^{TE})^2}{C_l^{TT}} \right]} \left[\left(\frac{8}{C_l^{BB}} - \frac{10}{C_l^{EE}} \right) + 4(2l+1) \left(\frac{(C_l^{EE} - C_l^{BB})}{C_l^{BB} C_l^{EE}} \right) \right] \\
&+ \sum_l C_l^{EE} \left[C_l^{EE} - \frac{(C_l^{TE})^2}{C_l^{TT}} \right]^{-1} \\
&+ \gamma^2 \sum_l \frac{(C_l^{EE} - C_l^{BB})^2}{C_l^{BB}} \left[C_l^{EE} - \frac{(C_l^{TE})^2}{C_l^{TT}} \right]^{-1} [8 + 4(2l+1)] \, .
\end{aligned}$$

Finally,

$$\left\langle \chi^2_{joint} \right\rangle = \sum_l 2 C_l^{EE} \left[C_l^{EE} - \frac{(C_l^{TE})^2}{C_l^{TT}} \right]^{-1} - \sum_l 2 \frac{(C_l^{TE})^2}{C_l^{TT}} \left[C_l^{EE} - \frac{(C_l^{TE})^2}{C_l^{TT}} \right]^{-1}$$

$$+\gamma^2 \sum_l C_l^{EE}\left[C_l^{EE}-\frac{(C_l^{TE})^2}{C_l^{TT}}\right]^{-1}\left\{4\left[\frac{C_l^{EE}-C_l^{BB}}{C_l^{BB}}+\frac{(C_l^{TE})^2}{C_l^{TT}C_l^{BB}}+(2l+1)\frac{(C_l^{TE})^2}{C_l^{TT}C_l^{BB}}\right]\right.$$
$$-2\frac{(C_l^{TE})^2}{C_l^{TT}}\left[\left(\frac{8}{C_l^{BB}}-\frac{10}{C_l^{EE}}\right)+4(2l+1)\left(\frac{C_l^{EE}-C_l^{BB}}{C_l^{BB}C_l^{EE}}\right)\right]$$
$$\left.+\frac{(C_l^{EE}-C_l^{BB})^2}{C_l^{BB}C_l^{EE}}[8+4(2l+1)]\right\}. \tag{3.27}$$

And the joint uncertainty becomes:

$$\sigma_{\text{joint}}=\left\{\sum_l C_l^{EE}\left[C_l^{EE}-\frac{(C_l^{TE})^2}{C_l^{TT}}\right]^{-1}\left\{4\left[\frac{C_l^{EE}-C_l^{BB}}{C_l^{BB}}+\frac{(C_l^{TE})^2}{C_l^{TT}C_l^{BB}}+(2l+1)\frac{(C_l^{TE})^2}{C_l^{TT}C_l^{BB}}\right]\right.\right.$$
$$-2\frac{(C_l^{TE})^2}{C_l^{TT}}\left(\frac{8}{C_l^{BB}}-\frac{10}{C_l^{EE}}+4(2l+1)\frac{C_l^{EE}-C_l^{BB}}{C_l^{BB}C_l^{EE}}\right)$$
$$\left.\left.+\frac{(C_l^{EE}-C_l^{BB})^2}{C_l^{BB}C_l^{EE}}[8+4(2l+1)]\right\}\right\}^{-\frac{1}{2}}. \tag{3.28}$$

Equation 3.28 represents the main result of this work and introduces a novel method for estimating the joint uncertainty derived from both EB and TB correlations.

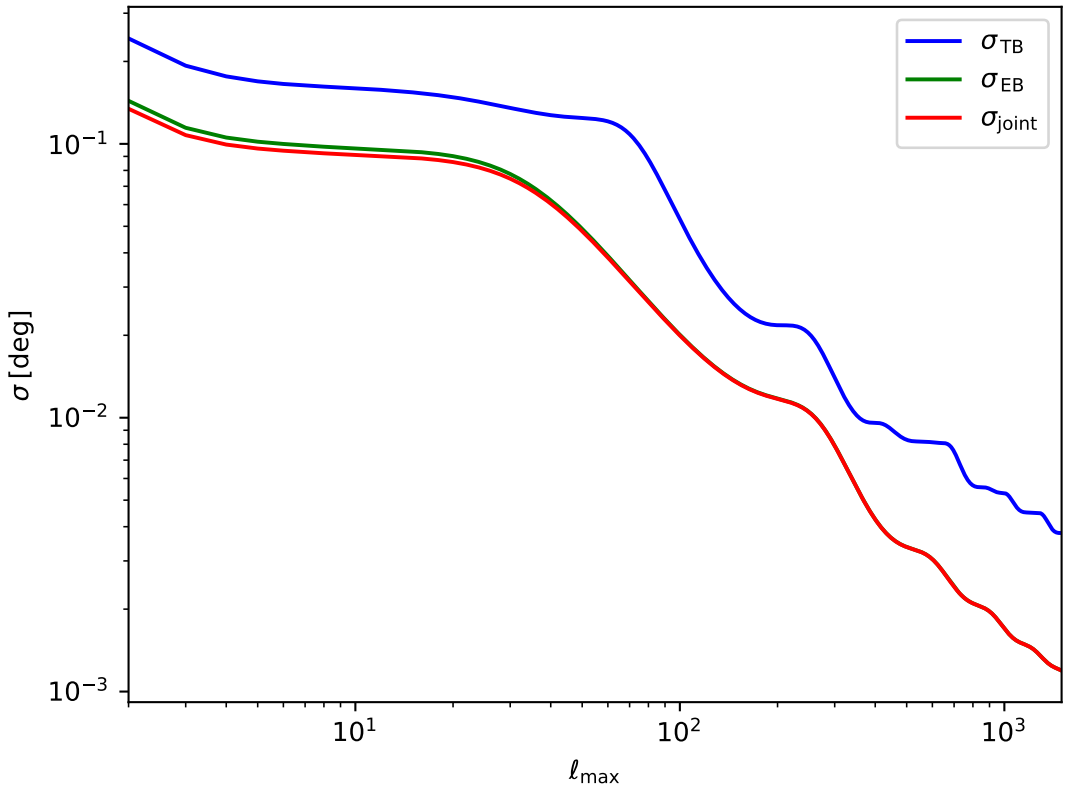

Figure 3.3: Comparison of the Joint Uncertainty with the Uncertainties from the EB-EB and TB-TB Correlations

In Figure 3.3, the red curve represents the combined uncertainty from both EB and TB correlations. This joint uncertainty curve lies below the individual σ_{EB} (green) and σ_{TB} (blue) curves across the multipole range ℓ, indicating that the combination of both correlations yields a slightly improved uncertainty estimate.

The main finding we obtain is that combining information from both EB and TB correlations offers a modest reduction in the total uncertainty. This effect is most prominent in the lower multipole range, where the combined correlation information more effectively constrains the uncertainty. However, the reduction is not large, and the EB component dominates over the joint uncertainty, with the TB component contributing less significantly. TB offers a complementary but less impactful contribution, therefore it is better to be used as a consistency check.

4

Conclusions

Cosmic birefringence refers to the rotation of the plane of polarization of the CMB photons caused by an interaction with a pseudoscalar field χ on its journey in the universe from the last scattering surface to the present day. This field couples to the dual of the electromagnetic field tensor via a Chern-Simons term. As a result, the Maxwell equations of the standard electromagnetism are modified with an additional term in the Lagrangian density: $\mathcal{L} = \mathcal{L}_{EM} + \mathcal{L}_{CS}$, where $\mathcal{L}_{CS} = (-\alpha_{em}/4f)\chi F\tilde{F}$. This term becomes effective when the χ varies in time, meaning that the time derivative of this field, χ' is non-zero. The varying nature of this pseudoscalar field violates the parity [27, 28]. The parity violation arises because $F\tilde{F} = -4\mathbf{B}\cdot\mathbf{E}$, electric field vector $\mathbf{E}$ and magnetic field vector $\mathbf{B}$ exhibit odd and even parity, respectively.

In this thesis, we explored the implications of this rotation on the CMB power spectra. We introduced the isotropic birefringence angle α, which quantifies the rotation of the E-mode and B-mode polarization components. This rotation generates non-zero TB and EB correlations in the observed power spectra, that are otherwise zero in a parity-conserved scenario. We assumed no parity violation at the last scattering surface ($TB = EB = 0$ initially), neglecting mechanisms breaking mirror symmetry in the early universe. We used the modified observed CMB spectra under ideal conditions (neglecting the noise) to derive D-estimators [41], which are harmonic-based estimators used to estimate the birefringence angle α. These estimators are based on the parameter β, which represents the estimator angle. When the birefringence angle equals the estimator angle ($\alpha = \beta$), it becomes possible to determine the birefringence angle by setting the D-estimators D_l^{TB} and D_l^{EB} to zero. This property ensures that the estimators remain unbiased for the theoretical spectra C_l^{TB} and C_l^{EB} when

$\beta = \alpha$. More technically, these estimators work because, in the intrinsic nature of the CMB, the EE and BB power spectra are not equal ($C_l^{EE} \neq C_l^{BB}$), and the cross-spectrum C_l^{TE} is inherently non-zero. These distinctions make it available for detecting any non-zero rotation angle β (see Eq.s 3.5 and 3.6).

We defined and analytically characterized these estimators and performed a χ^2 analysis under the Gaussian approximation to derive an analytical expression for the uncertainty of β for the EB and TB correlations, and their joint (combined) estimator. These analyzes include detailed computation of covariance matrices and uncertainties. From the χ^2 analysis for D_l^{EB} we have obtained the uncertainty for β, as given in Eq. 3.16 and shown in Figure 3.1. Eq. 3.16 demonstrate that our method is effective because $EE \gg BB$, which is a natural feature of the CMB polarization. We observe that the ratio of BB/EE is not constant and varies with ℓ, since EE exhibits an oscillatory behavior. This ratio, and consequently the uncertainty, becomes smallest when ℓ's are near the peaks of EE, due to the acoustic oscillations that occurred in the early universe. Similarly, from the χ^2 analysis for D_l^{TB} we have obtained the uncertainty for β, as given in Eq. 3.18 and shown in Figure 3.2. Our results from the analysis of TB correlation show that when the C_l^{EE} and C_l^{TE} terms dominate over C_l^{BB}, the uncertainty of β from the TB correlation is minimized.

Finally, we have performed a joint analysis of D_l^{EB} and D_l^{TB}, employing a joint χ^2 analysis that includes the cross-correlation between TB and EB. Following the same approach used for the other cases, we derived an analytical formula for the joint uncertainty under the Gaussian approximation. This expression, provided in Eq. 3.28 and shown in Figure 3.3, represents one of the main finding of this thesis. In Figure 3.3, we also compare the behavior of the joint uncertainty to the individual uncertainties derived from D_l^{EB} and D_l^{TB}. The results show that combining EB and TB slightly reduces the overall uncertainty, with the most noticeable improvement seen at lower multipoles, where the combined information provides tighter constraints. However, the EB component largely dominates the joint estimator, leaving the TB contribution with limited impact. Thus, treating TB independently as a consistency check may be a more practical approach.

Although the domination of EB in the joint estimator is already known in the literature, our work introduces a new analytical expression for the uncertainty of β for the joint estimator, that is not present in the literature. So far, these results have been developed in an idealized framework, considering only the CMB. In the future, we aim to investigate how our findings—particularly the behavior illustrated in Figure 3.3—are modified when non-idealities such as incomplete sky coverage, instrumental noise, and foreground residuals are included in the analysis. Addressing these non-idealities involves different strategies. Instrumental systematics require dedicated simulations, but other more standard effects, such as those mentioned above, can be addressed using the analytical expressions derived here or closely related ones. Consequently, these analytical expressions can be beneficial for

forecasting the expected performance for β in future CMB experiments, in cases where systematic effects are not overly complex.

Recent studies [1, 3, 4] have reported statistically significant non-zero birefringence angle, α, at confidence levels ranging from $2.4\,\sigma$ to $3.6\,\sigma$. Upcoming CMB experiments such as the ground-based CMB-S4 array [24], Simons Observatory [25], and the space mission LiteBIRD [22] promise to improve the precision of polarization measurements, particularly for the B-mode. These advancements in observational cosmology could illuminate new physics beyond the standard model and enhance our understanding of fundamental symmetries in the universe.

A Appendix

A.1 Covariance of C_l^{TB}

Using Eq. 3.2:

$$\begin{aligned}\langle D_l^{TB,o} D_{l'}^{TB,o}\rangle = &\left\langle \left[C_l^{TB,o}\cos 2\beta - C_l^{TE,o}\sin 2\beta\right]\right.\\ &\left.\cdot\left[C_{l'}^{TB,o}\cos 2\beta - C_{l'}^{TE,o}\sin 2\beta\right]\right\rangle\\ &= \langle C_l^{TB,o}C_{l'}^{TB,o}\rangle\cos^2 2\beta - \langle C_l^{TB,o}C_{l'}^{TE,o}\rangle\cos 2\beta\sin 2\beta\\ &- \langle C_l^{TE,o}C_{l'}^{TB,o}\rangle\cos 2\beta\sin 2\beta + \langle C_l^{TE,o}C_{l'}^{TE,o}\rangle\sin^2 2\beta\,.\end{aligned}$$

To compute $\langle D_l^{TB,o} D_{l'}^{TB,o}\rangle$, we first need to determine the expectation values of each individual component, using Equations 2.47, and 2.48:

1.

$$\begin{aligned}\langle C_l^{TB,o}C_{l'}^{TB,o}\rangle\cos^2 2\beta &= \left\langle\left[C_l^{TB}\cos 2\alpha + C_l^{TE}\sin 2\alpha\right]\left[C_{l'}^{TB}\cos 2\alpha + C_{l'}^{TE}\sin 2\alpha\right]\right\rangle\cos^2 2\beta\\ &= \langle C_l^{TB}C_{l'}^{TB}\rangle\cos^2 2\alpha\cos^2 2\beta + \langle C_l^{TB}C_{l'}^{TE}\rangle\cos 2\alpha\sin 2\alpha\cos^2 2\beta\\ &+ \langle C_l^{TE}C_{l'}^{TB}\rangle\cos 2\alpha\sin 2\alpha\cos^2 2\beta + \langle C_l^{TE}C_{l'}^{TE}\rangle\sin^2 2\alpha\cos^2 2\beta\end{aligned}$$

2.

$$\begin{aligned}\langle C_l^{TB,o} C_{l'}^{TE,o})\rangle \cos 2\beta \sin 2\beta &= \Big\langle \left[C_l^{TB}\cos 2\alpha + C_l^{TE}\sin 2\alpha\right]\left[(C_{l'}^{TE}\cos 2\alpha - C_{l'}^{TB}\sin 2\alpha\right]\Big\rangle \cos 2\beta \sin 2\beta \\ &= \langle C_l^{TB} C_{l'}^{TE}\rangle \cos^2 2\alpha \cos 2\beta \sin 2\beta - \langle C_l^{TB} C_{l'}^{TB}\rangle \cos 2\alpha \sin 2\alpha \cos 2\beta \sin 2\beta \\ &+ \langle C_l^{TE} C_{l'}^{TE}\rangle \cos 2\alpha \sin 2\alpha \cos 2\beta \sin 2\beta - \langle C_l^{TE} C_{l'}^{TB}\rangle \sin^2 2\alpha \cos 2\beta \sin 2\beta\end{aligned}$$

3.

$$\begin{aligned}\langle C_l^{TE,o} C_{l'}^{TB,o}\rangle \cos 2\beta \sin 2\beta &= \Big\langle \left[C_l^{TE}\cos 2\alpha - C_l^{TB}\sin 2\alpha\right]\left[C_{l'}^{TB}\cos 2\alpha + C_{l'}^{TE}\sin 2\alpha\right]\Big\rangle \cos 2\beta \sin 2\beta \\ &= \langle C_l^{TE} C_{l'}^{TB}\rangle \cos^2 2\alpha \cos 2\beta \sin 2\beta + \langle C_l^{TE} C_{l'}^{TE}\rangle \cos 2\alpha \sin 2\alpha \cos 2\beta \sin 2\beta \\ &- \langle C_l^{TB} C_{l'}^{TB}\rangle \cos 2\alpha \sin 2\alpha \cos 2\beta \sin 2\beta - \langle C_l^{TB} C_{l'}^{TE}\rangle \sin^2 2\alpha \cos 2\beta \sin 4\beta\end{aligned}$$

4.

$$\begin{aligned}\langle C_l^{TE,o} C_{l'}^{TE,o}\rangle \sin^2 2\beta &= \Big\langle \left[C_l^{TE}\cos 2\alpha - C_l^{TB}\sin 2\alpha\right]\left[C_{l'}^{TE}\cos 2\alpha - C_{l'}^{TB}\sin 2\alpha\right]\Big\rangle \sin^2 2\beta \\ &= \langle C_l^{TE} C_{l'}^{TE}\rangle \cos^2 2\alpha \sin^2 2\beta - \langle C_l^{TE} C_{l'}^{TB}\rangle \cos 2\alpha \sin 2\alpha \sin^2 2\beta \\ &- \langle C_l^{TB} C_{l'}^{TE}\rangle \cos 2\alpha \sin 2\alpha \sin^2 2\beta + \langle C_l^{TB} C_{l'}^{TB}\rangle \sin^2 2\alpha \sin^2 2\beta\end{aligned}$$

Now, let us combine all the terms we have computed individually:

$$\begin{aligned}\langle D_l^{TB,o} D_{l'}^{TB,o}\rangle \;&= \langle C_l^{TB} C_{l'}^{TB}\rangle \cos^2 2\alpha \cos^2 2\beta + \langle C_l^{TB} C_{l'}^{TE}\rangle \cos 2\alpha \sin 2\alpha \cos^2 2\beta \\ &+ \langle C_l^{TE} C_{l'}^{TB}\rangle \cos 2\alpha \sin 2\alpha \cos^2 2\beta + \langle C_l^{TE} C_{l'}^{TE}\rangle \sin^2 2\alpha \cos^2 2\beta \\ &- \langle C_l^{TB} C_{l'}^{TE}\rangle \cos^2 2\alpha \cos 2\beta \sin 2\beta + \langle C_l^{TB} C_{l'}^{TB}\rangle \cos 2\alpha \sin 2\alpha \cos 2\beta \sin 2\beta \\ &- \langle C_l^{TE} C_{l'}^{TE}\rangle \cos 2\alpha \sin 2\alpha \cos 2\beta \sin 2\beta + \langle C_l^{TE} C_{l'}^{TB}\rangle \sin^2 2\alpha \cos 2\beta \sin 2\beta \\ &- \langle C_l^{TE} C_{l'}^{TB}\rangle \cos^2 2\alpha \cos 2\beta \sin 2\beta - \langle C_l^{TE} C_{l'}^{TE}\rangle \cos 2\alpha \sin 2\alpha \cos 2\beta \sin 2\beta \\ &+ \langle C_l^{TB} C_{l'}^{TB}\rangle \cos 2\alpha \sin 2\alpha \cos 2\beta \sin 2\beta + \langle C_l^{TB} C_{l'}^{TE}\rangle \sin^2 2\alpha \cos 2\beta \sin 4\beta \\ &+ \langle C_l^{TE} C_{l'}^{TE}\rangle \cos^2 2\alpha \sin^2 2\beta - \langle C_l^{TE} C_{l'}^{TB}\rangle \cos 2\alpha \sin 2\alpha \sin^2 2\beta \\ &- \langle C_l^{TB} C_{l'}^{TE}\rangle \cos 2\alpha \sin 2\alpha \sin^2 2\beta + \langle C_l^{TB} C_{l'}^{TB}\rangle \sin^2 2\alpha \sin^2 2\beta \,.\end{aligned}$$

By applying the trigonometric identities for angle summation and subtraction, as introduced earlier, the expression above simplifies. Finally, the expectation value of the correlation between the

D-estimators for the TB-TB case becomes:

$$\langle D_l^{TB,o} D_{l'}^{TB,o} \rangle = \langle C_l^{TB} C_{l'}^{TB} \rangle \cos^2 2(\alpha - \beta) \tag{A.1}$$
$$+ \langle C_l^{TB} C_{l'}^{TE} \rangle \frac{1}{2} \sin 4(\alpha - \beta) \tag{A.2}$$
$$+ \langle C_l^{TE} C_{l'}^{TB} \rangle \frac{1}{2} \sin 4(\alpha - \beta) \tag{A.3}$$
$$+ \langle C_l^{TE} C_{l'}^{TE} \rangle \sin^2 2(\alpha - \beta). \tag{A.4}$$

Recalling Eq.s 3.6 and A.4, as shown previously:

$$\begin{aligned}
\left\langle \left(D_l^{TB,o} - D_l^{TB,o} \right) \left(D_{l'}^{TB,o} - D_{l'}^{TB,o} \right) \right\rangle &= \langle D_{l'}^{TB,o} D_{l'}^{TB,o} \rangle - \langle D_l^{TB,o} \rangle \langle D_{l'}^{TB,o} \rangle \\
&= \langle C_l^{TB} C_{l'}^{TB} \rangle \cos^2 2(\alpha - \beta) \\
&+ \langle C_l^{TB} C_{l'}^{TE} \rangle \frac{1}{2} \sin 4(\alpha - \beta) \\
&+ \langle C_l^{TE} C_{l'}^{TB} \rangle \frac{1}{2} \sin 4(\alpha - \beta) \\
&+ \langle C_l^{TE} C_{l'}^{TE} \rangle \sin^2 2(\alpha - \beta) \\
&- \langle C_l^{TE} \rangle \langle C_{l'}^{TE} \rangle \sin^2 2(\alpha - \beta) \,.
\end{aligned}$$

We now proceed by examining the expectation values of each angular power spectrum individually, applying Eq. 2.37:

1.

$$C_l^{TB} = \frac{1}{2l+1} \sum_{m=-l}^{l} a_{lm}^T (a_{lm}^B)^* \,,$$

and

$$\begin{aligned}
\langle C_l^{TB} C_{l'}^{TB} \rangle &= \frac{1}{2l+1} \frac{1}{2l'+1} \left\langle \sum_{m=-l}^{l} \sum_{m'=-l'}^{l'} a_{lm}^T (a_{lm}^B)^* a_{l'm'}^T (a_{l'm'}^B)^* \right\rangle \\
&= \frac{1}{2l+1} \frac{1}{2l'+1} \sum_{mm'} \langle a_{lm}^T (a_{lm}^B)^* a_{l'm'}^T (a_{l'm'}^B)^* \rangle \,.
\end{aligned}$$

Applying the Wick's theorem;

$$\langle C_l^{TB} C_{l'}^{TB} \rangle = \frac{1}{2l+1}\frac{1}{2l'+1}\sum_{mm'}\Big\{ \langle a_{lm}^T (a_{lm}^B)^* \rangle \langle a_{l'm'}^T (a_{l'm'}^B)^* \rangle + \langle a_{lm}^T a_{l'm'}^T \rangle \langle (a_{lm}^B)^* (a_{l'm'}^B)^* \rangle + \langle a_{lm}^T (a_{l'm'}^B)^* \rangle \langle (a_{lm}^B)^* a_{l'm'}^T \rangle \Big\} .$$

Using Eq.s 2.36 and 2.35 the above expression becomes:

$$= \frac{1}{2l+1}\frac{1}{2l'+1}\Big\{ \sum_m \sum_{m'} C_l^{TB} C_{l'}^{TB} + \sum_m \sum_{m'} C_l^{TT} \delta_{ll'} \delta_{m-m'} C_l^{BB} \delta_{ll'} \delta_{-mm'} + \sum_m \sum_{m'} C_l^{TB} \delta_{ll'} \delta_{mm'} C_l^{TB} \delta_{ll'} \delta_{mm'} \Big\} .$$

Using the property of Kronecker delta given in Eq. 3.8, and the sums over l, l', m, and m', we can now express the following:

$$\langle C_l^{TB} C_{l'}^{TB} \rangle = \frac{1}{(2l+1)^2}\Big\{ (2l+1)^2 C_l^{TB} C_{l'}^{TB} + \delta_{ll'} C_l^{TT} C_l^{BB} \sum_{mm'} \delta_{m-m'} + \delta_{ll'} (C_l^{TB})^2 \sum_{mm'} \delta_{mm'} \Big\}$$
$$= C_l^{TB} C_{l'}^{TB} + \frac{\delta_{ll'}}{2l+1}\left[C_l^{TT} C_l^{BB} + (C_l^{TB})^2 \right] .$$

Considering $C_l^{TB} = 0$, the absence of parity-violating physics at the last scattering surface,

$$\Rightarrow \langle C_l^{TB} C_{l'}^{TB} \rangle = \frac{\delta_{ll'}}{2l+1} C_l^{TT} C_l^{BB}.$$

2. Using

$$C_{l'}^{TE} = \frac{1}{2l+1}\sum_{m=-l'}^{l'} a_{l'm'}^T (a_{l'm'}^E)^* ,$$

we can now write:

$$\langle C_l^{TB} C_{l'}^{TE} \rangle = \frac{1}{2l+1}\frac{1}{2l'+1}\Big\langle \sum_{m=-l}^{l} \sum_{m'=-l'}^{l'} a_{lm}^T (a_{lm}^B)^* a_{l'm'}^T (a_{l'm'}^E)^* \Big\rangle$$

$$= \frac{1}{2l+1}\frac{1}{2l'+1}\sum_{mm'}\langle a^T_{lm}(a^B_{lm})^* a^T_{l'm'}(a^E_{l'm'})^*\rangle$$
$$= \frac{1}{2l+1}\frac{1}{2l'+1}\sum_{mm'}\Big\{\langle a^T_{lm}(a^B_{lm})^*\rangle\langle a^T_{l'm'}(a^E_{l'm'})^*\rangle + \langle a^T_{lm}a^T_{l'm'}\rangle\langle (a^B_{lm})^*(a^E_{l'm'})^*\rangle$$
$$+ \langle a^T_{lm}(a^E_{l'm'})^*\rangle\langle (a^B_{lm})^* a^T_{l'm'}\rangle\Big\}\,.$$

After some algebra, the above expression becomes:

$$\langle C^{TB}_l C^{TB}_{l'}\rangle = C^{TB}_l C^{TE}_{l'} + \frac{\delta_{ll'}}{2l+1}\left(C^{TT}_l C^{EB}_l + C^{TB}_l C^{TE}_l\right)\,.$$

Considering $C^{TB}_l, C^{EB}_l = 0$,

$$\langle C^{TB}_l C^{TB}_{l'}\rangle = 0\,.$$

3.

$$\langle C^{TE}_l C^{TB}_{l'}\rangle = \frac{1}{2l+1}\frac{1}{2l'+1}\Big\langle\sum_{m=-l}^{l}\sum_{m'=-l'}^{l'} a^T_{lm}(a^E_{lm})^* a^T_{l'm'}(a^B_{l'm'})^*\Big\rangle$$
$$= \frac{1}{2l+1}\frac{1}{2l'+1}\sum_{mm'}\langle a^T_{lm}(a^E_{lm})^* a^T_{l'm'}(a^B_{l'm'})^*\rangle$$
$$= \frac{1}{2l+1}\frac{1}{2l'+1}\sum_{mm'}\Big\{\langle a^T_{lm}(a^E_{lm})^*\rangle\langle a^T_{l'm'}(a^B_{l'm'})^*\rangle + \langle a^T_{lm}a^T_{l'm'}\rangle\langle (a^E_{lm})^*(a^B_{l'm'})^*\rangle$$
$$+ \langle a^T_{lm}(a^B_{l'm'})^*\rangle\langle (a^E_{lm})^* a^T_{l'm'}\rangle\Big\}$$

After some algebra, the above expression becomes:

$$\langle C^{TE}_l C^{TB}_{l'}\rangle = C^{TE}_l C^{TB}_{l'} + \frac{\delta_{ll'}}{2l+1}\left(C^{TT}_l C^{EB}_l + C^{TB}_l C^{TE}_l\right)\,.$$

Assuming $C^{TB}_l, C^{EB}_l = 0$,

$$\langle C^{TE}_l C^{TB}_{l'}\rangle = 0\,.$$

4.

$$\begin{aligned}\langle C_l^{TE} C_{l'}^{TE}\rangle &= \frac{1}{2l+1}\frac{1}{2l'+1}\Big\langle \sum_{m=-l}^{l}\sum_{m'=-l'}^{l'} a_{lm}^{T}(a_{lm}^{E})^{*} a_{l'm'}^{T}(a_{l'm'}^{E})^{*}\Big\rangle \\ &= \frac{1}{2l+1}\frac{1}{2l'+1}\sum_{mm'}\langle a_{lm}^{T}(a_{lm}^{E})^{*} a_{l'm'}^{T}(a_{l'm'}^{E})^{*}\rangle \\ &= \frac{1}{2l+1}\frac{1}{2l'+1}\sum_{mm'}\Big\{\langle a_{lm}^{T}(a_{lm}^{E})^{*}\rangle\langle a_{l'm'}^{T}(a_{l'm'}^{E})^{*}\rangle + \langle a_{lm}^{T}a_{l'm'}^{T}\rangle\langle (a_{lm}^{E})^{*}(a_{l'm'}^{E})^{*}\rangle \\ &+ \langle a_{lm}^{T}(a_{l'm'}^{E})^{*}\rangle\langle (a_{lm}^{E})^{*}a_{l'm'}^{T}\rangle\Big\}\end{aligned}$$

After some algebra, the above expression becomes:

$$\langle C_l^{TE} C_{l'}^{TE}\rangle = C_l^{TE} C_{l'}^{TE} + \frac{\delta_{ll'}}{2l+1}\left[C_l^{TT} C_l^{EE} + (C_l^{TE})^2\right] .$$

5. Following the same approach as shown previously in the EB case in Section 3.2.1:

$$\langle C_l^{TE}\rangle = C_l^{TE} ,$$

and

$$\langle C_{l'}^{TE}\rangle = C_{l'}^{TE} .$$

Then;

$$\langle C_l^{TE}\rangle\langle C_{l'}^{TE}\rangle = C_l^{TE} C_{l'}^{TE} .$$

Now, combining all the terms computed separately earlier:

$$\begin{aligned}\langle D_l^{TB,o} D_{l'}^{TB,o}\rangle &= \frac{\delta_{ll'}}{2l+1} C_l^{TT} C_l^{BB}\cos^2 2(\alpha-\beta) + C_l^{TE} C_{l'}^{TE}\sin^2 2(\alpha-\beta) \\ &+ \frac{\delta_{ll'}}{2l+1}\left(C_l^{TT} C_l^{EE} + (C_l^{TE})^2\right)\sin^2 2(\alpha-\beta) \\ &= \frac{\delta_{ll'}}{2l+1} C_l^{TT} C_l^{BB}(1-\sin^2 2(\alpha-\beta)) \\ &+ \frac{\delta_{ll'}}{2l+1}\left(C_l^{TT} C_l^{EE} + (C_l^{TE})^2\right)\sin^2 2(\alpha-\beta) + C_l^{TE} C_{l'}^{TE}\sin^2 2(\alpha-\beta)\end{aligned}$$

$$= \frac{\delta_{ll'}}{2l+1}\left(C_l^{TT}C_l^{EE} + (C_l^{TE})^2 - C_l^{TT}C_l^{BB}\right)\sin^2 2(\alpha-\beta)$$
$$+ \frac{\delta_{ll'}}{2l+1}C_l^{TT}C_l^{BB} + C_l^{TE}C_{l'}^{TE}\sin^2 2(\alpha-\beta)\,.$$

Rewriting the above expression, it becomes:

$$\langle D_l^{TB,o}D_{l'}^{TB,o}\rangle = \frac{\delta_{ll'}}{2l+1}\left[\left(C_l^{TT}C_l^{EE} + (C_l^{TE})^2 - C_l^{TT}C_l^{BB}\right)\sin^2 2(\alpha-\beta) + C_l^{TT}C_l^{BB}\right] + C_l^{TE}C_{l'}^{TE}\sin^2 2(\alpha-\beta)\,. \tag{A.5}$$

Now we can write:

$$\langle D_l^{TB,o}D_{l'}^{TB,o}\rangle - \langle D_l^{TB,o}\rangle\langle D_{l'}^{TB,o}\rangle = \frac{\delta_{ll'}}{2l+1}\left[\left(C_l^{TT}C_l^{EE} + (C_l^{TE})^2 - C_l^{TT}C_l^{BB}\right)\sin^2 2(\alpha-\beta) + C_l^{TT}C_l^{BB}\right]$$
$$+ C_l^{TE}C_{l'}^{TE}\sin^2 2(\alpha-\beta) - C_l^{TE}C_{l'}^{TE}\sin^2 2(\alpha-\beta)\,.$$

Finally, the covariance of TB-TB becomes:

$$\langle D_l^{TB,o}D_{l'}^{TB,o}\rangle - \langle D_l^{TB,o}\rangle\langle D_{l'}^{TB,o}\rangle = \frac{\delta_{ll'}}{2l+1}\left[\left(C_l^{TT}C_l^{EE} + (C_l^{TE})^2 - C_l^{TT}C_l^{BB}\right)\sin^2 2(\alpha-\beta) + C_l^{TT}C_l^{BB}\right]\,. \tag{A.6}$$

In the case $\alpha = \beta$, our result becomes:

$$\langle D_l^{TB,o}D_{l'}^{TB,o}\rangle - \langle D_l^{TB,o}\rangle\langle D_{l'}^{TB,o}\rangle = \frac{\delta_{ll'}}{2l+1}C_l^{TT}C_l^{BB}\,. \tag{A.7}$$

A.2 Cross-covariance of C_l^{TB}-C_l^{EB}

Using Eq.s 3.1 and 3.2, we can write:

$$\langle D_l^{TB,o}D_{l'}^{EB,o}\rangle = \left\langle\left[C_l^{TB,o}\cos 2\beta - C_l^{TE,o}\sin 2\beta\right]\right.$$
$$\left.\cdot\left[C_{l'}^{EB,o}\cos 4\beta - \frac{1}{2}(C_{l'}^{EE,o} - C_{l'}^{BB,o})\sin 4\beta\right]\right\rangle$$
$$= \langle C_l^{TB,o}C_{l'}^{EB,o}\rangle\cos 2\beta\cos 4\beta - \langle C_l^{TB,o}\frac{1}{2}(C_{l'}^{EE,o} - C_{l'}^{BB,o})\rangle\cos 2\beta\sin 4\beta$$
$$- \langle C_l^{TE,o}C_{l'}^{EB,o}\rangle\cos 4\beta\sin 2\beta + \langle C_l^{TE,o}\frac{1}{2}(C_{l'}^{EE,o} - C_{l'}^{BB,o})\rangle\sin 2\beta\sin 4\beta\,.$$

To compute $\langle D_l^{TB,o} D_{l'}^{EB,o} \rangle$, we must first evaluate the expectation values of each term, utilizing Equations 2.43, 2.46, 2.47, and 2.48:

1.

$$\begin{aligned}
\langle C_l^{TB,o} C_{l'}^{EB,o} \rangle \cos^2 4\beta = \Big\langle \big[C_l^{TB} \cos 2\alpha + C_l^{TE} \sin 2\alpha \big] \\
\cdot \left[C_{l'}^{EB} \cos 4\alpha + \frac{1}{2}(C_{l'}^{EE} - C_{l'}^{BB}) \sin 4\alpha \right] \Big\rangle \cos 2\beta \cos 4\beta \\
= \langle C_l^{TB} C_{l'}^{EB} \rangle \cos 2\alpha \cos 4\alpha \cos 2\beta \cos 4\beta \\
+ \langle C_l^{TB} \frac{1}{2}(C_{l'}^{EE} - C_{l'}^{BB}) \rangle \cos 2\alpha \sin 4\alpha \cos 2\beta \cos 4\beta \\
+ \langle C_l^{TE} C_{l'}^{EB} \rangle \cos 4\alpha \sin 2\alpha \cos 2\beta \cos 4\beta \\
+ \langle C_l^{TE} \frac{1}{2}(C_{l'}^{EE} - C_{l'}^{BB}) \rangle \sin 2\alpha \sin 4\alpha \cos 2\beta \cos 4\beta \,.
\end{aligned}$$

2.

$$\begin{aligned}
\langle C_l^{TB,o} \frac{1}{2}(C_{l'}^{EE,o} - C_{l'}^{BB,o}) \rangle \cos 2\beta \sin 4\beta = \Big\langle \big[C_l^{TB} \cos 2\alpha + C_l^{TE} \sin 2\alpha \big] \\
\cdot \left[\frac{1}{2}(C_{l'}^{EE} - C_{l'}^{BB}) \cos 4\alpha - C_{l'}^{EB} \sin 4\alpha \right] \Big\rangle \cos 2\beta \sin 4\beta \\
= \langle C_l^{TB} \frac{1}{2}(C_{l'}^{EE} - C_{l'}^{BB}) \rangle \cos 2\alpha \cos 4\alpha \cos 2\beta \sin 4\beta \\
- \langle C_l^{TB} C_{l'}^{EB} \rangle \cos 2\alpha \sin 4\alpha \cos 2\beta \sin 4\beta \\
+ \langle C_l^{TE} \frac{1}{2}(C_{l'}^{EE} - C_{l'}^{BB}) \rangle \cos 4\alpha \sin 2\alpha \cos 2\beta \sin 4\beta \\
- \langle C_l^{TE} C_{l'}^{EB} \rangle \sin 2\alpha \sin 4\alpha \cos 2\beta \sin 4\beta \,.
\end{aligned}$$

3.

$$\begin{aligned}
\langle C_l^{TE,o} C_{l'}^{EB,o} \rangle \cos 4\beta \sin 2\beta = \Big\langle \big[C_l^{TE} \cos 2\alpha - C_l^{TB} \sin 2\alpha \big] \\
\cdot \left[C_{l'}^{EB} \cos 4\alpha + \frac{1}{2}(C_{l'}^{EE} - C_{l'}^{BB}) \sin 4\alpha \right] \Big\rangle \cos 4\beta \sin 2\beta \\
= \langle C_l^{TE} C_{l'}^{EB} \rangle \cos 2\alpha \cos 4\alpha \cos 4\beta \sin 2\beta \\
+ \langle C_l^{TE} \frac{1}{2}(C_{l'}^{EE} - C_{l'}^{BB}) \rangle \cos 2\alpha \sin 4\alpha \cos 4\beta \sin 2\beta \\
- \langle C_l^{TB} C_{l'}^{EB} \rangle \cos 4\alpha \sin 2\alpha \cos 4\beta \sin 2\beta
\end{aligned}$$

$$- \langle C_l^{TB} \frac{1}{2}(C_{l'}^{EE} - C_{l'}^{BB}) \rangle \sin 2\alpha \sin 4\alpha \cos 4\beta \sin 2\beta \,.$$

4.

$$\begin{aligned}
\langle C_l^{TE,o} \frac{1}{2}(C_{l'}^{EE,o} - C_{l'}^{BB,o}) \rangle \sin 2\beta \sin 4\beta = \Big\langle \big[C_l^{TE} \cos 2\alpha - C_l^{TB} \sin 2\alpha \big] \\
\cdot \left[\frac{1}{2}(C_{l'}^{EE} - C_{l'}^{BB}) \cos 4\alpha - C_{l'}^{EB} \sin 4\alpha \right] \Big\rangle \sin 2\beta \sin 4\beta \\
= \langle C_l^{TE} \frac{1}{2}(C_{l'}^{EE} - C_{l'}^{BB}) \rangle \cos 2\alpha \cos 4\alpha \sin 2\beta \sin 4\beta \\
- \langle C_l^{TE} C_{l'}^{EB} \rangle \cos 2\alpha \sin 4\alpha \sin 2\beta \sin 4\beta \\
- \langle C_l^{TB} \frac{1}{2}(C_{l'}^{EE} - C_{l'}^{BB}) \rangle \cos 4\alpha \sin 2\alpha \sin 2\beta \sin 4\beta \\
+ \langle C_l^{TB} C_{l'}^{EB} \rangle \sin 2\alpha \sin 4\alpha \sin 2\beta \sin 4\beta \,.
\end{aligned}$$

Now, let us combine all the terms we have computed individually:

$$\begin{aligned}
\langle D_l^{TB,o} D_{l'}^{EB,o} \rangle \; &= \langle C_l^{TB} C_{l'}^{EB} \rangle \cos 2\alpha \cos 4\alpha \cos 2\beta \cos 4\beta \\
&+ \langle C_l^{TB} \frac{1}{2}(C_{l'}^{EE} - C_{l'}^{BB}) \rangle \cos 2\alpha \sin 4\alpha \cos 2\beta \cos 4\beta \\
&+ \langle C_l^{TE} C_{l'}^{EB} \rangle \cos 4\alpha \sin 2\alpha \cos 2\beta \cos 4\beta \\
&+ \langle C_l^{TE} \frac{1}{2}(C_{l'}^{EE} - C_{l'}^{BB}) \rangle \sin 2\alpha \sin 4\alpha \cos 2\beta \cos 4\beta \\
&- \langle C_l^{TB} \frac{1}{2}(C_{l'}^{EE} - C_{l'}^{BB}) \rangle \cos 2\alpha \cos 4\alpha \cos 2\beta \sin 4\beta \\
&+ \langle C_l^{TB} C_{l'}^{EB} \rangle \cos 2\alpha \sin 4\alpha \cos 2\beta \sin 4\beta \\
&- \langle C_l^{TE} \frac{1}{2}(C_{l'}^{EE} - C_{l'}^{BB}) \rangle \cos 4\alpha \sin 2\alpha \cos 2\beta \sin 4\beta \\
&+ \langle C_l^{TE} C_{l'}^{EB} \rangle \sin 2\alpha \sin 4\alpha \cos 2\beta \sin 4\beta \\
&- \langle C_l^{TE} C_{l'}^{EB} \rangle \cos 2\alpha \cos 4\alpha \cos 4\beta \sin 2\beta \\
&- \langle C_l^{TE} \frac{1}{2}(C_{l'}^{EE} - C_{l'}^{BB}) \rangle \cos 2\alpha \sin 4\alpha \cos 4\beta \sin 2\beta \\
&+ \langle C_l^{TB} C_{l'}^{EB} \rangle \cos 4\alpha \sin 2\alpha \cos 4\beta \sin 2\beta \\
&+ \langle C_l^{TB} \frac{1}{2}(C_{l'}^{EE} - C_{l'}^{BB}) \rangle \sin 2\alpha \sin 4\alpha \cos 4\beta \sin 2\beta \\
&+ \langle C_l^{TE} \frac{1}{2}(C_{l'}^{EE} - C_{l'}^{BB}) \rangle \cos 2\alpha \cos 4\alpha \sin 2\beta \sin 4\beta
\end{aligned}$$

$$
\begin{aligned}
&- \langle C_l^{TE} C_{l'}^{EB} \rangle \cos 2\alpha \sin 4\alpha \sin 2\beta \sin 4\beta \\
&- \langle C_l^{TB} \frac{1}{2} (C_{l'}^{EE} - C_{l'}^{BB}) \rangle \cos 4\alpha \sin 2\alpha \sin 2\beta \sin 4\beta \\
&+ \langle C_l^{TB} C_{l'}^{EB} \rangle \sin 2\alpha \sin 4\alpha \sin 2\beta \sin 4\beta \,.
\end{aligned}
$$

Simplifying the expression above by applying the trigonometric identities for angle summation and subtraction, as introduced earlier, the expectation value of the correlation between the D-estimators for the TB-EB case becomes:

$$
\begin{aligned}
\langle D_l^{TB,o} D_{l'}^{EB,o} \rangle = &\langle C_l^{TB} C_{l'}^{EB} \rangle \cos 2(\alpha - \beta) \cos 4(\alpha - \beta) && \text{(A.8)} \\
&+ \langle C_l^{TB} \frac{1}{2} (C_{l'}^{EE} - C_{l'}^{BB}) \rangle \cos 2(\alpha - \beta) \sin 4(\alpha - \beta) && \text{(A.9)} \\
&+ \langle C_l^{TE} C_{l'}^{EB} \rangle \frac{1}{2} \sin 4(\alpha - \beta) && \text{(A.10)} \\
&+ \langle C_l^{TE} \frac{1}{2} (C_{l'}^{EE} - C_{l'}^{BB}) \rangle \sin 4(\alpha - \beta) \sin 2(\alpha - \beta). && \text{(A.11)}
\end{aligned}
$$

Recalling Eq.s 3.6, 3.5, and A.11, we can write:

$$
\begin{aligned}
\left\langle \left(D_l^{TB,o} - D_l^{EB,o} \right) \left(D_{l'}^{TB,o} - D_{l'}^{EB,o} \right) \right\rangle = &\langle C_l^{TB} C_{l'}^{EB} \rangle \cos 2(\alpha - \beta) \cos 4(\alpha - \beta) \\
&+ \langle C_l^{TB} \frac{1}{2} (C_{l'}^{EE} - C_{l'}^{BB}) \rangle \cos 2(\alpha - \beta) \sin 4(\alpha - \beta) \\
&+ \langle C_l^{TE} C_{l'}^{EB} \rangle \sin 2(\alpha - \beta) \cos 4(\alpha - \beta) \\
&+ \langle C_l^{TE} \frac{1}{2} (C_{l'}^{EE} - C_{l'}^{BB}) \rangle \sin 2(\alpha - \beta) \sin 4(\alpha - \beta) \\
&- \langle C_l^{TE} \rangle \frac{1}{2} \left(\langle C_{l'}^{EE} \rangle - \langle C_{l'}^{BB} \rangle \right) \sin 2(\alpha - \beta) \sin 4(\alpha - \beta) \,.
\end{aligned}
$$

We now proceed by examining the expectation values of each angular power spectrum individually, applying Eq. 2.37:

1.

$$
\langle C_l^{TB} C_{l'}^{EB} \rangle = \frac{1}{2l+1} \frac{1}{2l'+1} \sum_{mm'} \langle a_{lm}^T (a_{lm}^B)^* a_{l'm'}^E (a_{l'm'}^B)^* \rangle
$$

Applying the Wick's theorem;

$$\langle C_l^{TB} C_{l'}^{EB} \rangle = \frac{1}{2l+1}\frac{1}{2l'+1}\sum_{mm'}\Big\{ \langle a_{lm}^T (a_{lm}^B)^* \rangle \langle a_{l'm'}^E (a_{l'm'}^B)^* \rangle + \langle a_{lm}^T a_{l'm'}^E \rangle \langle (a_{lm}^B)^* (a_{l'm'}^B)^* \rangle + \langle a_{lm}^T (a_{l'm'}^B)^* \rangle \langle (a_{lm}^B)^* a_{l'm'}^E \rangle \Big\} .$$

Using Eq.s 2.36, the property of Kronecker delta in Eq. 3.8, the sums over l, l', m, m', and Eq. 2.35, we can now express the following:

$$\langle C_l^{TB} C_{l'}^{TB} \rangle = C_l^{TB} C_{l'}^{EB} + \frac{\delta_{ll'}}{2l+1}\left(C_l^{TE} C_l^{BB} + C_l^{TB} C_l^{EB} \right) .$$

Considering $C_l^{TB}, C_l^{EB} = 0$ at the last scattering surface with no parity-violating physics:

$$\langle C_l^{TB} C_{l'}^{EB} \rangle = \frac{\delta_{ll'}}{2l+1} C_l^{TE} C_l^{BB} .$$

2.

$$\begin{aligned}
\langle C_l^{TE} \frac{1}{2}(C_{l'}^{EE} - C_{l'}^{BB}) \rangle &= \langle \frac{1}{2} C_l^{TE} C_{l'}^{EE} - \frac{1}{2} C_l^{TE} C_{l'}^{BB} \rangle \\
&= \frac{1}{2}\langle C_l^{TE} C_{l'}^{EE} \rangle - \frac{1}{2}\langle C_l^{TE} C_{l'}^{BB} \rangle \\
&= \frac{1}{2}\frac{1}{2l+1}\frac{1}{2l'+1}\sum_{mm'}\langle a_{lm}^T (a_{lm}^E)^* a_{l'm'}^E (a_{l'm'}^E)^* \rangle \\
&- \frac{1}{2}\frac{1}{2l+1}\frac{1}{2l'+1}\sum_{mm'}\langle a_{lm}^T (a_{lm}^E)^* a_{l'm'}^B (a_{l'm'}^B)^* \rangle \\
&= \frac{1}{2}\frac{1}{2l+1}\frac{1}{2l'+1}\sum_{mm'}\Big\{ \langle a_{lm}^T (a_{lm}^E)^* \rangle \langle a_{l'm'}^E (a_{l'm'}^E)^* \rangle + \langle a_{lm}^T a_{l'm'}^E \rangle \langle (a_{lm}^E)^* (a_{l'm'}^E)^* \rangle \\
&+ \langle a_{lm}^T a_{l'm'}^E \rangle \langle (a_{lm}^E)^* a_{l'm'}^E \rangle \Big\} - \frac{1}{2}\frac{1}{2l+1}\frac{1}{2l'+1}\sum_{mm'}\Big\{ \langle a_{lm}^T (a_{lm}^E)^* \rangle \langle a_{l'm'}^B (a_{l'm'}^B)^* \rangle \\
&+ \langle a_{lm}^T a_{l'm'}^B \rangle \langle (a_{lm}^E)^* (a_{l'm'}^B)^* \rangle + \langle a_{lm}^T (a_{l'm'}^B)^* \rangle \langle (a_{lm}^E)^* a_{l'm'}^B \rangle \Big\}
\end{aligned}$$

After some algebra, the above expression becomes:

$$\langle C_l^{TE} \frac{1}{2}(C_{l'}^{EE} - C_{l'}^{BB}) \rangle = \frac{1}{2} C_l^{TE} C_{l'}^{EE} + \frac{\delta_{ll'}}{2l+1} C_l^{TE} C_l^{EE} - \frac{1}{2} C_l^{TE} C_{l'}^{BB} - \frac{\delta_{ll'}}{2l+1} C_l^{TE} C_l^{BB} .$$

Considering $C_l^{TB}, C_l^{EB} = 0$:

$$\langle C_l^{TE} \frac{1}{2}(C_{l'}^{EE} - C_{l'}^{BB})\rangle = \frac{1}{2} C_l^{TE}(C_{l'}^{EE} - C_{l'}^{BB}) + \frac{\delta_{ll'}}{2l+1} C_l^{TE} C_l^{EE} \,.$$

3.

$$\begin{aligned}
\langle C_l^{TB} \frac{1}{2}(C_{l'}^{EE} - C_{l'}^{BB})\rangle &= \langle \frac{1}{2} C_l^{TB} C_{l'}^{EE} - \frac{1}{2} C_l^{TB} C_{l'}^{BB}\rangle \\
&= \frac{1}{2}\langle C_l^{TB} C_{l'}^{EE}\rangle - \frac{1}{2}\langle C_l^{TB} C_{l'}^{BB}\rangle \\
&= \frac{1}{2}\frac{1}{2l+1}\frac{1}{2l'+1}\sum_{mm'}\langle a_{lm}^T (a_{lm}^B)^* a_{l'm'}^E (a_{l'm'}^E)^*\rangle \\
&- \frac{1}{2}\frac{1}{2l+1}\frac{1}{2l'+1}\sum_{mm'}\langle a_{lm}^T (a_{lm}^B)^* a_{l'm'}^B (a_{l'm'}^B)^*\rangle \\
&= \frac{1}{2}\frac{1}{2l+1}\frac{1}{2l'+1}\sum_{mm'}\Big\{ \langle a_{lm}^T (a_{lm}^B)^*\rangle\langle a_{l'm'}^E (a_{l'm'}^E)^*\rangle + \langle a_{lm}^T a_{l'm'}^E\rangle\langle (a_{lm}^B)^* (a_{l'm'}^E)^*\rangle \\
&+ \langle a_{lm}^T a_{l'm'}^E\rangle\langle (a_{lm}^B)^* a_{l'm'}^E\rangle\Big\} - \frac{1}{2}\frac{1}{2l+1}\frac{1}{2l'+1}\sum_{mm'}\Big\{ \langle a_{lm}^T (a_{lm}^B)^*\rangle\langle a_{l'm'}^B (a_{l'm'}^B)^*\rangle \\
&+ \langle a_{lm}^T a_{l'm'}^B\rangle\langle (a_{lm}^B)^* (a_{l'm'}^B)^*\rangle + \langle a_{lm}^T (a_{l'm'}^B)^*\rangle\langle (a_{lm}^B)^* a_{l'm'}^B\rangle\Big\}
\end{aligned}$$

After some algebra, the above expression becomes:

$$\langle C_l^{TB} \frac{1}{2}(C_{l'}^{EE} - C_{l'}^{BB})\rangle = \frac{1}{2} C_l^{TB} C_{l'}^{EE} + \frac{\delta_{ll'}}{2l+1} C_l^{TE} C_l^{EB} - \frac{1}{2} C_l^{TB} C_{l'}^{BB} - \frac{\delta_{ll'}}{2l+1} C_l^{TB} C_l^{BB} \,.$$

Considering $C_l^{TB}, C_l^{EB} = 0$:

$$\langle C_l^{TB} \frac{1}{2}(C_{l'}^{EE} - C_{l'}^{BB})\rangle = 0 \,.$$

4.

$$\begin{aligned}
\langle C_l^{TE} C_{l'}^{EB}\rangle &= \frac{1}{2l+1}\frac{1}{2l'+1}\sum_{mm'}\langle a_{lm}^T (a_{lm}^E)^* a_{l'm'}^E (a_{l'm'}^B)^*\rangle \\
&= \frac{1}{2l+1}\frac{1}{2l'+1}\sum_{mm'}\Big\{ \langle a_{lm}^T (a_{lm}^E)^*\rangle\langle a_{l'm'}^E (a_{l'm'}^B)^*\rangle + \langle a_{lm}^T a_{l'm'}^E\rangle\langle (a_{lm}^E)^* (a_{l'm'}^B)^*\rangle \\
&+ \langle a_{lm}^T (a_{l'm'}^B)^*\rangle\langle (a_{lm}^E)^* a_{l'm'}^E\rangle\Big\}
\end{aligned}$$

After some algebra, the above expression becomes:

$$\langle C_l^{TE} C_{l'}^{TE} \rangle = C_l^{TE} C_{l'}^{EB} + \frac{\delta_{ll'}}{2l+1} C_l^{TE} C_l^{EB} \frac{\delta_{ll'}}{2l+1} C_l^{TB} C_l^{EE} \,.$$

Considering $C_l^{TB}, C_l^{EB} = 0$

$$\langle \langle C_l^{TE} C_{l'}^{TE} \rangle = 0 \,.$$

5.

$$\begin{aligned} \langle C_l^{TE} \rangle \frac{1}{2} \langle C_{l'}^{EE} - C_{l'}^{BB} \rangle &= \frac{1}{2} \langle C_l^{TE} \rangle \langle C_{l'}^{EE} \rangle - \frac{1}{2} \langle C_l^{TE} \rangle \langle C_{l'}^{BB} \rangle \\ &= C_l^{TE} \frac{1}{2} (C_{l'}^{EE} - C_{l'}^{BB}) \end{aligned}$$

Now, combining all the terms computed separately earlier:

$$\begin{aligned} \langle D_l^{TB,o} D_{l'}^{EB,o} \rangle = &\frac{\delta_{ll'}}{2l+1} C_l^{TE} C_l^{BB} \cos 2(\alpha-\beta) \cos 4(\alpha-\beta) \\ &+ \frac{1}{2} C_l^{TE} (C_{l'}^{EE} - C_{l'}^{BB}) \sin 2(\alpha-\beta) \sin 4(\alpha-\beta) \\ &+ \frac{\delta_{ll'}}{2l+1} C_l^{TE} C_l^{EE} \sin 2(\alpha-\beta) \sin 4(\alpha-\beta) \,, \end{aligned} \tag{A.12}$$

and

$$\begin{aligned} \langle D_l^{TB,o} D_{l'}^{EB,o} \rangle - \langle D_l^{TB,o} \rangle \langle D_{l'}^{EB,o} \rangle = &\frac{\delta_{ll'}}{2l+1} C_l^{TE} C_l^{BB} \cos 2(\alpha-\beta) \cos 4(\alpha-\beta) \\ &+ \frac{1}{2} C_l^{TE} (C_{l'}^{EE} - C_{l'}^{BB}) \sin 2(\alpha-\beta) \sin 4(\alpha-\beta) \\ &+ \frac{\delta_{ll'}}{2l+1} C_l^{TE} C_l^{EE} \sin 2(\alpha-\beta) \sin 4(\alpha-\beta) \\ &- \frac{1}{2} C_l^{TE} (C_{l'}^{EE} - C_{l'}^{BB}) \sin 2(\alpha-\beta) \sin 4(\alpha-\beta) \,. \end{aligned}$$

Finally, the covariance of TB-EB becomes:

$$\begin{aligned} \langle D_l^{TB,o} D_{l'}^{EB,o} \rangle - \langle D_l^{TB,o} \rangle \langle D_{l'}^{EB,o} \rangle = &\frac{\delta_{ll'}}{2l+1} \Big[C_l^{TE} C_l^{BB} \cos 2(\alpha-\beta) \cos 4(\alpha-\beta) \\ &+ C_l^{TE} C_l^{EE} \sin 2(\alpha-\beta) \sin 4(\alpha-\beta) \Big] \,. \end{aligned} \tag{A.13}$$

In the case $\alpha = \beta$, our result becomes:

$$\langle D_l^{TB,o} D_{l'}^{EB,o} \rangle - \langle D_l^{TB,o} \rangle \langle D_{l'}^{EB,o} \rangle = \frac{\delta_{ll'}}{2l+1} C_l^{TE} C_l^{BB} \,. \tag{A.14}$$

A.3 Cross-covariance of C_l^{EB}-C_l^{TB}

Using Eq.s 3.1 and 3.2, we can write:

$$\begin{aligned}
\langle D_l^{EB,o} D_{l'}^{TB,o} \rangle &= \left\langle \left[C_{l'}^{EB,o} \cos 4\beta - \frac{1}{2}(C_l^{EE,o} - C_l^{BB,o}) \sin 4\beta \right] \right. \\
&\quad \left. \cdot \left[C_{l'}^{TB,o} \cos 2\beta - C_{l'}^{TE,o} \sin 2\beta \right] \right\rangle \\
&= \langle C_l^{EB,o} C_{l'}^{TB,o} \rangle \cos 2\beta \cos 4\beta - \langle \frac{1}{2}(C_l^{EE,o} - C_l^{BB,o}) C_{l'}^{TB,o} \rangle \cos 2\beta \sin 4\beta \\
&\quad - \langle C_l^{EB,o} C_{l'}^{TE,o} \rangle \cos 4\beta \sin 2\beta + \langle \frac{1}{2}(C_l^{EE,o} - C_l^{BB,o}) C_{l'}^{TE,o} \rangle \sin 2\beta \sin 4\beta \,.
\end{aligned}$$

We can see that the above expression is identical to $\langle D_l^{TB,o} D_{l'}^{EB,o} \rangle$ except for the multipoles l and l', however yielding the same results as in Eq.s A.12 and A.14 after applying Wick's theorem with the rules used in previous sections. Therefore we can write:

$$\begin{aligned}
\langle D_l^{EB,o} D_{l'}^{TB,o} \rangle &= \frac{\delta_{ll'}}{2l+1} C_l^{TE} C_l^{BB} \cos 2(\alpha - \beta) \cos 4(\alpha - \beta) \\
&\quad + \frac{1}{2} C_l^{TE} (C_{l'}^{EE} - C_{l'}^{BB}) \sin 2(\alpha - \beta) \sin 4(\alpha - \beta) \\
&\quad + \frac{\delta_{ll'}}{2l+1} C_l^{TE} C_l^{EE} \sin 2(\alpha - \beta) \sin 4(\alpha - \beta) \,,
\end{aligned} \tag{A.15}$$

and

$$\langle D_l^{EB,o} D_{l'}^{TB,o} \rangle - \langle D_l^{EB,o} \rangle \langle D_{l'}^{TB,o} \rangle = \frac{\delta_{ll'}}{2l+1} C_l^{TE} C_l^{BB} \,. \tag{A.16}$$

References

[1] Y. Minami, E. Komatsu, New extraction of the cosmic birefringence from the planck 2018 polarization data, Phys. Rev. Lett. 125 (2020) 221301. doi:10.1103/PhysRevLett.125.221301.

[2] P. Diego-Palazuelos, J. R. Eskilt, Y. Minami, M. Tristram, R. M. Sullivan, A. J. Banday, R. B. Barreiro, H. K. Eriksen, K. M. Górski, R. Keskitalo, E. Komatsu, E. Martínez-González, D. Scott, P. Vielva, I. K. Wehus, Cosmic birefringence from the planck data release 4, Phys. Rev. Lett. 128 (2022) 091302. doi:10.1103/PhysRevLett.128.091302.

[3] J. R. Eskilt, Frequency-dependent constraints on cosmic birefringence from the lfi and hfi planck data release 4, A & A 662 (2022) A10. doi:10.1051/0004-6361/202243269.

[4] J. R. Eskilt, E. Komatsu, Improved constraints on cosmic birefringence from the wmap and planck cosmic microwave background polarization data, Phys. Rev. D 106 (2022) 063503. doi:10.1103/PhysRevD.106.063503.

[5] G. F. Smoot, C. L. Bennett, A. Kogut, E. L. Wright, J. Aymon, N. W. Boggess, E. S. Cheng, G. de Amici, S. Gulkis, M. G. Hauser, G. Hinshaw, P. D. Jackson, M. Janssen, E. Kaita, T. Kelsall, P. Keegstra, C. Lineweaver, K. Loewenstein, P. Lubin, J. Mather, S. S. Meyer, S. H. Moseley, T. Murdock, L. Rokke, R. F. Silverberg, L. Tenorio, R. Weiss, D. T. Wilkinson, Structure in the COBE Differential Microwave Radiometer First-Year Maps, The Astrophysical Journal Letters 396 (1992) L1. doi:10.1086/186504.

[6] C. L. Bennett, D. Larson, J. L. Weiland, N. Jarosik, G. Hinshaw, N. Odegard, K. M. Smith, R. S. Hill, B. Gold, M. Halpern, E. Komatsu, M. R. Nolta, L. Page, D. N. Spergel, E. Wollack, J. Dunkley, A. Kogut, M. Limon, S. S. Meyer, G. S. Tucker, E. L. Wright, Nine-year wilkinson microwave anisotropy probe (wmap) observations: Final maps and results, The Astrophysical Journal Supplement Series 208 (2) (2013) 20. doi:10.1088/0067-0049/208/2/20.

[7] N. Aghanim, Y. Akrami, M. Ashdown, J. Aumont, C. Baccigalupi, M. Ballardini, A. J. Banday, R. B. Barreiro, N. Bartolo, S. Basak, R. Battye, K. Benabed, J.-P. Bernard, M. Bersanelli,

P. Bielewicz, J. J. Bock, J. R. Bond, J. Borrill, F. R. Bouchet, F. Boulanger, M. Bucher, C. Burigana, R. C. Butler, E. Calabrese, J.-F. Cardoso, J. Carron, A. Challinor, H. C. Chiang, J. Chluba, L. P. L. Colombo, C. Combet, D. Contreras, B. P. Crill, F. Cuttaia, P. de Bernardis, G. de Zotti, J. Delabrouille, J.-M. Delouis, E. Di Valentino, J. M. Diego, O. Doré, M. Douspis, A. Ducout, X. Dupac, S. Dusini, G. Efstathiou, F. Elsner, T. A. Enßlin, H. K. Eriksen, Y. Fantaye, M. Farhang, J. Fergusson, R. Fernandez-Cobos, F. Finelli, F. Forastieri, M. Frailis, A. A. Fraisse, E. Franceschi, A. Frolov, S. Galeotta, S. Galli, K. Ganga, R. T. Génova-Santos, M. Gerbino, T. Ghosh, J. González-Nuevo, K. M. Górski, S. Gratton, A. Gruppuso, J. E. Gudmundsson, J. Hamann, W. Handley, F. K. Hansen, D. Herranz, S. R. Hildebrandt, E. Hivon, Z. Huang, A. H. Jaffe, W. C. Jones, A. Karakci, E. Keihänen, R. Keskitalo, K. Kiiveri, J. Kim, T. S. Kisner, L. Knox, N. Krachmalnicoff, M. Kunz, H. Kurki-Suonio, G. Lagache, J.-M. Lamarre, A. Lasenby, M. Lattanzi, C. R. Lawrence, M. Le Jeune, P. Lemos, J. Lesgourgues, F. Levrier, A. Lewis, M. Liguori, P. B. Lilje, M. Lilley, V. Lindholm, M. López-Caniego, P. M. Lubin, Y.-Z. Ma, J. F. Macías-Pérez, G. Maggio, D. Maino, N. Mandolesi, A. Mangilli, A. Marcos-Caballero, M. Maris, P. G. Martin, M. Martinelli, E. Martínez-González, S. Matarrese, N. Mauri, J. D. McEwen, P. R. Meinhold, A. Melchiorri, A. Mennella, M. Migliaccio, M. Millea, S. Mitra, M.-A. Miville-Deschênes, D. Molinari, L. Montier, G. Morgante, A. Moss, P. Natoli, H. U. Nørgaard-Nielsen, L. Pagano, D. Paoletti, B. Partridge, G. Patanchon, H. V. Peiris, F. Perrotta, V. Pettorino, F. Piacentini, L. Polastri, G. Polenta, J.-L. Puget, J. P. Rachen, M. Reinecke, M. Remazeilles, A. Renzi, G. Rocha, C. Rosset, G. Roudier, J. A. Rubiño-Martín, B. Ruiz-Granados, L. Salvati, M. Sandri, M. Savelainen, D. Scott, E. P. S. Shellard, C. Sirignano, G. Sirri, L. D. Spencer, R. Sunyaev, A.-S. Suur-Uski, J. A. Tauber, D. Tavagnacco, M. Tenti, L. Toffolatti, M. Tomasi, T. Trombetti, L. Valenziano, J. Valiviita, B. Van Tent, L. Vibert, P. Vielva, F. Villa, N. Vittorio, B. D. Wandelt, I. K. Wehus, M. White, S. D. M. White, A. Zacchei, A. Zonca, Planck2018 results: Vi. cosmological parameters, Astronomy & Astrophysics 641 (2020) A6. doi:10.1051/0004-6361/201833910.
URL http://dx.doi.org/10.1051/0004-6361/201833910

[8] N. Aghanim, Y. Akrami, F. Arroja, M. Ashdown, J. Aumont, C. Baccigalupi, M. Ballardini, A. J. Banday, R. B. Barreiro, N. Bartolo, S. Basak, R. Battye, K. Benabed, J.-P. Bernard, M. Bersanelli, P. Bielewicz, J. J. Bock, J. R. Bond, J. Borrill, F. R. Bouchet, F. Boulanger, M. Bucher, C. Burigana, R. C. Butler, E. Calabrese, J.-F. Cardoso, J. Carron, B. Casaponsa, A. Challinor, H. C. Chiang, L. P. L. Colombo, C. Combet, D. Contreras, B. P. Crill, F. Cuttaia, P. de Bernardis, G. de Zotti, J. Delabrouille, J.-M. Delouis, F.-X. Désert, E. Di Valentino,

C. Dickinson, J. M. Diego, S. Donzelli, O. Doré, M. Douspis, A. Ducout, X. Dupac, G. Efstathiou, F. Elsner, T. A. Enßlin, H. K. Eriksen, E. Falgarone, Y. Fantaye, J. Fergusson, R. Fernandez-Cobos, F. Finelli, F. Forastieri, M. Frailis, E. Franceschi, A. Frolov, S. Galeotta, S. Galli, K. Ganga, R. T. Génova-Santos, M. Gerbino, T. Ghosh, J. González-Nuevo, K. M. Górski, S. Gratton, A. Gruppuso, J. E. Gudmundsson, J. Hamann, W. Handley, F. K. Hansen, G. Helou, D. Herranz, S. R. Hildebrandt, E. Hivon, Z. Huang, A. H. Jaffe, W. C. Jones, A. Karakci, E. Keihänen, R. Keskitalo, K. Kiiveri, J. Kim, T. S. Kisner, L. Knox, N. Krachmalnicoff, M. Kunz, H. Kurki-Suonio, G. Lagache, J.-M. Lamarre, M. Langer, A. Lasenby, M. Lattanzi, C. R. Lawrence, M. Le Jeune, J. P. Leahy, J. Lesgourgues, F. Levrier, A. Lewis, M. Liguori, P. B. Lilje, M. Lilley, V. Lindholm, M. López-Caniego, P. M. Lubin, Y.-Z. Ma, J. F. Macías-Pérez, G. Maggio, D. Maino, N. Mandolesi, A. Mangilli, A. Marcos-Caballero, M. Maris, P. G. Martin, M. Martinelli, E. Martínez-González, S. Matarrese, N. Mauri, J. D. McEwen, P. D. Meerburg, P. R. Meinhold, A. Melchiorri, A. Mennella, M. Migliaccio, M. Millea, S. Mitra, M.-A. Miville-Deschênes, D. Molinari, A. Moneti, L. Montier, G. Morgante, A. Moss, S. Mottet, M. Münchmeyer, P. Natoli, H. U. Nørgaard-Nielsen, C. A. Oxborrow, L. Pagano, D. Paoletti, B. Partridge, G. Patanchon, T. J. Pearson, M. Peel, H. V. Peiris, F. Perrotta, V. Pettorino, F. Piacentini, L. Polastri, G. Polenta, J.-L. Puget, J. P. Rachen, M. Reinecke, M. Remazeilles, C. Renault, A. Renzi, G. Rocha, C. Rosset, G. Roudier, J. A. Rubiño-Martín, B. Ruiz-Granados, L. Salvati, M. Sandri, M. Savelainen, D. Scott, E. P. S. Shellard, M. Shiraishi, C. Sirignano, G. Sirri, L. D. Spencer, R. Sunyaev, A.-S. Suur-Uski, J. A. Tauber, D. Tavagnacco, M. Tenti, L. Terenzi, L. Toffolatti, M. Tomasi, T. Trombetti, J. Valiviita, B. Van Tent, L. Vibert, P. Vielva, F. Villa, N. Vittorio, B. D. Wandelt, I. K. Wehus, M. White, S. D. M. White, A. Zacchei, A. Zonca, Planck2018 results: I. overview and the cosmological legacy of planck, Astronomy & Astrophysics 641 (2020) A1. doi:10.1051/0004-6361/201833880.

[9] D. Baumann, Cosmology, Cambridge University Press, 2022.

[10] D. Brout, D. Scolnic, B. Popovic, A. G. Riess, A. Carr, J. Zuntz, R. Kessler, T. M. Davis, S. Hinton, D. Jones, W. D. Kenworthy, E. R. Peterson, K. Said, G. Taylor, N. Ali, P. Armstrong, P. Charvu, A. Dwomoh, C. Meldorf, A. Palmese, H. Qu, B. M. Rose, B. Sanchez, C. W. Stubbs, M. Vincenzi, C. M. Wood, P. J. Brown, R. Chen, K. Chambers, D. A. Coulter, M. Dai, G. Dimitriadis, A. V. Filippenko, R. J. Foley, S. W. Jha, L. Kelsey, R. P. Kirshner, A. Möller, J. Muir, S. Nadathur, Y.-C. Pan, A. Rest, C. Rojas-Bravo, M. Sako, M. R. Siebert, M. Smith, B. E. Stahl, P. Wiseman, The pantheon+ analysis: Cosmological constraints, The Astrophysical Journal 938 (2) (2022) 110. doi:10.3847/1538-4357/ac8e04.

[11] S. Perlmutter, G. Aldering, G. Goldhaber, R. A. Knop, P. Nugent, P. G. Castro, S. Deustua, S. Fabbro, A. Goobar, D. E. Groom, I. M. Hook, A. G. Kim, M. Y. Kim, J. C. Lee, N. J. Nunes, R. Pain, C. R. Pennypacker, R. Quimby, C. Lidman, R. S. Ellis, M. Irwin, R. G. McMahon, P. Ruiz-Lapuente, N. Walton, B. Schaefer, B. J. Boyle, A. V. Filippenko, T. Matheson, A. S. Fruchter, N. Panagia, H. J. M. Newberg, W. J. Couch, T. S. C. Project, Measurements of Ω and Λ from 42 high-redshift supernovae, The Astrophysical Journal 517 (2) (1999) 565. doi:10.1086/307221.

[12] A. G. Riess, A. V. Filippenko, P. Challis, A. Clocchiatti, A. Diercks, P. M. Garnavich, R. L. Gilliland, C. J. Hogan, S. Jha, R. P. Kirshner, B. Leibundgut, M. M. Phillips, D. Reiss, B. P. Schmidt, R. A. Schommer, R. C. Smith, J. Spyromilio, C. Stubbs, N. B. Suntzeff, J. Tonry, Observational evidence from supernovae for an accelerating universe and a cosmological constant, The Astronomical Journal 116 (3) (1998) 1009. doi:10.1086/300499.

[13] D. J. Eisenstein, I. Zehavi, D. W. Hogg, R. Scoccimarro, M. R. Blanton, R. C. Nichol, R. Scranton, H.-J. Seo, M. Tegmark, Z. Zheng, S. F. Anderson, J. Annis, N. Bahcall, J. Brinkmann, S. Burles, F. J. Castander, A. Connolly, I. Csabai, M. Doi, M. Fukugita, J. A. Frieman, K. Glazebrook, J. E. Gunn, J. S. Hendry, G. Hennessy, Z. Ivezić, S. Kent, G. R. Knapp, H. Lin, Y.-S. Loh, R. H. Lupton, B. Margon, T. A. McKay, A. Meiksin, J. A. Munn, A. Pope, M. W. Richmond, D. Schlegel, D. P. Schneider, K. Shimasaku, C. Stoughton, M. A. Strauss, M. SubbaRao, A. S. Szalay, I. Szapudi, D. L. Tucker, B. Yanny, D. G. York, Detection of the baryon acoustic peak in the large-scale correlation function of sdss luminous red galaxies, The Astrophysical Journal 633 (2) (2005) 560. doi:10.1086/466512.

[14] L. Anderson, E. Aubourg, S. Bailey, F. Beutler, V. Bhardwaj, M. Blanton, A. S. Bolton, J. Brinkmann, J. R. Brownstein, A. Burden, C.-H. Chuang, A. J. Cuesta, K. S. Dawson, D. J. Eisenstein, S. Escoffier, J. E. Gunn, H. Guo, S. Ho, K. Honscheid, C. Howlett, D. Kirkby, R. H. Lupton, M. Manera, C. Maraston, C. K. McBride, O. Mena, F. Montesano, R. C. Nichol, S. E. Nuza, M. D. Olmstead, N. Padmanabhan, N. Palanque-Delabrouille, J. Parejko, W. J. Percival, P. Petitjean, F. Prada, A. M. Price-Whelan, B. Reid, N. A. Roe, A. J. Ross, N. P. Ross, C. G. Sabiu, S. Saito, L. Samushia, A. G. Sánchez, D. J. Schlegel, D. P. Schneider, C. G. Scoccola, H.-J. Seo, R. A. Skibba, M. A. Strauss, M. E. C. Swanson, D. Thomas, J. L. Tinker, R. Tojeiro, M. V. Magaña, L. Verde, D. A. Wake, B. A. Weaver, D. H. Weinberg, M. White, X. Xu, C. Yèche, I. Zehavi, G.-B. Zhao, The clustering of galaxies in the SDSS-III Baryon Oscillation Spectroscopic Survey: baryon acoustic oscillations in the Data Releases 10

and 11 Galaxy samples, Monthly Notices of the Royal Astronomical Society 441 (1) (2014) 24–62. doi:10.1093/mnras/stu523.

[15] D. Baumann, Tasi lectures on primordial cosmology (2018). arXiv:1807.03098. URL https://arxiv.org/abs/1807.03098

[16] E. M. Leitch, J. M. Kovac, C. Pryke, J. E. Carlstrom, N. W. Halverson, W. L. Holzapfel, M. Dragovan, B. Reddall, E. S. Sandberg, Measurement of polarization with the degree angular scale interferometer, Nature 420 (6917) (2002) 763–771. doi:10.1038/nature01271.

[17] Y. Akrami, F. Arroja, M. Ashdown, J. Aumont, C. Baccigalupi, M. Ballardini, A. J. Banday, R. B. Barreiro, N. Bartolo, S. Basak, K. Benabed, J.-P. Bernard, M. Bersanelli, P. Bielewicz, J. J. Bock, J. R. Bond, J. Borrill, F. R. Bouchet, F. Boulanger, M. Bucher, C. Burigana, R. C. Butler, E. Calabrese, J.-F. Cardoso, J. Carron, A. Challinor, H. C. Chiang, L. P. L. Colombo, C. Combet, D. Contreras, B. P. Crill, F. Cuttaia, P. de Bernardis, G. de Zotti, J. Delabrouille, J.-M. Delouis, E. Di Valentino, J. M. Diego, S. Donzelli, O. Doré, M. Douspis, A. Ducout, X. Dupac, S. Dusini, G. Efstathiou, F. Elsner, T. A. Enßlin, H. K. Eriksen, Y. Fantaye, J. Fergusson, R. Fernandez-Cobos, F. Finelli, F. Forastieri, M. Frailis, E. Franceschi, A. Frolov, S. Galeotta, S. Galli, K. Ganga, C. Gauthier, R. T. Génova-Santos, M. Gerbino, T. Ghosh, J. González-Nuevo, K. M. Górski, S. Gratton, A. Gruppuso, J. E. Gudmundsson, J. Hamann, W. Handley, F. K. Hansen, D. Herranz, E. Hivon, D. C. Hooper, Z. Huang, A. H. Jaffe, W. C. Jones, E. Keihänen, R. Keskitalo, K. Kiiveri, J. Kim, T. S. Kisner, N. Krachmalnicoff, M. Kunz, H. Kurki-Suonio, G. Lagache, J.-M. Lamarre, A. Lasenby, M. Lattanzi, C. R. Lawrence, M. Le Jeune, J. Lesgourgues, F. Levrier, A. Lewis, M. Liguori, P. B. Lilje, V. Lindholm, M. López-Caniego, P. M. Lubin, Y.-Z. Ma, J. F. Macías-Pérez, G. Maggio, D. Maino, N. Mandolesi, A. Mangilli, A. Marcos-Caballero, M. Maris, P. G. Martin, E. Martínez-González, S. Matarrese, N. Mauri, J. D. McEwen, P. D. Meerburg, P. R. Meinhold, A. Melchiorri, A. Mennella, M. Migliaccio, S. Mitra, M.-A. Miville-Deschênes, D. Molinari, A. Moneti, L. Montier, G. Morgante, A. Moss, M. Münchmeyer, P. Natoli, H. U. Nørgaard-Nielsen, L. Pagano, D. Paoletti, B. Partridge, G. Patanchon, H. V. Peiris, F. Perrotta, V. Pettorino, F. Piacentini, L. Polastri, G. Polenta, J.-L. Puget, J. P. Rachen, M. Reinecke, M. Remazeilles, A. Renzi, G. Rocha, C. Rosset, G. Roudier, J. A. Rubiño-Martín, B. Ruiz-Granados, L. Salvati, M. Sandri, M. Savelainen, D. Scott, E. P. S. Shellard, M. Shiraishi, C. Sirignano, G. Sirri, L. D. Spencer, R. Sunyaev, A.-S. Suur-Uski, J. A. Tauber, D. Tavagnacco, M. Tenti, L. Toffolatti, M. Tomasi, T. Trombetti, J. Valiviita, B. Van Tent, P. Vielva, F. Villa, N. Vittorio, B. D. Wandelt, I. K. Wehus, S. D. M.

White, A. Zacchei, J. P. Zibin, A. Zonca, Planck2018 results: X. constraints on inflation, Astronomy & Astrophysics 641 (2020) A10. doi:10.1051/0004-6361/201833887.

[18] U. Seljak, M. Zaldarriaga, Signature of gravity waves in the polarization of the microwave background, Physical Review Letters 78 (11) (1997) 2054–2057. doi:10.1103/physrevlett.78.2054.

[19] P. A. R. Ade, Z. Ahmed, R. W. Aikin, K. D. Alexander, D. Barkats, S. J. Benton, C. A. Bischoff, J. J. Bock, R. Bowens-Rubin, J. A. Brevik, I. Buder, E. Bullock, V. Buza, J. Connors, J. Cornelison, B. P. Crill, M. Crumrine, M. Dierickx, L. Duband, C. Dvorkin, J. P. Filippini, S. Fliescher, J. Grayson, G. Hall, M. Halpern, S. Harrison, S. R. Hildebrandt, G. C. Hilton, H. Hui, K. D. Irwin, J. Kang, K. S. Karkare, E. Karpel, J. P. Kaufman, B. G. Keating, S. Kefeli, S. A. Kernasovskiy, J. M. Kovac, C. L. Kuo, N. A. Larsen, K. Lau, E. M. Leitch, M. Lueker, K. G. Megerian, L. Moncelsi, T. Namikawa, C. B. Netterfield, H. T. Nguyen, R. O'Brient, R. W. Ogburn, S. Palladino, C. Pryke, B. Racine, S. Richter, A. Schillaci, R. Schwarz, C. D. Sheehy, A. Soliman, T. St. Germaine, Z. K. Staniszewski, B. Steinbach, R. V. Sudiwala, G. P. Teply, K. L. Thompson, J. E. Tolan, C. Tucker, A. D. Turner, C. Umiltà, A. G. Vieregg, A. Wandui, A. C. Weber, D. V. Wiebe, J. Willmert, C. L. Wong, W. L. K. Wu, H. Yang, K. W. Yoon, C. Zhang, Constraints on primordial gravitational waves using planck, wmap, and new bicep2/keck observations through the 2015 season, Phys. Rev. Lett. 121 (2018) 221301. doi:10.1103/PhysRevLett.121.221301.

[20] M. Kamionkowski, A. Kosowsky, A. Stebbins, Statistics of cosmic microwave background polarization, Phys. Rev. D 55 (1997) 7368–7388. doi:10.1103/PhysRevD.55.7368.

[21] P. A. R. Ade, Z. Ahmed, M. Amiri, D. Barkats, R. B. Thakur, C. A. Bischoff, D. Beck, J. J. Bock, H. Boenish, E. Bullock, V. Buza, J. R. Cheshire, J. Connors, J. Cornelison, M. Crumrine, A. Cukierman, E. V. Denison, M. Dierickx, L. Duband, M. Eiben, S. Fatigoni, J. P. Filippini, S. Fliescher, N. Goeckner-Wald, D. C. Goldfinger, J. Grayson, P. Grimes, G. Hall, G. Halal, M. Halpern, E. Hand, S. Harrison, S. Henderson, S. R. Hildebrandt, G. C. Hilton, J. Hubmayr, H. Hui, K. D. Irwin, J. Kang, K. S. Karkare, E. Karpel, S. Kefeli, S. A. Kernasovskiy, J. M. Kovac, C. L. Kuo, K. Lau, E. M. Leitch, A. Lennox, K. G. Megerian, L. Minutolo, L. Moncelsi, Y. Nakato, T. Namikawa, H. T. Nguyen, R. O'Brient, R. W. Ogburn, S. Palladino, T. Prouve, C. Pryke, B. Racine, C. D. Reintsema, S. Richter, A. Schillaci, R. Schwarz, B. L. Schmitt, C. D. Sheehy, A. Soliman, T. S. Germaine, B. Steinbach, R. V. Sudiwala, G. P. Teply, K. L. Thompson, J. E. Tolan, C. Tucker, A. D. Turner, C. Umiltà, C. Vergès, A. G. Vieregg, A. Wandui, A. C.

Weber, D. V. Wiebe, J. Willmert, C. L. Wong, W. L. K. Wu, H. Yang, K. W. Yoon, E. Young, C. Yu, L. Zeng, C. Zhang, S. Zhang, Improved constraints on primordial gravitational waves using planck, wmap, and bicep/keck observations through the 2018 observing season, Physical Review Letters 127 (15) (Oct. 2021). doi:10.1103/physrevlett.127.151301.

[22] L. Montier, B. Mot, P. de Bernardis, B. Maffei, G. Pisano, F. Columbro, J. E. Gudmundsson, S. Henrot-Versillé, L. Lamagna, J. Montgomery, T. Prouvé, M. Russell, G. Savini, S. Stever, K. L. Thompson, M. Tsujimoto, C. Tucker, B. Westbrook, P. A. Ade, A. Adler, E. Allys, K. Arnold, D. Auguste, J. Aumont, R. Aurlien, J. Austermann, C. Baccigalupi, A. J. Banday, R. Banerji, R. B. Barreiro, S. Basak, J. Beall, D. Beck, S. Beckman, J. Bermejo, M. Bersanelli, J. Bonis, J. Borrill, F. Boulanger, S. Bounissou, M. Brilenkov, M. Brown, M. Bucher, E. Calabrese, P. Campeti, A. Carones, F. J. Casas, A. Challinor, V. Chan, K. Cheung, Y. Chinone, J. F. Cliche, L. Colombo, J. Cubas, A. Cukierman, D. Curtis, G. D'Alessandro, N. Dachlythra, M. De Petris, C. Dickinson, P. Diego-Palazuelos, M. Dobbs, T. Dotani, L. Duband, S. Duff, J. M. Duval, K. Ebisawa, T. Elleflot, H. K. Eriksen, J. Errard, T. Essinger-Hileman, F. Finelli, R. Flauger, C. Franceschet, U. Fuskeland, M. Galloway, K. Ganga, J. R. Gao, R. Genova-Santos, M. Gerbino, M. Gervasi, T. Ghigna, E. Gjerløw, M. L. Gradziel, J. Grain, F. Grupp, A. Gruppuso, T. de Haan, N. W. Halverson, P. Hargrave, T. Hasebe, M. Hasegawa, M. Hattori, M. Hazumi, D. Herman, D. Herranz, C. A. Hill, G. Hilton, Y. Hirota, E. Hivon, R. A. Hlozek, Y. Hoshino, E. de la Hoz, J. Hubmayr, K. Ichiki, T. Iida, H. Imada, K. Ishimura, H. Ishino, G. Jaehnig, T. Kaga, S. Kashima, N. Katayama, A. Kato, T. Kawasaki, R. Keskitalo, T. Kisner, Y. Kobayashi, N. Kogiso, A. Kogut, K. Kohri, E. Komatsu, K. Komatsu, K. Konishi, N. Krachmalnicoff, I. Kreykenbohm, C.-L. L. Kuo, A. Kushino, J. V. Lanen, M. Lattanzi, A. T. Lee, C. Leloup, F. Levrier, E. Linder, T. Louis, G. Luzzi, T. Maciaszek, D. Maino, M. Maki, S. Mandelli, E. Martinez-Gonzalez, S. Masi, T. Matsumura, A. Mennella, M. Migliaccio, Y. Minami, K. Mitsuda, G. Morgante, Y. Murata, J. A. Murphy, M. Nagai, Y. Nagano, T. Nagasaki, R. Nagata, S. Nakamura, T. Namikawa, P. Natoli, S. Nerval, T. Nishibori, H. Nishino, C. O'Sullivan, H. Ogawa, H. Ogawa, S. Oguri, H. Ohsaki, I. S. Ohta, N. Okada, N. Okada, L. Pagano, A. Paiella, D. Paoletti, G. Patanchon, J. Peloton, F. Piacentini, G. Polenta, D. Poletti, G. Puglisi, D. Rambaud, C. Raum, S. Realini, M. Reinecke, M. Remazeilles, A. Ritacco, G. Roudil, J. A. Rubino-Martin, H. Sakurai, Y. Sakurai, M. Sandri, M. Sasaki, D. Scott, J. Seibert, Y. Sekimoto, B. Sherwin, K. Shinozaki, M. Shiraishi, P. Shirron, G. Signorelli, G. Smecher, R. Stompor, H. Sugai, S. Sugiyama, A. Suzuki, J. Suzuki, T. L. Svalheim, E. Switzer, R. Takaku, H. Takakura, S. Takakura, Y. Takase, Y. Takeda, A. Tartari, E. Tay-

lor, Y. Terao, H. Thommesen, B. Thorne, T. Toda, M. Tomasi, M. Tominaga, N. Trappe, M. Tristram, M. Tsuji, J. Ullom, G. Vermeulen, P. Vielva, F. Villa, M. Vissers, N. Vittorio, I. Wehus, J. Weller, J. Wilms, B. Winter, E. J. Wollack, N. Y. Yamasaki, T. Yoshida, J. Yumoto, M. Zannoni, A. Zonca, Overview of the medium and high frequency telescopes of the litebird space mission, in: M. Lystrup, N. Batalha, E. C. Tong, N. Siegler, M. D. Perrin (Eds.), Space Telescopes and Instrumentation 2020: Optical, Infrared, and Millimeter Wave, SPIE, 2020. doi:10.1117/12.2562243.

[23] E. Allys, K. Arnold, J. Aumont, R. Aurlien, S. Azzoni, C. Baccigalupi, A. J. Banday, R. Banerji, R. B. Barreiro, N. Bartolo, L. Bautista, D. Beck, S. Beckman, M. Bersanelli, F. Boulanger, M. Brilenkov, M. Bucher, E. Calabrese, P. Campeti, A. Carones, F. J. Casas, A. Catalano, V. Chan, K. Cheung, Y. Chinone, S. E. Clark, F. Columbro, G. D'Alessandro, P. de Bernardis, T. de Haan, E. de la Hoz, M. De Petris, S. D. Torre, P. Diego-Palazuelos, M. Dobbs, T. Dotani, J. M. Duval, T. Elleflot, H. K. Eriksen, J. Errard, T. Essinger-Hileman, F. Finelli, R. Flauger, C. Franceschet, U. Fuskeland, M. Galloway, K. Ganga, M. Gerbino, M. Gervasi, R. T. Génova-Santos, T. Ghigna, S. Giardiello, E. Gjerløw, J. Grain, F. Grupp, A. Gruppuso, J. E. Gudmundsson, N. W. Halverson, P. Hargrave, T. Hasebe, M. Hasegawa, M. Hazumi, S. Henrot-Versillé, B. Hensley, L. T. Hergt, D. Herman, E. Hivon, R. A. Hlozek, A. L. Hornsby, Y. Hoshino, J. Hubmayr, K. Ichiki, T. Iida, H. Imada, H. Ishino, G. Jaehnig, N. Katayama, A. Kato, R. Keskitalo, T. Kisner, Y. Kobayashi, A. Kogut, K. Kohri, E. Komatsu, K. Komatsu, K. Konishi, N. Krachmalnicoff, C. L. Kuo, L. Lamagna, M. Lattanzi, A. T. Lee, C. Leloup, F. Levrier, E. Linder, G. Luzzi, J. Macias-Perez, T. Maciaszek, B. Maffei, D. Maino, S. Mandelli, E. Martínez-González, S. Masi, M. Massa, S. Matarrese, F. T. Matsuda, T. Matsumura, L. Mele, M. Migliaccio, Y. Minami, A. Moggi, J. Montgomery, L. Montier, G. Morgante, B. Mot, Y. Nagano, T. Nagasaki, R. Nagata, R. Nakano, T. Namikawa, F. Nati, P. Natoli, S. Nerval, F. Noviello, K. Odagiri, S. Oguri, H. Ohsaki, L. Pagano, A. Paiella, D. Paoletti, A. Passerini, G. Patanchon, F. Piacentini, M. Piat, G. Pisano, G. Polenta, D. Poletti, T. Prouvé, G. Puglisi, D. Rambaud, C. Raum, S. Realini, M. Reinecke, M. Remazeilles, A. Ritacco, G. Roudil, J. A. Rubino-Martin, M. Russell, H. Sakurai, Y. Sakurai, M. Sasaki, D. Scott, Y. Sekimoto, K. Shinozaki, M. Shiraishi, P. Shirron, G. Signorelli, F. Spinella, S. Stever, R. Stompor, S. Sugiyama, R. M. Sullivan, A. Suzuki, T. L. Svalheim, E. Switzer, R. Takaku, H. Takakura, Y. Takase, A. Tartari, Y. Terao, J. Thermeau, H. Thommesen, K. L. Thompson, M. Tomasi, M. Tominaga, M. Tristram, M. Tsuji, M. Tsujimoto, L. Vacher, P. Vielva, N. Vittorio, W. Wang, K. Watanuki, I. K. Wehus, J. Weller, B. Westbrook, J. Wilms, B. Winter, E. J. Wollack, J. Yu-

moto, M. Zannoni, Probing cosmic inflation with thelitebirdcosmic microwave background polarization survey, Progress of Theoretical and Experimental Physics 2023 (4) (Nov. 2022). doi:10.1093/ptep/ptac150.

[24] K. N. Abazajian, P. Adshead, Z. Ahmed, S. W. Allen, D. Alonso, K. S. Arnold, C. Baccigalupi, J. G. Bartlett, N. Battaglia, B. A. Benson, C. A. Bischoff, J. Borrill, V. Buza, E. Calabrese, R. Caldwell, J. E. Carlstrom, C. L. Chang, T. M. Crawford, F.-Y. Cyr-Racine, F. D. Bernardis, T. de Haan, S. di Serego Alighieri, J. Dunkley, C. Dvorkin, J. Errard, G. Fabbian, S. Feeney, S. Ferraro, J. P. Filippini, R. Flauger, G. M. Fuller, V. Gluscevic, D. Green, D. Grin, E. Grohs, J. W. Henning, J. C. Hill, R. Hlozek, G. Holder, W. Holzapfel, W. Hu, K. M. Huffenberger, R. Keskitalo, L. Knox, A. Kosowsky, J. Kovac, E. D. Kovetz, C.-L. Kuo, A. Kusaka, M. L. Jeune, A. T. Lee, M. Lilley, M. Loverde, M. S. Madhavacheril, A. Mantz, D. J. E. Marsh, J. McMahon, P. D. Meerburg, J. Meyers, A. D. Miller, J. B. Munoz, H. N. Nguyen, M. D. Niemack, M. Peloso, J. Peloton, L. Pogosian, C. Pryke, M. Raveri, C. L. Reichardt, G. Rocha, A. Rotti, E. Schaan, M. M. Schmittfull, D. Scott, N. Sehgal, S. Shandera, B. D. Sherwin, T. L. Smith, L. Sorbo, G. D. Starkman, K. T. Story, A. van Engelen, J. D. Vieira, S. Watson, N. Whitehorn, W. L. K. Wu, Cmb-s4 science book, first edition (2016).
URL https://arxiv.org/abs/1610.02743

[25] P. Ade, J. Aguirre, Z. Ahmed, S. Aiola, A. Ali, D. Alonso, M. A. Alvarez, K. Arnold, P. Ashton, J. Austermann, H. Awan, C. Baccigalupi, T. Baildon, D. Barron, N. Battaglia, R. Battye, E. Baxter, A. Bazarko, J. A. Beall, R. Bean, D. Beck, S. Beckman, B. Beringue, F. Bianchini, S. Boada, D. Boettger, J. R. Bond, J. Borrill, M. L. Brown, S. M. Bruno, S. Bryan, E. Calabrese, V. Calafut, P. Calisse, J. Carron, A. Challinor, G. Chesmore, Y. Chinone, J. Chluba, H.-M. S. Cho, S. Choi, G. Coppi, N. F. Cothard, K. Coughlin, D. Crichton, K. D. Crowley, K. T. Crowley, A. Cukierman, J. M. D'Ewart, R. Dünner, T. de Haan, M. Devlin, S. Dicker, J. Didier, M. Dobbs, B. Dober, C. J. Duell, S. Duff, A. Duivenvoorden, J. Dunkley, J. Dusatko, J. Errard, G. Fabbian, S. Feeney, S. Ferraro, P. Fluxà, K. Freese, J. C. Frisch, A. Frolov, G. Fuller, B. Fuzia, N. Galitzki, P. A. Gallardo, J. T. G. Ghersi, J. Gao, E. Gawiser, M. Gerbino, V. Gluscevic, N. Goeckner-Wald, J. Golec, S. Gordon, M. Gralla, D. Green, A. Grigorian, J. Groh, C. Groppi, Y. Guan, J. E. Gudmundsson, D. Han, P. Hargrave, M. Hasegawa, M. Hasselfield, M. Hattori, V. Haynes, M. Hazumi, Y. He, E. Healy, S. W. Henderson, C. Hervias-Caimapo, C. A. Hill, J. C. Hill, G. Hilton, M. Hilton, A. D. Hincks, G. Hinshaw, R. Hložek, S. Ho, S.-P. P. Ho, L. Howe, Z. Huang, J. Hubmayr, K. Huffenberger, J. P. Hughes, A. Ijjas, M. Ikape, K. Irwin, A. H. Jaffe, B. Jain, O. Jeong, D. Kaneko,

E. D. Karpel, N. Katayama, B. Keating, S. S. Kernasovskiy, R. Keskitalo, T. Kisner, K. Kiuchi, J. Klein, K. Knowles, B. Koopman, A. Kosowsky, N. Krachmalnicoff, S. E. Kuenstner, C.-L. Kuo, A. Kusaka, J. Lashner, A. Lee, E. Lee, D. Leon, J. S.-Y. Leung, A. Lewis, Y. Li, Z. Li, M. Limon, E. Linder, C. Lopez-Caraballo, T. Louis, L. Lowry, M. Lungu, M. Madhavacheril, D. Mak, F. Maldonado, H. Mani, B. Mates, F. Matsuda, L. Maurin, P. Mauskopf, A. May, N. McCallum, C. McKenney, J. McMahon, P. D. Meerburg, J. Meyers, A. Miller, M. Mirmelstein, K. Moodley, M. Munchmeyer, C. Munson, S. Naess, F. Nati, M. Navaroli, L. Newburgh, H. N. Nguyen, M. Niemack, H. Nishino, J. Orlowski-Scherer, L. Page, B. Partridge, J. Peloton, F. Perrotta, L. Piccirillo, G. Pisano, D. Poletti, R. Puddu, G. Puglisi, C. Raum, C. L. Reichardt, M. Remazeilles, Y. Rephaeli, D. Riechers, F. Rojas, A. Roy, S. Sadeh, Y. Sakurai, M. Salatino, M. S. Rao, E. Schaan, M. Schmittfull, N. Sehgal, J. Seibert, U. Seljak, B. Sherwin, M. Shimon, C. Sierra, J. Sievers, P. Sikhosana, M. Silva-Feaver, S. M. Simon, A. Sinclair, P. Siritanasak, K. Smith, S. R. Smith, D. Spergel, S. T. Staggs, G. Stein, J. R. Stevens, R. Stompor, A. Suzuki, O. Tajima, S. Takakura, G. Teply, D. B. Thomas, B. Thorne, R. Thornton, H. Trac, C. Tsai, C. Tucker, J. Ullom, S. Vagnozzi, A. v. Engelen, J. V. Lanen, D. D. V. Winkle, E. M. Vavagiakis, C. Vergès, M. Vissers, K. Wagoner, S. Walker, J. Ward, B. Westbrook, N. Whitehorn, J. Williams, J. Williams, E. J. Wollack, Z. Xu, B. Yu, C. Yu, F. Zago, H. Zhang, N. Zhu, The simons observatory: science goals and forecasts, Journal of Cosmology and Astroparticle Physics 2019 (02) (2019) 056–056. doi:10.1088/1475-7516/2019/02/056.

[26] M. Zaldarriaga, U. Seljak, Gravitational lensing effect on cosmic microwave background polarization, Physical Review D 58 (2) (Jun. 1998). doi:10.1103/physrevd.58.023003.

[27] E. Komatsu, New physics from the polarized light of the cosmic microwave background, Nature Reviews Physics 4 (7) (2022) 452–469. doi:10.1038/s42254-022-00452-4.

[28] M. Li, X. Zhang, Cosmological *cpt* violating effect on cmb polarization, Phys. Rev. D 78 (2008) 103516. doi:10.1103/PhysRevD.78.103516.

[29] A. Hoseinpour, M. Zarei, G. Orlando, N. Bartolo, S. Matarrese, Cmb *v* modes from photon-photon forward scattering revisited, Phys. Rev. D 102 (2020) 063501. doi:10.1103/PhysRevD.102.063501.

[30] S. M. Carroll, G. B. Field, R. Jackiw, Limits on a lorentz- and parity-violating modification of electrodynamics, Phys. Rev. D 41 (1990) 1231–1240. doi:10.1103/PhysRevD.41.1231.

[31] S. Nakagawa, F. Takahashi, M. Yamada, Cosmic birefringence triggered by dark matter domination, Phys. Rev. Lett. 127 (2021) 181103. doi:10.1103/PhysRevLett.127.181103.

[32] I. Obata, Implications of the cosmic birefringence measurement for the axion dark matter search, Journal of Cosmology and Astroparticle Physics 2022 (09) (2022) 062. doi:10.1088/1475-7516/2022/09/062.

[33] R.-P. Zhou, D. Huang, C.-Q. Geng, Cosmic birefringence from neutrino and dark matter asymmetries, Journal of Cosmology and Astroparticle Physics 2023 (07) (2023) 053. doi:10.1088/1475-7516/2023/07/053.

[34] A. Greco, N. Bartolo, A. Gruppuso, A new solution for the observed isotropic cosmic birefringence angle and its implications for the anisotropic counterpart through a boltzmann approach, Journal of Cosmology and Astroparticle Physics 2024 (10) (2024) 028. doi:10.1088/1475-7516/2024/10/028.

[35] K. Murai, F. Naokawa, T. Namikawa, E. Komatsu, Isotropic cosmic birefringence from early dark energy, Physical Review D 107 (4) (Feb. 2023). doi:10.1103/physrevd.107.l041302.

[36] S. Gasparotto, I. Obata, Cosmic birefringence from monodromic axion dark energy, Journal of Cosmology and Astroparticle Physics 2022 (08) (2022) 025. doi:10.1088/1475-7516/2022/08/025.

[37] T. Fujita, K. Murai, H. Nakatsuka, S. Tsujikawa, Detection of isotropic cosmic birefringence and its implications for axionlike particles including dark energy, Physical Review D 103 (4) (Feb. 2021). doi:10.1103/physrevd.103.043509.

[38] A. Greco, N. Bartolo, A. Gruppuso, Cosmic birefrigence: cross-spectra and cross-bispectra with cmb anisotropies, Journal of Cosmology and Astroparticle Physics 2022 (03) 050. doi:10.1088/1475-7516/2022/03/050.

[39] A. Greco, N. Bartolo, A. Gruppuso, Probing axions through tomography of anisotropic cosmic birefringence, Journal of Cosmology and Astroparticle Physics 2023 (05) (2023) 026. doi:10.1088/1475-7516/2023/05/026.

[40] S. Arcari, N. Bartolo, A. Greco, A. Gruppuso, M. Lattanzi, P. Natoli, Conversations in the dark: cross-correlating birefringence and lss to constrain axions, Journal of Cosmology and Astroparticle Physics 2024 (10) (2024) 101. doi:10.1088/1475-7516/2024/10/101.

[41] A. Gruppuso, G. Maggio, D. Molinari, P. Natoli, A note on the birefringence angle estimation in cmb data analysis, Journal of Cosmology and Astroparticle Physics 2016 (05) (2016) 020. doi:10.1088/1475-7516/2016/05/020.

[42] N. Aghanim, M. Ashdown, J. Aumont, C. Baccigalupi, M. Ballardini, A. J. Banday, R. B. Barreiro, N. Bartolo, S. Basak, K. Benabed, J.-P. Bernard, M. Bersanelli, P. Bielewicz, L. Bonavera, J. R. Bond, J. Borrill, F. R. Bouchet, C. Burigana, E. Calabrese, J.-F. Cardoso, J. Carron, H. C. Chiang, L. P. L. Colombo, B. Comis, D. Contreras, F. Couchot, A. Coulais, B. P. Crill, A. Curto, F. Cuttaia, P. de Bernardis, A. de Rosa, G. de Zotti, J. Delabrouille, F.-X. Désert, E. Di Valentino, C. Dickinson, J. M. Diego, O. Doré, A. Ducout, X. Dupac, S. Dusini, F. Elsner, T. A. Enßlin, H. K. Eriksen, Y. Fantaye, F. Finelli, F. Forastieri, M. Frailis, E. Franceschi, A. Frolov, S. Galeotta, S. Galli, K. Ganga, R. T. Génova-Santos, M. Gerbino, Y. Giraud-Héraud, J. González-Nuevo, K. M. Górski, A. Gruppuso, J. E. Gudmundsson, F. K. Hansen, S. Henrot-Versillé, D. Herranz, E. Hivon, Z. Huang, A. H. Jaffe, W. C. Jones, E. Keihänen, R. Keskitalo, K. Kiiveri, N. Krachmalnicoff, M. Kunz, H. Kurki-Suonio, J.-M. Lamarre, M. Langer, A. Lasenby, M. Lattanzi, C. R. Lawrence, M. Le Jeune, J. P. Leahy, F. Levrier, M. Liguori, P. B. Lilje, V. Lindholm, M. López-Caniego, Y.-Z. Ma, J. F. Macías-Pérez, G. Maggio, D. Maino, N. Mandolesi, M. Maris, P. G. Martin, E. Martínez-González, S. Matarrese, N. Mauri, J. D. McEwen, P. R. Meinhold, A. Melchiorri, A. Mennella, M. Migliaccio, M.-A. Miville-Deschênes, D. Molinari, A. Moneti, G. Morgante, A. Moss, P. Natoli, L. Pagano, D. Paoletti, G. Patanchon, L. Patrizii, L. Perotto, V. Pettorino, F. Piacentini, L. Polastri, G. Polenta, J. P. Rachen, B. Racine, M. Reinecke, M. Remazeilles, A. Renzi, G. Rocha, C. Rosset, M. Rossetti, G. Roudier, J. A. Rubiño-Martín, B. Ruiz-Granados, M. Sandri, M. Savelainen, D. Scott, C. Sirignano, G. Sirri, L. D. Spencer, A.-S. Suur-Uski, J. A. Tauber, D. Tavagnacco, M. Tenti, L. Toffolatti, M. Tomasi, M. Tristram, T. Trombetti, J. Valiviita, F. Van Tent, P. Vielva, F. Villa, N. Vittorio, B. D. Wandelt, I. K. Wehus, A. Zacchei, A. Zonca, Planck-intermediate results: Xlix. parity-violation constraints from polarization data, Astronomy & Astrophysics 596 (2016) A110. doi:10.1051/0004-6361/201629018.

[43] R. A. Fisher, On the mathematical foundations of theoretical statistics, Philosophical Transactions of the Royal Society of London. Series A, Containing Papers of a Mathematical or Physical Character 222 (1922) 309–368. doi:10.1098/rsta.1922.0009.

[44] F. Zhang (Ed.), The Schur Complement and Its Applications, Numerical Methods and Algorithms, Springer, 2005. doi:https://doi.org/10.1007/b105056.